Order Number 9020788

Temperature effect on dye laser spectra and optical properties of organic dyes

Moghaddasi, Jalil, Ph.D.

City University of New York, 1990

U·M·I
300 N. Zeeb Rd.
Ann Arbor, MI 48106

TEMPERATURE EFFECT ON DYE LASER SPECTRA AND OPTICAL PROPERTIES OF ORGANIC DYES

by

JALIL MOGHADDASI

A dissertation submitted to the Graduate Faculty in Engineering in partial fulfillment of the requirements for the degree of Doctor of philosophy, The City University of New York.

1990

This manuscript has been read and accepted for the Graduate Faculty in Engineering in satisfaction of the dissertation requirement for the degree of Doctor of philosophy.

1/16/90
Date

Chair of Examining Committe

1/16/90
Date

Jacques E. Benveniste
Executive Officer

Professor S. Ahmed

Dr. M. Ali

Professor R. Dorsinville

Dr. D. Kokkinos

Professor J. Manassah

Professor L. Roytman

Supervisory Committee

The City University of New York

ABSTRACT

TEMPERATURE EFFECT ON DYE LASER SPECTRA AND OPTICAL PROPERTIES OF ORGANIC DYES

by

Jalil Moghaddasi

Advisor: S. Ahmed, Professor and Chairman of Electrical Engineering Department.

The thesis describes the effects of temperature on dye laser spectra and optical prorerties of organic dyes. The study involved an investigation of the changes in absorption and fluorescence spectra of laser dyes on the efficiency of lasing and threshold power of cw dye lasers as the temperature of the dye solutions varied. An important role is stablished for the variation of concentration ratios with temperature of different types of dye in solution in shaping the threshold power and lasing efficiency of dye-based active liquids. The study of the possibility of increasing the lasing stability of active media is also especially important . In this connection, in the present work number of experiments were carried out to study the spectra-luminescence and lasing characteristics of number of Rhodamine dyes in different solvents, different concentration at different temperature. We examine the mechanism of the influence of intermolecular relaxation on the characteristic of the induced emission of the solutions. A theoretical basis is also

stablished for a hypotheses on the active role of the solvent as a factor that facilitates the conditions for the development of the lasing of the solutions. These factors have potential impact in improving dye laser characteristics and will result in substantial differences in attainable operating performance of at least some dye lasers. The study of temperature effects will be extended for examination of optical properties of organic dyes. An analytical expression for the real part of the complex refractive index is obtained in terms of the absorption coefficient. This result is then combined with the general reflectance expression to predict the reflectance of an absorbing medium at any given wavelength, soley in terms of the absorption coefficient of the medium at that wavelength and the angle of incidence. Experiments were also carried out for measurements of reflection intensity at low temperature. Four areas are investigated:1) Temperature effects on absorption and Fluorescence spectra of dye solutions, 2) Temperature effects on lasing efficiency and threshold power of dye solutions, 3) Comprehensive examination of temperature effects on the lasing characteristics of Rhodamine cw dye lasers 4) Temperature effects on optical reflective properties of Rhodamine dyes.

ACKNOWLEDGEMENTS

I would like to take this opportunity to express my sincere thanks to my parents, whose many sacrifices lead me to pursue higher education.

It is a great pleasure to acknowledge my deep appreciation to my mentor, S. Ahmed, professor and Chairman of Electrical Engineering Department of The City College of The City University of New York, for his patient guidance, rigorous training, continued encouragement, numerous invaluable suggestions and discussions during the course of this research, and most of all for his help selecting and changing my thesis subject.

As a recipient of a Loral Fellowship I would like to take this opportunity to express my appreciation and gratitude to Mr. Bernard L. Schwartz, Chairman of the Board and Chief Executive Officer, and Mr. Joseph Browdy, Vice-president, of Loral incorporation for their continued support of my research.

I wish to express my sincere thanks to the faculty of the Electrical Engineering Department for their instruction and help, especially to professor M. Ali for his invaluable suggestions and Professor P. Karmel for his continuos encouragement during the course of this undertaking.

To My Parents

Table of Contents

Page

Chapter 3

Chapter 4

Chapter 5

List of Figures

Page

Page

Page

CHAPTER 1

INTRODUCTION

1.1 Temperature Effect on Dye Laser Spectrum

A study of the temperature effect on fluorescence and lasing characteristics of dye lasers is of obvious scientific interest in the practical utilization of this type of laser. Temperature effects on dye laser solutions open the possibility of changes in spectroscopic and energy characteristics of dyes and hence of laser action from them. As the temperature of a dye solution is increased, higher vibrational levels of the ground state are populated according to a Boltzmann-distribution,[1-3] and more and more transitions occur from these to higher sublevels of the first excited singlet state. Consequently, the absorption spectrum becomes broader and the superposition of so many levels blurs most of the vibrational fine structure of the band, while cooling of the solution usually reduces the spectral width and enhances any vibrational features that may be present. As a concequence, absorption, fluorescence, lasing output, and threshold energy are sensetive to change in temperature. The correct choice of solvent and optimal temperature of the solutions of dyes therefore opens the feasibility of improving laser characteristics.

In this work, the spectral-luminescent and lasing properties of solutions of Rhodamine dyes in different solvents are

compared with the energy parameters characterizing intermolecular relaxation process and their variations with temperatures of dye solutions. An important role is also stablished for the variation of concentration ratios with temperature of different types of dye in solution in shaping the lasing characteristics of dye-based active liquids. The association of dye moleccules is an important manifestation of the interaction in solutions with temperature, and it has marked influence on all their optical properties.

In the last few years, a fairly large amount of varied experimental material has accumulated in the literature concerning the characteristic features of the stimulated emission of activated liquid systems and, in particular, the lasing spectra of solutions of organic substances (chiefly dyes).Unfortunately, the possibility of a logical and well-founded interpretation of all the accumulated established facts, some of which are fairly general in character, is as still extremely limited Thus for example, existing theories,[4-7] which have played a major role in the study of laser action in solutions of dyes and which are now being widely used in calculations of lasers,[8-9] nevertheless remain phenomenological theories, in which no account is taken of a large number of factors that are in fact fundamental characteristics of dye laser systems.

An explanation of the temperature effect on the spectrum and lasing efficiency of dye solutions can not be taken to be

quite complete in the framework of the theory of universal intermolecular interactions. This follows from the properties of their structure, typical for dye molecules. The dye always possesses one or some specific polar groups which, in the majority of cases, enter into specific interactions with the dye molecules. As a consequence, the dyes in solutions are often represented simultaneously in several forms with quite close spectral-luminescence characteristics. Variations in the state of these forms may be accompanied by variation in the absorption and luminescence spectra of the entire ensamble of impurity centers.

As mentioned above there are serious grounds for believing that it is allowance for intermolecular interactions and the associated characteristic features of the condensed state of matter that may in a number of cases be of decisive importantance of a correct understanding of the physical nature of the observed laser phenomena. These factors coupled with the thermal excitation of highrer levels and consequent broadening, of absorption and fluorescence spectra are also examined in this thesis research for their potential impact in improving dye lasers charecteristics.

1.2 Thesis Statement and Organisation

The goal of the thesis research is to study the following areas: 1) investigation of temperature effects on absorption and fluorescence spectra of dye solutions, 2) temperature effects on lasing efficiency and threshold power of dye solutions, 3) Comprehensive examination of temperature effects on the lasing charactetistics of Rhodamine cw dye lasers., and 4) Temperature effects on optical properties of Rhodamine dyes.

1.3 References

1. M. Bass and J. I. Steinfeld, IEEE. J. Quantum Electronics. Vol. 4, PP. 53-58, Feb. (1968).

2. P. P. Sorokin and J. R. Lankard, IBM J. Research and Develop. Vol 11, PP. 148, March (1967).

3. F. P. Schafer, pp. 9-29, (1977).

4. A. M. Samson, Methode of Calculation for Organic-Dye Laser with Monochromatic Excitation. Institute of Physics, Academy of science of USSR (1970).

5. G. C. Orner and M. R. Topp, Chem. Phys. Letter. PP. 36, 265, (1975).

6. T. F. Deutsch, M. Bass, P. Meyer, and S. Protopapa Appl. Phys. Letters, Vol. 11, PP. 379-381, (1967).

7. R. T. Kuznetsova. Fofova, and V. I. Danilva. Appl. Phys. PP. 1475, (1980).

8. Yu. Mazurenko and N.G. Bakhshiev, Opt. Spectrosc. PP. 490, (1977).

9. B. B. McFarland, Appl. Phys. Letters, Vol. 10, PP. 208-209, April (1967).

CHAPTER 2

TEMPERATURE EFFECTS ON ABSORPTION AND FLUORESCENCE SPECTRA OF DYE SOLUTIONS

2.1 Introduction and background

The first part of the thesis research was to investigate the temperature effects on absorption and fluorescence spectra of dye solutions. The spectral-luminescent and intermolecular interactions of solutions of Rhodamin dyes have been compared with the energy prameters characterizing intermolecular relaxation processes with variations in the temperature of the solution over wide range.

In this chapter we review the molecular interactions and stimulated emission spectra of fluid activated systems,[1-8] and present measurements of fluorescence and absorption of Rhodamine dyes in different solvents as the temperature of the dye solution is reduced. The interpretation of the results is soght in terms of the intermolecular interactions and associated characteristics are important in the condensed state as well as in terms of thermal excitation of higher levels. Ideas concerning the general regularities of the effect of relaxation and fluctuation intermolecular processes in the liquid phase of a substance on various characteristics of stimulated emission

of solutions are presented. It is shown that on the basis of the presented ideas with one point of view one can succeed in qualitatively interpreting a significant number of presently established experimental facts related to the energetic spectral parameters of the generation of organic solutions. The opinion is expressed that the processes of intermolecular interactions play an important, in many cases the determining, role in the examined effect, actively contributing to inverse population of the electronic-Vibrational states of the activator molecules.

When molecules are illuminated by monochromatic radiation with a wavelength within their resonance absorption band, a portion of the radiation is absorbed (Resonance Absorption). Some of the absorbed radiation will be re-emitted as fluorescence radiation by the molecules over a broad spectral range characteristic of the specific molecular species. In that process, each excited molecule decays by isotropically re-emitting a photon spontaneously. This fluorescence radiation will be in all directions. We found that the laser emission of Rhodamine B in ethanol shifted towards shorter wavelengths with decreasing temperature. This is caused by the narrowing of the fluorescence and the absorption band with decreasing temperature which results in higher gain and fewer absorption losses near the fluorescence peak. The solvent has also an important influence on the wavelength and efficiency of the dye-laser emission.

2.2 VIBRATIONAL-ELECTRONIC SPECTRA

2.2.1 The Franck Condon principle

Although quantum mechanics imposes no restrictions on the change in the vibrational quantum number during an electronic transition[1-3], the vibrational lines in a progression are not all observed to be of the same intensity. In some spectra the (0,0) transition is the strongest, in others the intensity increases to a maximum at some value of v', while in yet others only a few vibrational lines with high v' ,are seen, follow by a continuum. All these types of spectra are readily explicable in terms of the franck-Condon principle which states that an electronic transition takes place so rapidly that a vibrating molecule does not change its internuclear distance appreciably during transition.

Classical theory would suggest that the oscillating atom would spend most of its time on the curve at the turning point of its motion, since it is moving most slowly there; quantum theory, while agreeing with this view for high values of the vibrational quantum numbers, shows that for v =0 the atom is most likely to be found at the center of its motion, at the equilibrium internuclear distance $r_{eq.}$ For v =1, 2, 3, ... the most probable positions steadily approach the extremities until, for high v , the quantal and classical pictures merge. This behaviour is shown in Fig. 2.1.1 where we plot the probability distribution in each vibrational state against internuclear

distance. Fig. 2.1.1 shows the variation of Ψ_2 with internuclear distance, where Ψ is the vibrational wave function. Fig. 2.1.2 shows three possibilities. In (a) we show the upper electronic state having the same equilibrium internuclear distance as the lower. Now the frank-Condon principle suggests that a transition occurs vertically on this diagram, since the internuclear distance does not change, and so if we consider the molecule to be initially in the ground state both electronically (ε'') and vibrationally ($v'' = 0$), then the most probable transition is that of indicated by the vertical line in Fig. 2.1.2 (a). Thus the strongest spectral line of the v'' =0 progression will be the (0,0). However, the quantum theory only says that the probability of finding the oscillating atom is greatest at the equilibrium distance in the v =0 state, It allows some, although small, chance of the atom being near the extremities of its vibrational motion. Hence there is chance of the transition starting from the ends of the $v'' = 0$ state and finishing in the $v' = 1,2$, etc., states. The (1,0), (2,0), etc. lines diminish rapidly in intensity, however, as shown at the foot of Fig. 2.1.2 (a).

In Fig. 2.1.2(b) we show the case where the excited electronic state has a slightly greater internuclear separation than the ground state. Now a vertical transition from the $v'' = 0$ level will most likely occur into the upper vibrational state v' =2, transition to lower and higher v' states being less likely; in general the upper state most probably reached will depened

on the difference between the equlibrium separations in the lower and upper state. In Fig. 2.1.2(c) the upper state separation is drown as considerably greater than that in the lower state and we see that, firstly, the vibrational level to which a transition takes place has a high v' value. Further, transitions can now occur to a state where the excited molecule has energy in excess of its own dissociation energy. From such states the molecule will dissociate without any vibrations and, since the atoms which are formed may take up any value of kinetic energy, the transitions are not quantized and a continuum results. This is shown at the foot of the figure.

2.2.2 Vibronic absorption transitions

The total energy (E_t) of a molecule in its electronic ground state (excluding translational energy, and internal nuclear energy) [4],

$$E_t = E_e + E_v + E_r$$

is the sum of three components, the electronic energy (E_e), the vibrational energy (E_v), and the rotational energy (E_r).

Similarly, the total energy (E'_t) of a molecule in an excited electronic state

$$E'_t = E'_e + E'_v + E'_r$$

is the sum of its electronic, vibrational and rotational components, E'_e , E'_v , and E'_r , respectivily. If we define an absorption transition as

$$\Delta E_x = E'_x - E_x$$

where x = t, e, v or r, then $\Delta E_x \sim 10\ cm^{-1}$, $\Delta E_v \sim 1000\ cm^{-1}$, and $\Delta Ee \sim 30{,}000\ cm^{-1}$

Transitions involving only ΔE_r ($\Delta E_e = \Delta E_v$) yield the rotational absorption spectrum, which occurs in the far infrared region. Translations involving ΔE_v and ΔE_r ($\Delta E_e = 0$) yield the vibrational and vibrational- rotational absorption spectrum, which occurs in the near infra-red region. Transitions involving ΔE_e and E_v yield the electronic and electronic-vibrational absorption spectrum, which occurs in the visible and ultraviolet region. A state involving electronic and vibrational energy is refered to as a vibronic state, and a

transition between two such states is a vibronic transition Each electronic absorption transition ΔE_e gives rise to an absorption band system, each band of which corresponds to a different value of ΔE_v.

Let us consider a molecule in which only one vibrational mode is dominant, so that it approximates to a harmonic oscillator. If the energy of the fundamental vibrational mode in the ground electronic state is E_{1v} , then

$$E_t = E_e + (m + \frac{1}{2}) E_{1v}$$

where m=0, 1, 2, ...is the vibrational quantum number. If the energy of the fundamental vibrational mode in the excited electronic state is E'_{uv}, then

$$E'_t = E'_e + (n + \frac{1}{2}) E'_{uv}$$

where n= 0, 1, 2, 3, ... If the ground state system is thermal equilibrium at absolute temperature T, the fraction f_m of ground state molecules in a vibrationally excited state m is determined by the Boltzmann factor,

$$f_m = \exp (-mE_{1v}/KT)$$

where K is Boltzmann's constant. Since E_{1v}= 1000 cm^{-1}, and KT=200 cm^{-1} at room temperature, $f_1 = e^{-5} = 6.7 \times 10^{-3}$, $f_2 = e^{-10}$, etc. over 0.99 of the molecules are in the zero-point vibrational level of energy

$$E_t = E_e + \frac{1}{2} E_{1v}$$

The transitions constituting the main electronic absorption spectrum are given by

$$\Delta E_t = (E'_e - E_e) + \frac{1}{2} (E'_{uv} - E_{1v}) + nE'_{uv}$$

$$=(E'_e - E_e) + nE'_{uv}$$

since $E'_{uv} = E_{1v}$. The lowest energy vibronic transition in a given band system (n=0) is described as the 0-0 transition. The transition to the n^{th} vibrational level of E't is the o-n vibronic transition. The main electronic absorption spectrum thus yields data about the vibrational levels (nE'uv) of the excited electronic states Fig. 2.2.1.

2.2.3 Vibronic fluorescence transitions

Luminescence is the emission of photons from electronically excited states. Luminescence is divided into two types, depending upon the nature of the ground and the excited states [5]. In a singlet excited state, the electron in the higher- energy orbital has the opposite spin orientation as the second electron in the lower orbital. These two electrons are said to be paired. In the triplet states these electrons are unpaired, that is, their spins have the same orientation. Return to the ground state from an excited singlet state does not require an electron to change its spin orientation. A change in spin orientation is needed for a triplet state to return to the singlet ground state. Fluorescence is the emission which results from the return to the lower orbital of the paired electron. Such transitions are quantum mechanically "allowed" and the emissive rates are typically near 10^8 sec^{-1}. These high emissive rates result in fluorescence lifetimes near 10^{-8}sec or 10 nsec. The lifetime is the average period of time a fluorophore remains in the excited state.

The S_1 - S_0 fluorescence transition is the inverse of S_0 - S_1 absorption transition. Provided the lifetime of the excited electronic singlet state S_1 is sufficiently long for the excited molecules to attain thermal equilibrium, the fluorescence emission occurs primarily from the Zero-point vibrational level of S_1. This condition is generally valid if the molecules are in a condensed medium, in solution, but it may not be true in a

rarefied vapour, in which the molecules cannot lose their excess vibrational energy in collisions. In solution the fluorescence spectrum corresponds to $10 \rightarrow 0m$ vibronic transitions to the various vibrational levels (m) of the ground electronic singlet state (S_0). The fluorescence spectrum thus yields data about the vibrational levels of the ground electronic state Fig. 2.2.1.

We define the molecular fluorescence quantum efficiency q_{FM} as the ratio of the number of fluorescence photons emitted by a system of molecules in dilute solution to the number of molecules excited into S_1 (=the number of absorbed photons). The molecular fluorescence quantum intensity at frequncyν, normalized by the relation, [6]

$$q_{FM} = \int_0^{\bar{}} F(v)dv$$

In the general case of a large dye molecule, many normal vibrations of differing frequencies are coupled to the electronic transition. Further more, collisional and electrostatic perturbations, caused by the surrounding solvent molecules broaden the individual lines of such vibranic sublevel of every electronic state, including the ground state, has superimposed on it a ladder of rotationally excited sublevels. These are

extremely broadened because of the frequent collisions with solvent molecules which hinder the rotational movement so that there is a quasicontinuum of states superimposed on every electronic level. The population of these levels in contact with thermalized solvent molecules is determined by a Boltzmann distribution.

After an electronic transition, which, as describe above, lead to a nonequilibrium state (Franck-Condon state) the approach to thermal equilibrium is very fast in liquid solutions at room temperature. The reason is that a large molecule experiences at least 10^{12} collision/sec with solvent molecules, so that equilibrium is reached in a time of the order of one picosecond. Thus, the absorption is practically continuous all over the absorption band. The same is true for the fluorescence emission corresponding to the transition from the electronically excited state of molecule to the ground state.This results in a mirror image of the absorption band displaced towards lower wave numbers by reflection at the wave number of the purely electronic transition. This condition exists, since the emissive transitions start from vibrational ground state of the first excited electronic state S_1 and end in vibrationally excited sublevels of the electronic ground state. The resulting typical form of the absorption and fluorescence spectrum of an organic dye is given in Fig. 2.2.2

2.2.4 Emission spectra

The uptake of ultraviolet or visible radiation by a molecule results in the formation of an excited state or state of high energy. Such energy rich states are relatively short lived and rapidly lose the absorbed energy to return to the stable ground state. There are types of intermolecular process whereby molecules can lose excess energy. One is classified as radiative since energy is lost by the emission of radiation, and the other as non-radiative since radiaion is not emitted during energy loss. The former process is of importance in the present context since it gives rise to emission spectra.

The radiation emitted during a radiative transition is termed fluorescence when the transition is between states of the same multiplicity and phosphorescence when the transition is between states of different multiplicity. That is, the emitted radiation is fluorescence for the $S_1 \rightarrow S_0$ transition and phosphorescence for the $T_1 \rightarrow S_0$ transition. The relationship between the absorption spectrum of a molecule with a singlet ground state and its fluorescence and phosphorescence spectra is seen in Fig. 2.2.3. On absorption of radiation the molecule may be excited to an upper vibrational level of first excited singlet state or end up in such a level after deactivation from an upper excited singlet state. The excess vibrational energy is

rapidly lost by collisional deactivation and the molecule finishes up in the vibrational level.

Fluorescence arises from the radiative transitions from the lowest vibrational level of the S_1 state to the various vibrational levels of the S_0 state. If the spacings of the vibrational levels in the excited state are similar to those in the ground state there will be an approximate "mirror image" relationship between the absorption and fluorescence spectra. The spacing between the bands in the absorption spectrum is equal to the difference in energy between the vibrational levels of the excited state while that between the bands in the fluorescence spectrum is equal to the difference in energy between the vibrational levels of the ground state. Although the $0 \rightarrow 0$ transitions in absorption and fluorescence are shown to have the same energy in Fig. 2.2.3. this may not in fact be the case, and in the absorption and fluorescence spectra the band arising from the $0 \rightarrow 0$ transitions may be slightly displaced. Consideration of Fig. 2.2.3. helps to explain why this can occur.

If the excited state S_1 has a different solvation equilibrium from the ground state S_0 there will be a reorientation of the solvent cage after excitation and the more stable equilibrium state of S_1 will be formed. Foluorescence emission from this latter state will give a non-equilibrium ground state of higher energy than the original equilibrium ground state. Thus the $0 \rightarrow 0$ fluorescence transition will be of lower energy (lower

wave number) than original $0 \rightarrow 0$ absorption transition. Phosphorescence results from the radiative transition of the lowest vibrational level of the T_1 state to the various vibrational levels of the S_0 state. Since the energy of the T_1 state is lower than that of the S_1 state the phosphorescence spectrum is observed at lower wave number values than the fluorescence spectrum. Since transitions between states of different multiplicity are forbidden the phosphorescence spectrum is weak. On the other hand, fluorescence is relatively intense since it corresponds to a transition between states of the same multiplicity.

The intensities of vibrational bands in fluorescence and phosphorescence spectra vary in a similar manner to bands in absorption spectra. Again this is most readily discussed in relation to diatomic molecules. Typical potential energy curves for the S_0 and S_1 states of a diatomic molecule are shown in Fig. 2.2.4. Here the excited state curve is displaced to greater internuclear separation than the ground state curve. The Franck-Condon principle applies to emission as well as to absorption, and emission processes can be represented by vertical lines connecting the initial and final states. In the situation represented in Fig. 2.2.5 the $0 \rightarrow 1$ transition is the most probable and the fluorescence spectrum may appear as shown.

2.2.5 Temperature effects on internal conversion and intersystem crossing of intramolecular decay processes

The deactivation of excited state molecules via intermolecular interactions is a frequent occurence in photochemical systems. The major routes for the dissipation of the excitation energy in the photo-excited species are energy transfer to an acceptor molecule, and chemical reaction with a suitable reactant. Intermolecular and intramolecular deactivation processes occur concurrently and all deactivation steps have to be taken into account when considering the kinetics of a photochemical system. The processes which can contribute to the deactivation of an excited state molecule and which may have to be considered in the kinetic analysis as radiative emission, internal conversion, intersystem crossing, energy transfer, chemical reaction.

The absorption of radiation leads to excited state molecules which rapidly convert to the $V'=0$ levels of the S_1 and T_1 states. If the excited state molecules do not participate in a chemical reaction they will all revert unchanged to the original ground state and the quantum yield for the re-formation of the ground state will be unity. This maybe expressed as

ϕ = no. of ground state molecules re-formed / no. of ground state molecules initially excited = 1

The processes whereby molecules starting in the $V' = 0$ level of the S_1 state can return to the ground state are summarized in Fig. 2.2.6. Each of these processes will have a quantum yield defined by the expression:

$\phi_{process}$ = no. of molecules deactivated by the process / no. of ground state molecules initially excited

An alternative expression is:

$\phi_{process}$ = rate of process / rate of absorption of radiation

If there is no photochemical reaction and no energy loss from excited states by intermolecular quenching then the sum of the quantum yields for the deactivation processes originating from the S_1 state will equal unity. This can be written in the form

$$\phi_f + \phi_{ic} + \phi_{isc}(S_1 \rightarrow T_1) = 1 \qquad (2.2.1)$$

Where ϕ_f , ϕ_{ic} and ϕ_{isc} are respectively the quantum yields for fluorescence, internal conversion and intersystem crossing.

When there is no photochemical reaction or energy loss by intermolecular quenching all the molecules which cross over to the T_1 state will decay either by emitting phosphorescence or

by intersystem crossing to the S_0 state. The following expression will be applicable in these circumstances:

$$\phi_{isc}(S_1 \rightarrow T_1) = \phi_p + \phi_{isc}(T_1 \rightarrow S_0) \qquad (2.2.2)$$

Where ϕ_p and ϕ_{isc} are the quantum yields for phosphorescence and intersystem crossing.

Each decay process occurs at a rate which is represented by one of the unimolecular rate constants K_f , K_{ic}, $K_{isc}(S_1 \rightarrow T_1)$, K_p and $K_{isc}(T_1 \rightarrow S_0)$. The quantum yield for each process is related to these rate constants by the expression

$$\phi_{process} = K_{process} / \sum K_i \qquad (2.2.3)$$

where $\sum K_i$ is the sum of the rate constants for each of the processes.

The observed radiative lifetimes of the S_1 and T_1 states are determined by the rates of the deactivation processes originating from the state, and are given by the equation

$$\tau = \frac{1}{\sum K_i} \qquad (2.2.4)$$

The extent to which each of the processes of internal conversion, intersystem crossing, fluorescence and phosphorescence contribute to the return of excited state molecules to the ground state varies for different molecular systems, and within the one system varies for different environmental conditions. Whether the deactivation of excited state molecules occurs primarily from S_1 state or from the T_1 state depends on a number of factors, some of which are outlined below. These factors affect the rate of the $S_1 \rightarrow T_1$ intersystem crossing relative to the rates of fluorescence and $S_1 \rightarrow S_0$ internal conversion; if K_{isc} is large compared to K_f and K_{ic} then deactivation from the T_1 state will be the main route to the ground state. One factor which determines the relative magnitudes of K_{isc}, K_f and K_{ic} is the energy gap, $\Delta E(S_1 - T_1)$, between the $V' = 0$ levels of the S_1 and T_1 states.

The rate of internal conversion from the S_1 state to the S_0 state is dependent upon the energy gap, $\Delta E(S_1 - S_0)$, between the lowest vibrational levels of the S_1 and S_0 states; the smaller the energy gap the greater the rate of internal conversion. Similarly the rate of the $T_1 \rightarrow S_0$ intersystem crossing is dependent upon the energy difference between the lowest vibrational levels of the T_1 and S_0 states. As the energy differnce decreases so the rate of the $T_1 \rightarrow S_0$

intersystem crossing increases relative to the rate of phosphorescence.

The rate of fluorescence can be enhanced relative to other processes deactivating the S_1 state by changing the temperature of the system. The fluorescence quantum yield, ϕ_f , varies with temperature according to the equation:

$$\log\left(\frac{1}{\phi_f} - A\right) = \frac{B}{T} \qquad (2.2.5)$$

where B is a constant, A is equal to $(1 + \sum K_i' \tau)$ with τ being the observed radiative lifetime of the S_1 state and $\sum K_i'$ the sum of the rate constants for deactivation of the S_1 state by processes other than fluorescence. It can be seen from Equation (2.2.5) that fluorescence yield can be increased by decreasing the temperature of the system. The rate of the $S_1 \rightarrow T_1$ intersystem crossing can be enhance relative to the rate of fluorescence and $S_1 \rightarrow S_0$ internal conversion by substituting a heavy atom into the molecule or by using solvents containing heavy atoms. The increase rate for the $S_1 \rightarrow T_1$ intersystem crossing is shown up by the higher values for ϕ_p and the lower values for ϕ_f in the systems with heavy atom present. The presence of heavy atoms also increases the rate of the $T_1 \rightarrow S_0$ intersystem crossing and reduces the phosphorescence lifetime of the T_1 state. Electronic transitions occur at rates rapid relative to the

rate of internuclear motion in molecules. Hence during an electronic transition, each nucleus in the molecule remains essentially stationary. (The Franck-Condon principle). Accordingly, when a molecule in its ground state absorbs a photon, it reaches to an excited state in which the molecular geometry and solvent configuration are those characteristics of the ground state. Solvent reorientation then occurs approximately 10^{-11} to 10^{-12} second after excitation, producing an equilibrium excited state. In this equilibrium excited state, the solvent configuration is optimal for the geometry and electron distribution of the molecule. Emission occures from the equilibrium excited state forming a Franck-Condon ground state. Solvent relaxation then occurs forming the equilibrium ground state. It is evident that ground and excited states involved in absorption and fluorescence are different. Accordingly there is no reason to expect precise correspondence between absorption and fluorescence effects.

In most polar molecules, the excited state is more polar than the ground state. Hence an increase in polarity of the solvent produces a greater stabilization of the excited state than of the ground state. Consequently a shift in both absorbance and fluorescence spectra to lower energy, or longer wavelengths (red shift), is usually observed as the dielectric constant of the solvent increases.[1-9]

The magnitude of the red shift of fluorescence emission to longer wavelengths on the specific nature of the solute-

solvent interactions. Several of the important types are; 1) permanent dipole-dipole interactions between solute and solvent, 2) interactions involving one permanent dipole and one induced dipole, and 3) interactions involving one transition dipole and one induced dipole.The fluorescence spectrum will be influence by one or more of these categories; the general effect is termed an electrostatic effect.

The fluorescent intensities of aromatic compounds can also be affected by electrostatic solvent effects. These effects are generally significant if both solute and solvent are non-polar. For polar solute-solvent pairs, electrostatic intensity perturbations are minor relative to those produced by specific short range interactions such as complex formation. Fluorescence often varies with solvent and this is due to the dielectric constant of the solvent, which will be discussed in chapter 3, and quenching by solvent molecules and ionization.

2.3 Luminescence in solutions of organic dyes at low temperature

2.3.1 Temperature Tuning of an organic Dye Laser

Dependence of the luminescence spectra on the frequency of exciting light is known at room temperature for solutions of organic dyes in different solvents.[17] It is known that the spectral characteristics of complex molecules in solution depend strongly on orientational interactions with the solvent.[18-19] Orientation effects determined in particular the shift of the luminescence spectra towards shorter wavelenghts, found for a number of substances on lowering the temperature of the dye solutions.[20] In the present thesis research we shall indicate how the orientational interaction of the molecule in the solutions can also lead to a dependence of the luminescence spectra on the frequency of the exciting light at low temperature.

The spectra properties of complex molecules in polar solvents can be described by a model involving four levels , as shown in Fig. 2.3.1. It is assumed in this scheme that all unexcited molecules are concentrated on level 1', since the equilibrium configuration of the surrounding solvent molecules corresponds to this level. Under such conditions the location of the pair of levels 1" - 2" with respect to the levels 1'-2' is unimportant to the extent that the absorption and fluorescence spectra are determined only by the frequency of

the transitions 1'-2' and 2"-1". For this reason sometimes instead of the energy-level scheme of Fig. 2.3.1a, one considers the scheme of Fig. 2.3.1b, in which the states 1' and 1" are located at the same level.

Both these schemes, though, describe only approximately the spectral properties of the solution, since the thermal molecular motion is not taken into account. If the temperature of the medium is not zero, the thermal motions inhibit the establishment of equilibrium configurations in the solvent. It follows that even in the case when the life time τ of the excited level of the dye molecule is many times longer than relaxation time τ_R of the medium, the equilibrium states 1' and 2" will exist in solution together with the non-equilibrium states 1" and 2'. In order to determine the probability of attaining states with equilibrium and non-equilibrium configuration, it will be necessary to consider not only the solute molecule, but also an appropriate elementary volume (cell) of the solution consisting of a dye molecule and the surrounding envelope of solvent molecules. The energy of such an elementary cell can be expressed as a sum of terms that can be considered approximately independent:

$$E = \sum_i E_i + E_j + w$$

Here E_i is the potential energy of the isolated i-th molecule of the solvent which is part of the elementary cell; E_j is the potential energy of an isolated fluorescence molecule; w is the total mutual interaction energy of the molecules in the elementary cell. In the present case we are considering only the orientational interactions, namely the interaction caused by the presence of permanent dipole moments on the solute and solvent molecules. The energy-level scheme of the cell being considered is actually more complex. because of the thermal motion of the molecules, a large number of cell configurations exist, which are not equilibrium configurations either for the ground or for the excited state of the fluorescing molecule. This leads to inhomogeneous broadening of the solution spectra. Since the processes of absorption and emission of light being consider are connected with electronic-vibrational transitions in the dye molecules but not in the solvent, only changes of the quantities E_i and w need to be considered, while the sum $\sum_i E_i$ can be assumed to remain constant and can be neglected.

2.3.2 Temperature dependence of luminescence spectra

The characteristic short-wavelength shift in the luminescence spectrum, observed during polar solutions of complex molecules and corresponding to the temperature region in which the orientational dipole relaxation time of the solvent (τ_R) is comparable with the luminescence lifetime (τ_f). This pecularity of solutions in polar media is due to the following reasons. If the dipole moment of a molecule varies during its excitation, the energy of its dipole-dipole interaction with the surrounding medium should also vary. The change in the interaction energy takes place at the rate of the orientational relaxation in solvent; therefore, the degree of its completeness and the shift in the luminescence spectrum depend on the relationship of the times τ_R and τ_f and, consequently, on the temperature. The position of the luminescence spectrum as a function of the time t that the molecule is in the excited state is described according to Ref. 21 , by the expression

$$\xi(t) = \xi_0 - \frac{1}{hc}(K_0 - K_\infty)(U_e^0 - U_g^0)^2 A(t), \qquad (2.3.1)$$

where ξ_0 is the position of the spectrum at t=0, in the absence of relaxation), $K(\varepsilon)$ is the function of the dielectric constant ε

$$K(\varepsilon)=\frac{2(\varepsilon-1)}{(2\varepsilon+1)-2(\varepsilon-1)\frac{\alpha}{a^3}}\frac{1}{a^3} \quad ,$$

(2.3.2)

α is the polarizability of the solute molecule, a is the molecular radius, $K_0=K(\varepsilon)$; $K_\infty = K(n^2)$, ε_0 is the static ε value, n is the index of refraction in the optical region, u_0^g and u_e^0 are the dipole moments of the solute molecule in the ground and excited states, and A(t) is a dimensionless function that varies from 0 to 1 and describes the relaxation kinetics of the medium field acting on the molecule. Function A(t) is dependent on the relaxation characteristics of the orientational polarization of the solvent and can be determined by a fourier transformation of the spectrum $K(\omega)$

$$A(t)\,(K_0-K_\infty)=\frac{1}{2\pi}\int_0^t\left\{\int_{-\infty}^{+\infty}[K(\omega)-K_\infty]\,e^{-j\omega t}\,d\omega\right\}dt$$

(2.3.3)

The spectrum $K(\omega)$ is associated through equation (2.3.2) with the spectrum of the complex dielectric constant $\varepsilon(\omega)$. The experimentally observed luminescence spectrum is the sum of

the instanteneous spectra emitted at various moments of time t. For the center of gravity of the total spectrum

$$\bar{\nu} = \int_{\nu}\int_{t} \nu I(\nu, t)\, d\nu dt \;/\; \int_{\nu}\int_{t} I(\nu, t) d\nu dt$$

it is not difficult to obtain

$$\bar{\nu} = \bar{\nu}_0 - (\bar{\nu}_0 - \bar{\nu}_-)\tau_f^{-1}\int_0^{\infty} A(t)e^{-t/\tau_f}dt, \qquad (2.3.4)$$

$$(\bar{\nu}_0 - \bar{\nu}_-) = \frac{1}{hc}(K_0 - K_-)(U_e^0 - U_g^0)^2 \qquad (2.3.5)$$

where ν_0 and ν_- are the position of the spectrum at t=0 and t=∞. Equation (4) permits determining the temperature dependence of the spectrum if the dependence of the function A(t) at the temperature is known. The simplest approximation for A(t) results from the polar Deby liquid model,[22] according to which relaxation of polarization of a dielectric takes place exponentially. In this case A(t) = 1-exp(-t/τR), and the temperature dependence of the luminescence spectrum for the modle is determined by the expression:

$$\bar{\nu} = \bar{\nu}_0 - (\bar{\nu}_0 - \bar{\nu}_\infty)\frac{\tau_f}{\tau_f + \tau_R} \qquad (2.3.6)$$

As is known, detailed studies of the dielectric properties of polar liquid lead to the conclusion that the relaxation process is more complex than the Deby model would seem to indicate,[23-25]. In the improve model relaxation is characterized by the sum of several simple exponential processes with sharply differing times.

Let us consider the application of this more realistic model to a study of temperature dependence of the luminescence spectrum. In the approximation of several (N) relaxation times the spectrum $\varepsilon(\omega)$ should consist of N shifted Debye bands, each of which corresponds to

its own relaxation time $\tau_d^{(k)}$

$$\varepsilon(\omega) = n^2 + \sum_{k=1}^{N} \frac{\varepsilon_0^{(k)} - \varepsilon_\infty^{(k)}}{1 - i\omega\tau_d^{(k)}}, \qquad (2.3.7)$$

where $\varepsilon_0^{(k)}$ and $\varepsilon_\infty^{(k)}$ are real values, in which case $\varepsilon_\infty^{(k)} = \varepsilon_0^{(k+1)}, \varepsilon_0^{(1)} = \varepsilon_0, \varepsilon_\infty^{(N)} = n^2, \tau_d^{(k+1)} \ll \tau_d^{(k)}, \tau_d^1 = \tau_d$ is the relaxation time corresponding to the fundamental (low-frequency) band.

By applying Eq. (2.3.2) to Eq. (2.3.7) and taking into account the fact that the $\tau_d^{(k)}$ values differ by tens and, consequently, the individual $\varepsilon^{(k)}(\omega)$ bands are weakly overlaped, we find

$$K(\omega) = K(n^2) + \sum_{k=1}^{N} \frac{K_0^{(k)} - K_\infty^{(k)}}{1 - i\omega\tau_R^{(k)}}, \tag{2.3.8}$$

$$\tau_R^{(k)} = \tau_d^{(k)} \frac{(2\varepsilon_\infty^{(k)} + 1) - (\varepsilon_\infty^{(k)} - 1)\frac{2}{3}}{(2\varepsilon_0^{(k)} + 1) - (\varepsilon_0^{(k)} - 1)\frac{2}{3}}, \tag{2.3.9}$$

where $K_\infty^{(k)} = K_0^{(k+1)}, K_0^1 = K(\varepsilon_0)$, and $K_\infty^{(N)} = K(n^2)$. The function A(t) resulting from Eqs. (2.3.8) and (2.3.3) contains N exponents characterized by different time constants $\tau_R^{(k)}$. Substituting A(t) into Eq. (4), we obtain

$$\bar{\nu} = \bar{\nu}_0 - \sum_{k=1}^{N} (\bar{\nu}_0^{(k)} - \bar{\nu}_\infty^{(k)}) \frac{\tau_f}{\tau_f + \tau_R^{(k)}}, \tag{2.3.10}$$

$$(\bar{\nu}_0^{(k)} - \bar{\nu}_\infty^{(k)}) = \frac{1}{hc}(K_0^{(k)} - K_\infty^{(k)})(U_e^0 - U_g^0)^2. \tag{2.3.11}$$

The temperature shift of luminescence spectrum according to Eq. (2.3.10) appeare more complex than according to Eq.(2.3.6). When the solution is cooled, the relaxation times $\tau_R^{(k)}$ increase (just as $\tau_d^{(k)}$). Therefore, temperature regions corresponding to the conditions $\tau_f \approx \tau_R^{(1)}, \tau_f \approx \tau_R^{(2)}$, etc. , in each of which there is a partial shift in the spectrum by the value $(\nu_0^{(k)} - \nu_-^{(k)})$. [26-27]

2.4 Experimental

2.4.1 The experimental arrangement

Figure 2.4.1 shows the arrangement used to measure fluorescence intensity of Rhodamin dyes in different solvents under cw argon laser excitation as the temperature of the dye solution varied. The experimental arrangement was assemdled on a horizontal table. A collimated light beam was obtained from a tunable cw dye laser. By appropriate geometric arrangement of mirrors, the incidence of the laser beam on the dye solution surface obtained and fluorescence intensity determined using a spectrometer in conjunction with a detector. An additional detector used to monitor the output of cw dye laser. To increase sensitivity and accuracy, a phase lock loop amplifier could also be used in conjunction with the detector.

2.4.2 Experimental results

Experimental measurements were carried out to determine and measure the temperature effects on fluorescence and absorption spectra of Rhodamine dyes in different solvent as the temperature of the dye solution is reduced.

Figure 2.4.2-2.4.22 show the experimental results of fluorescence and absorption of Rhodamine B, Rhodamine 6G, and Rhodamine 110 in Ethylalcohol, Methanol, and Ethylene glycol, as the temperature of the dye solution varied within the interval from room temperature ($23\,C^{\circ}$) down to $-60\,C^{\circ}$.

2.5 REFERENCES

1. N.G. Bakhshiev, Opt. Spectrosc. Vol 32, PP. 1151 (1972).

2. N. G. Bakhshiev and B.S. Neporent, Opt. Spectrosc. Vol16, PP. 191 (1970).

3. P.P. Sorokin and J.R. Lankard, IBM J Research and develop. Vol. 10, pp. 162-163, March (1966).

4. F. P. Shafer, W. Schmidt, and J. Volez Vol. 9, PP. 306-309, October (1966).

5. M. L. Spaeth and D. P. Bortfield , Appl. Phys. Letters, Vol. 10 PP. 179-181, September (1966).

6. P. P. Sorokin and J. R. Lankard, IBM J. Research and Develop. Vol 11, PP. 148, March (1967).

7. B. B. Snavely, O. G. Peterson, and R. F. Reithel, Appl. Phys Letters, Vol. 11, PP. 275-276, November (1967).

8. A. Yariv and J. P. Gordon, IEEE, Vol. 51, PP. 4-29, January (1963).

9. M. Bass and J. I. Steinfeld, IEEE J. Quantum Electronics Vol. 4, PP. 53-58, February (1968).

10. B. H. Soffer and B. B. McFarland, Appl. Phys. Letters, Vol. 10, PP. 266-267, May (1967).

11. N. G. Bakhshiev, Opt. Spectrosc. Vol. 10, PP. 717 (1961).

12. N. G. Bakhshiev, I.V. Piterskaya, and A. V. Altaskaya, Opt. Spectrosc. Vol. 28, PP. 897 (1970).

13. N. G. Bakhshiev, Opt. Spectrosc. Vol. 32, PP. 979 (1972).

14. N. G. Bakhshiev, Opt. Spectrosc. Vol. 32, PP. 1151(1972).

15. S. K. Garg and C. P. Smyth, J. Phys. Chem. Vol. 69, PP. 1294 (1965).

16. B. B. Snavely and O. G. Peterson, IEEE Journal of Quantum Electronics, Vol. QE-4, Vol. 10, October (1968).

17. L. V. Levshin and D. M. Akbarova, Zh. Prikl. Spectrosc., 3, 441 (1965).

18. E. S. Mcrae and M. Kasha, J. Chem. Phys. 28, 721 (1958).

19. V. I. Permogorov, L. A. Serdyukova, and M. A. Frank Kamenetskii, Opt. Spectrosc. Vol. 36, PP. 503 (1974).

20. T. E. Sharp and H. M. Rosenstock. J. Chem. Phys. Vol. 41, PP. 3453 (1964).

21. Yu. T. Mazurenko and N.G. Bakhshiev, Opt. Spectrosc. Vol. 28, PP. 490 (1970).

CHAPTER 3

TEMPERATURE EFFECTS ON LASING EFFICIENCY AND THRESHOLD POWER OF DYE SOLUTIONS

3.1 Introduction and background

The effect of changes in absorption and fluorescence spectra of laser dyes on the efficiency of lasing and threshold power of cw dye lasers are investigated in this chapter. The mechanism of the temperature effect on the lasing and spectral characteristics of solutions of Rhodamine dyes in different solvents are also studied. An important role is stablished for the variation of concentration ratios with temperature of different types of dye in solution in shaping the threshold power and lasing efficiency of dye-based active liquids. The spectral-luminescent and lasing properties (lasing frequency and lasing threshold) of solutions of Rhodamine dyes in different solvents have been compared with the energy parameters characterizing intermolecular relaxation processes with variations in the temperature of the dye solution. The regular change in the frequency and threshold intensity of pumping when the solution is cooled is chiefly a concequence of a change in the relative arrangement of the equilibrium and Franck-Condon states of the activator molecule as a result of a change in the state of aggregation of the solvent. This chapter also presents the experimental results of the nature of the

temperature effect on the lasing efficiency and threshold power of dye solutions under cw laser excitation.

The study of the effect of the medium on the luminescence properties and photochemical stability of lasing organic compounds is required in order to make a deliberate election of orgar ic luminophores and solvents, used as active laser media. Under the action of the excited light , photochemical transformations occur in the solvent, as well as irreversible photodecomposition of dye molecules, which degrade the luminescence and generating characteristics of the active media in liquid lasers. The data available in the literature on these problems[1-3] do not permit drawing final conclusions concerning the mechanism by which the solvent affects the lasing efficiency and the photochemical stability of active media based on rhodamine dyes. For this reson, it is important to investigate the influence of solvent and temperature on laser radiation of rhodamine dyes in order to optimize the lasing characteristics of active media. The study of the possibility of increasing the lasing stability of real active media is especially important. In this connection, in the present thesis we studied the spectral-luminescence and generating characteristics of a number of rhodamine dyes in different solvents, as temperature of the dye solution decreased, and the effect of the addition of some compounds on the lasing stability of active media.

3.2 Intermolecular relaxation processes

3.2.1 Theoretical explanation of intermolecular relaxation processes

The vast majority of photochemical reaction occure when a molecule is raised to either the first excited singlet state S_1 or the first triplet state T_1 [4-7]. Molecules in these states possess a large excess of energy and although this facilitates chemical reaction these highly energetic molecules are short lived and can often lose their excess energy and return to the stable ground state before reaction can occur. The likelihood of a photochemical reaction is dependent, therefore, upon the rates of the reaction processes as compared to the rates of the reaction processes. The three types of process whereby the energy of electronically excited molecules can be dissipated are:

(1) Radiationless transitions from one electronic state to another (no radiation emitted during energy loss).

(2) Radiative transitions between electronic states (radiation emitted during energy loss).

(3) Electronic energy transfer between molecules.

In most cases, processes 1 and 2 are intermolecular and process 3 is intermolecular. Internal conversion is the term given to the radiationless process where by a molecule transfers from one electronic state to another electronic state of

the same multiplicity. Intersystem crossing is the term given to the process when the transfer involves electronic states of different multiplicity. we begin the examination with the problem concerning the effect of medium (solvent) on such an important characteristic as the generation threshold.[1-5] The nature of the solvent, its composition, aggregate state, and also temperature exert a substantial effect on the threshold intensity of the pumping. In liquid solutions at room temperature ($\tau_R << t_e$) the generation thereshold of dye solutions sharply increases during the transition from polar solvents to nonpolar. As the temperature of the dye solution decreases the threshold at first is markedly lowered and then with future cooling, as a rule, begins to increase, leading finally to the collapse of generation ($t_e << \tau_R$). The fact that as the temperature is reduced the value of the quantum yield of spontaneous luminescence sharply increases.

3.2.2 Intermolecular processes for the dissipation of electronic energy

Actually, it is well known that the threshold of pumping U_{th} in the general case is smaller, the higher the last level of a laser transition is located on an energy scale, in respect to the level occurring for the act of absorption. With respect to the examined intermolecular processes the quantity ΔE_g^{FC} serves as a measure of the indicated energy gap, so that we have

$$U_{th} = U_{th.}\,(\Delta E_g^{FC}).$$

The threshold increase in the transition from the $\tau_R \ll t_e$ condition to $t_e \ll \tau_R$ is explained by the fact that in the liquid polar solvent always $0 < \Delta E_g^{FC}$ on account of the orientational intermolecular relaxation, whereas in the frozen glassy solution $\Delta E_g^{FC} \equiv 0$ at $\tau_R \ll t_e$

$$\Delta E_g^{FC} \approx \left(\frac{\varepsilon_1 - 1}{\varepsilon_1 + 2} - \frac{n_1^2 - 1}{n_1^2 + 2}\right)$$

where ε_1 and n_1 are the local dielectric constant and index of reflection of near neighbors of the acceptor molecules (in the case of an individual solvent the quantities ε_1 and n_1 can be identified with corresponding macroscopic values of ε and n). Since for nonpolar solvents $\varepsilon \sim n^2$, under these conditions $\Delta E_g^{FC} \sim 0$, the generation threshold is high. In the transition to ($n^2 < \varepsilon$) the value is $0 < \Delta_g^{FC}$, According to which the threshold is reduced. This same result can be achieved, by the use of a mixed solvent which is explaind by the preeminent solvation of the activator molecule by molecules of the polar component.

3.3. The energy gap ΔE_g^{FC}

3.3.1 A detailed mathematical expression for ΔE_g^{FC}

A working formula for calculating ΔE_g^{FC} when $\tau_R << t_e$ (liquid solutions) [16-18],

$$\Delta E_g^{FC} = \frac{1}{2}\mu_e^{eq} R_{e(or)}^{eq} - \frac{1}{2}\mu_g^{FC} R_{g(ind)}^{FC} - \mu_g^{FC} R_{e(or)}^{eq} + \frac{1}{2} R_g^{FC} \alpha R_g^{FC} + \frac{1}{2}\mu_g R_g^{eq} \tag{3.31}$$

where

$$\mu_i^{eq} = \mu_i + \alpha R_i^{eq} \tag{3.3.2}$$

$$\mu_j^{Fc} = \mu_j + \alpha R_j^{FC} \tag{3.3.3}$$

here $R^m_{i(or)}$, $R^n_{j(ind)}$ are orientational and induced electronic components of the reaction fields R_i^m and R_i^n , μ_g and μ_e are electric dipole moments of a free activator molecule in the corresponding states, α is polarizability of the molecule. Expressions for the fields $R^{eq}_{e(or)}$, $R^{FC}_{(ind)}$ and R_q^{eq} in Eq. (1) can be adopted, [2-4] for example,

$$R^{eq}_{e(or)} = \frac{2}{r^3}\mu_e \frac{2\varepsilon_0 + 1}{\varepsilon_0 + 2}\left(\frac{\varepsilon_0 - 1}{2\varepsilon_0 + 1} - \frac{n_0^2 - 1}{2n_0^2 + 1}\right) \tag{3.3.4}$$

where ε_0 and n_0 are the static dielectric constant and index of reflection of the solvent, and r is the Onsager radius of the activator molecule.

We must note that Eq. (3.3.1) allows us to determine the average energy gap ΔE_g^{FC} . However, fluctuation distribution of this quantity due to statistical intermolecular processes in the

liquid phase is not included in the equation. In Eq. (3.3.1), we must include not only orientational and induced-electronic components of the reactionfield due to the orientations of the molecules of the surrounding with respect to the activator molecule and the polarization of electronic shells of solvent molecules, but also an induced atomic component which is due to the displacement of the nuclei in the molecules of the surroundings.

The process of stablishing this type of polarization occurs over $10^{-12} - 10^{-14}$ sec, atomic intermolecular relaxation is commensurable in time to intermolecular relaxation. This does not allow us as yet to separate the contribution of these two different types of relaxation to the stimulated emission characteristic. The larger $\Delta\nu = \nu_{max}^{lum} - \nu_{max}^{las}$, the higher the threshold and vice versa. These results enable us to express several specific preliminary reasons regarding the selection of the activator and solvent characteristics from which we can expect a lowering of the lasing threshold due to processes of orientational intermolecular relaxation. In the case of individual solvents we must give preference to liquids with a large dielectric constant ε_0 and small n_o, tacking appropriate account of the orientational relaxation time τ_R and ensuring that condition $t_e > \tau_R$ is satisfied. This imposes certain requirements on the temperature range for observing lasing. It is thus necessary to bear in mind that the energy gap ΔE_g^{FC} will be higher for molecules of those activators which are

characterized by a more significant variation in the dipole moment under laser excitation.

Thus, for a correct approach to evaluate any prospective solution in the stimulated emission, knowledge not only of the standard spectroscopic characteristics of system, but also considration of a number of solvent characteristics and parameters of the activator molecule in the ground and excited states are necessary. According to foregoing, other conditions being equal, we can expect a minimum lasing threshold for a given system under the condition $\Delta E_g^{FC} \rightarrow \Delta_{g(max)}^{FC}$.

3.4 Improvement in the performance of Rhodamine B cw dye lasers

3.4.1 EXPERIMENTAL: RESULTS AND ANALYSIS

The lasing characteristics of a cw circulating dye laser, RhB solution in ethylene glycol, were obtained by pumping with the 488-nm output of an Argon laser. A heat exchanger with liquid nitrogen was used for cooling of the solution in the circulating resevoir shown in Fig. 3.4.1. The temperature dependence of the lasing characteristics were obtained for four different concentrations, 2×10^{-4}, 3×10^{-4}, 4×10^{-4}, and 5×10^{-5} moles/liter using broadband mirrors for the dye laser.

Fig.3.4.2. shows typical behavior of the fluorescence and absorption spectra of RhB solution in ethylene glycol at two

temperatures, 23^0C, and -5^0C, respectively. The flourescence spectra shown in Fig. 3.4.2 were also excited with the 488-nm output of an Argon laser. As expected, the fluorescence spectrum narrows with decreasing temperature, however, there is no appreciable shift in its peak. Since lasing occurs on the long wavelength side of the fluorescence peak, the fluorescence spectrum "pulls" the lasing wavelength towards lower values as the spectrum narrows with decreasing temperature. This effect is more pronounced at higher concentrations where the increased absorption has forced the lasing wavelength farther from the peak. This may be seen in Fig. 3.4.2 where the lasing wavelengths have been indicated for various concentrations. It can also be seen, however, that especially at higher concentrations, fluorescence narrowing alone is not sufficient to explain the total shift with temperature. It is possible that the gradual increase of triplet-triplet absorption, at higher concentrations, provide the additional amount of absorption at these shorter wavelengths necessary to explain the total shift.

Figs. 3.4.3 and 3.4.4. show the temperature dependence of the lasing threshold and lasing radiation at various concentrations. It can be seen from Fig. 3.4.3. that in the initial stage of cooling, for all concentrations, as T drops from 23^0C to -5^0C, there is a considerable reduction in the lasing threshold. It can also be seen from Fig. 3.4.3. that the reduction is more significant at a concentrations of 3×10^{-4} moles/liter. This significant reduction in the lasing threshold, cannot be

explained in the framework of a model of universal intermolecular interactions which, as a general rule, predict an increase in the lasing threshold with reduction in temperature [15-22]. However, as shown in Fig. 3.4.2, this significant reduction in the lasing threshold is explained by the fact that as the temperature is reduced the value of the quantum yield of spontaneous luminescence sharply increases, overriding any possible negative effects due to intermolecular relaxation processes. As might be expected, as shown in Fig. 4, at temperature of -5^0C and concentrations of 3×10^{-4} moles/liter, where the lasing threshold is minimum, the lasing ouput power also reaches a maximum.

It can be expected that with further cooling ($T < -5^0$C), the lasing threshold, would begins, as a rule, to increase, leading finally to the collapse of lasing ($\tau_R >> \tau_f$ and $\Delta E_g^{Fc} \approx 0$) [16-19].

To further illustrate the temperature dependence of the lasing characteristics, measurements of the lasing threshold and ouput power, versus wavelength, at two different temperatures, were carried out again, this time for single-frequency regimes. These measurements are shown in Figs. 3.4.5. and 3.4.6. for concentrations of 2×10^{-4}, 3×10^{-4} moles/liter, respectively. As expected, for all wavelengths, through out the entire spectrum of interest, all values, obtained at -5^0C, for lasing threshold and output power, are, lower and higher, respectively, than those obtained at 23^0C.

Finally, it should be pointed out that these results are in contrast to the results obtained for most other dye solutions (e.g. solutions of Rhodamine 6G in methanol, Rhodamine C in methanol and 3-amino-N-methylphthalimide in glycerol) [20-23], where quantum yields are already high at room temperature, and where cooling has initially little or no impact, and further cooling results in reduction in laser output and increase in threshold requirements, in conformity with the theory of universal intermolecular interactions.

In conclusion, it has been shown that, for the case of RhB-ethylene glycol laser solution, cooling from room temperature to -5^0C can result in significant increases in cw dye laser output, and related reductions in threshold power requirements. These results are explained by the fact that as the temperature is reduced the value of the quantum yield of spontaneous luminescence for RhB sharply increases, overriding possible negative effects due to intermolecular relaxation processes. An understanding of the temperature effect on the spectrum and lasing efficiency of dye solutions, particularly for the initial stage of cooling, is therefore seem to require an explanation beyond the framework of the theory of universal intermolecular interactions.

Finally, it should be noted that attempts at a more comperhensive explanation of temperature effects would be complicated because of the complex structure of dye molecules. Dyes always possesses one or more specific polar groups

(auxochromes) [23], which, in most of the cases, enter into specific interactions with the dye molecules. These interactions are responsible for the existence of dyes in several different forms, consequently, dyes in solutions are often represented simultaneously in several forms with similar spectral-luminescence characteristics.

3.5 REFERENCES:

[1] Joseph R. Lakowicz, Principles of flourescence spectroscopy, third edition, Plenum press, New York, (1986).

[2] M. U. Belyi, and A. B. Leontev. Opt. Spektrosc. Vol. 34, PP. 715-721, April (1972).

[3] F. P. Schafer, Dye lasers, second revised edition, Springer-Verlag Berlin Heidelberg New York, (1977).

[4] N. G. Bakhshiev and Yu. T. Mazurenko, Optical Spectrosc. PP. 25, (1970).

[5] N. G. Bakshiev and I. V. Piterskaya, Opt. Spectrosc. PP21, (1966).

[6] V. P. Klochkov and S. M. Korotkov, Opt. Spectrosc. PP. 16, (1970).

[7] A. V. Aristov and Yu. s. Maslyukov, Opt. Specrosc. PP. 835, (1968).

[8] N. G. Bakshiev, Opt. Spectrosk. Vol. 32, PP. 1151, (1972).

[9] N. G. Bakshiev, O. P. Grin, and V. I. Studenov, Opt. Spectrosk. Vol. 39, PP. 54-59 (July 1975).

[10] N. G. Bakshiev, Opt. Spectrosk. Vol. 32, PP. 979, (1972).

[11] V. A. Alekseev, L. K. Denisov, V. I. Kozintsev, and N. A. Kozlov. J. Appl. Spectrosc. Vol. 31, PP. 848, (1979).

[12] L. V. Levshin, T. D. Slavnova, and V. I. Yuzhakov. J. Appl. Spectrosc. Vol. 24, PP. 698, (1976).

[13] V. I. Studenov, N. G. Bakhshiev, and V. S. Smirnov. Reports of the 7th-All-Union conference, PP. 406, (1974).

[14] A. N. Rubinov and V. I. Tomin Opt. Spektrosk. Vol. 29, PP. 1802, (1970).

[15] A. V. Aristov, N. G. Bakhshiev, and I. V. Piterskaya. Opt. Spektrosk. Vol. 30, PP. 143, (1971).

[16] V. I. Studenov, and N. G. Bakhshiev. Opt. Spektrosk. Vol. 36, PP. 392 (1974).

[17] V. I. Studenov, I. V. Piterskaya, and N. G. Bakhshiev. Opt. Spektrosk. Vol. 39, PP. 308, (1975).

[18] N. G. Bakhshiev, The Spectroscopy of intermolecular interactions, Nauka, Leningrad, (1972).

[19] N. G. Bakshiev, Opt. Spectrosk. Vol. 32, PP. 1151, (1972).

[20] N. G. Bakhshiev, and V. I. Studenov. Opt. Spektrosc. Vol. 33, PP. 62-65 (1972).

[21] V. I. Studenov, and N. G. Bakhshiev. Opt. Spektrosk. Vol. 39, PP. 661-665, October (1975).

[22] N. V. Korol' Kova, and B. M. Uzhinov. Zhurnal prikladnoi Spektroskopii, Vol 39, No. 3, pp. 406-412, September (1983).

[23] V. M. Krasnoshchekov, A. B. Nikolaev, and V. V. Rylkov. Opt. Spektrosk. Vol. 54, PP. 118-122, January (1983).

CHAPTER 4

COMPREHENSIVE EXAMINATION OF TEMPERATURE EFFECTS ON THE LASING CHARACTERISTICS OF RHODAMINE cw DYE LASERS

4.1 INTRODUCTION

The mechanisms of temperature effects on the fluorescence and absorption spectra of organic dye solutions have received considerable attention [1-3]. However, the nature of temperature effects on the lasing characteristics of organic dye solutions, when used as a lasing media under laser excitation, is still unclear [4-20]. Extensive experimental and theoretical data available in the literature [10-23], devoted to uncover temperature effects on the lasing characteristics of dye solutions, when used as a lasing media under laser excitation, particularly at the initial stage of cooling, do not permit drawing final conclusions concerning the mechanisms by which the temperature affects the lasing characteristics of these dyes when used as a lasing media. Interpretations of the experimental results, as well as theoretical calculations [15-22], concerning temperature effects on the lasing characteristics of dye solutions, are, entirely based on the the framework of the theory of universal intermolecular interactions [5-18]. An understanding of the temperature effects, particularly for the

initial stage of cooling, as will be discussed, on the spectrum and lasing efficiency of dye solutions, require an explanation beyond the framework of the theory of universal intermolecular interactions.

This paper examines these effects in laser-pumped cw dye lasers, and shows them to be of considerable practical significance in some special cases.

The optical excitation of a molecule and its subsequent emission of spontaneous luminescence or stimulated radiation results in a series of intermolecular processes (orientational, translational, etc.), which occurr in both the ground and excited states [6-11]. The orientational relaxation processes have a substantial effects not only on the spontaneous luminescence spectrum but also on the stimulated emission spectrum of the solution [15-22].

To examine these processes, it is necessary, because of the finite duration τ_f (10^{-8} - 10^{-9} Sec), of the excited states of the molecules studied, to consider the relationship between this quantity and the orientation relaxation time, τ_R (10^{-11} - 10^{-12} Sec), of the surrounding molecules, i. e., to take into account the degree of reorientation of the surroundings, caused by the change in the electric properties of the molecule upon excitation. Under conditions where the role of stimulated emission processes predominates, the average time t during which the molecules stay in the excited states decrease sharply and can become comparable to the orientation relaxation time τ_R for the molecules of the medium at room temperature. In

fact, when the threshold pumping level is substantially exceeded, the condition $\tau_f \approx \tau_R$ can be realized in ordinary liquid luminescing solutions at room temperature [15]. The results of [7-10], show that at temperatures for which $\tau_f >> \tau_R$ (total relaxation) or for which $\tau_f \approx \tau_R$ (partial relaxation), energy level scheme for electronic states of complex molecules in polar solvents can be approximated by a model involving four levels, as shown in Fig. 4.1.1. As a result of intermolecular relaxation processes, which reestablish equilibrium between the excited molecules and the solvent, optically excited molecules decay to an equilibrium level, 3, with a probability of $P_{23} = 1/\tau_R$. Then, emit in the transition $3 \rightarrow 4$, entering the ground Franck-Condon level 4.

Obviously the more rapidly the relaxation processes take place, the greater the probabilities P_{23} and P_{41}, and the less populated are the final Franck-Condon levels for the absorption and emission events 2 and 4 are as compared with the equilibrium levels 1 and 3. This fact creates favorable conditions for the development of an inverse population of level 3 as compared with level 4. The gap ΔE_g^{Fc} characterizes the difference in the position of the lower electronic laser level, 4, and the ground state electronic level, which is the original level for absorption (excitation). It has been established [16-17] that the lasing threshold, as expected [18-19], is on the whole lower, the greater the value of ΔE_g^{Fc} for a given lasing solution.

In the case of a frozen solution, for which $\tau_R >> \tau_f$, intermolecular relaxation of orientational type greatly reduced ($\Delta E_g^{Fc} = \Delta E_e^{Fc} \approx 0$), and the four-level scheme is effectively reduced to a two-level scheme. Mathematical expressions, for ΔE_g^{Fc} as well as the whole theoretical treatment of the theory of universal intermolecular interactions, given in the literature [11-15], are very complicated and in our opinion cannot be taken to be complete. Extensive experimental and theoretical data [16-22], devoted to uncover temperature effects on the lasing characteristics of dye solutions, when used as a lasing media under laser excitation, reveal that in the initial stage of cooling there is a slight decrease in the threshold pumping intensity, and then with further cooling, as a rule, threshold requirements begin to increase greatly, leading finally to the collapse of lasing ($\tau_R >> \tau_f$ and $\Delta E_g^{Fc} \approx 0$). While the theory of universal intermolecular interactions, for the two limiting cases, $\tau_f >> \tau_R$ and $\tau_R >> \tau_f$, is in good agreement with the experimental results, it can not explain, as will be shown, the significant reduction in threshold pumping intensity in the initial stage of cooling (for Rhodamine B in ethylene glycol), neither can it give, in general, satisfactory results in the case of a gradual transition from a four-level scheme to two-level scheme in the arrangement of the electronic levels.

The present work is devoted to a further study of temperature effects on the lasing characteristics of dye solutions, when used as a lasing media under laser excitation,

particularly at the initial stage of cooling ($T \approx 23^0C$ to -5^0C) where the theory of universal intermolecular interactions cannot be used to interpret the experimental results. We report experimental results of the temperature effects on the cw lasing and flourescence characteristics of Rhodamine dyes (Rhodamine B, Rhodamine 6G, and Rhodamine 110) in ethylene glycol for different concentrations.

4.2. EXPERIMENTAL: RESULTS AND ANALYSIS

The lasing characteristics of a cw circulating dye lasers, Rhodamine B, Rhodamine 6G, and Rhodamine 110 in ethylene glycol, were obtained by pumping with the 488-nm output of an Argon laser shown in Fig. 4.2.1. A heat exchanger with liquid nitrogen was used for cooling of the solution in the circulating resevoir. The temperature dependence of the lasing characteristics were obtained at a concentrations of 3×10^{-4} moles/liter using broadband mirrors for the dye lasers.

Figs. 4.2.2, 4.2.3, and 4.2.4 show typical behavior of the fluorescence spectra, at various temperatures, for RhB, R6G, and Rh110 solutions in ethylene glycol respectively. These flourescence spectra were also excited with the 488-nm output of an Argon laser. As expected, the fluorescence spectra, for the three dye solutions, narrow with decreasing temperature, however, there is no appreciable shift in their peaks. It can also be seen that, while the quantum yeild of RhB sharply increases with decreasing temperature, however, for both R6G and

Rh110 solutions, there is a sharp reduction in their quantum yields with decreasing temperature. There are almost no variations with varying the temperature, where lasing occurs, on the long wavelength side of the absorption peaks, with a slight shift in the absorption peaks.

The experimental results for the temperature dependence of the lasing threshold and lasing radiation are shown in Figs. 4.2.5 and 4.2.6 respectively. It can be seen from Fig. 4.2.5 that at the initial stage of cooling, in the case of Rhodamine B, as T drops from 23^0C to -5^0C, there is a considerable reduction in the lasing threshold. However, in the case of Rhodamine 6G and Rhodamine 110 there is a slight reduction in the lasing threshold.

For the case of RhB, this significant reduction in the lasing threshold, cannot be explained in the framework of a model of universal intermolecular interactions which, as a general rule, predict an increase in the lasing threshold with reduction in temperature [15-22]. Obviously, at the initial stage of cooling, down to a certain temperature (-5^0C), where negative effects due to intermolecular relaxation processes are almost absent, there is a linear correlation between the lasing threshold and the quantum yield for fluorescence. Thus, as shown in Fig. 4.2.2, this significant reduction in the lasing threshold is explained by the fact that as the temperature is reduced the value of the quantum yield of spontaneous luminescence

sharply increases, overriding any possible negative effects due to intermolecular relaxation processes. With further cooling ($T < -5^0C$), despite the continious increase in the fluorescence quantum yield (fig. 4.2.2), negative effects due to intermolecular relaxation processes begin to dominate, with the result that the lasing threshold, would begins, as a rule, to increase, leading finally to the collapse of lasing ($\tau_R >> \tau_f$ and $\Delta E_g^{Fc} \approx 0$) [16-19].

Given the fact that the fluorescence quantum yield, for both Rhodamine 6G and Rhodamine 110, decreases with reduction in temperature (Figs. 4.2.3 and 4.2.4), then, the slight decrease, at the initial stage of cooling, of lasing threshold of Rhodamine 6G and Rhodamine 110 (fig. 4.2.5) cannot be explained with the help of the model just examined above. However, this slight reduction could be related to a decrease in the induced losses due to triplet-triplet absorption which could be caused by an increase in the amount of oxygen present as the temperature of the solution is reduced [24]. As is well known, oxygen is a quencher of the triplet state of dye molecules [25-26]. Hence, its presence in a solution strongly modifies such parameters as the intersystems crossing rate constant and the life time of the triplet states [27-28]. Consequently, a decrease in the concentrations of oxygen in a solution leads to an increase in the losses due more intense T-T absorption which, in turn, brings about a decrease in the laser output and an increase in the threshold pumping energy.

Thus, it is necessary, in order to bring about this slight reduction, at the initial stage of cooling, in the lasing threshold of Rhodamine 6G and Rhodamine 110, that positive effects due to the reduction in the triplet states losses override any possible negative effects due to both intermolecular relaxation processes and the reduction in the fluorescence quantum yield.

With further cooling ($T < -5^0C$), however, this time, negative effects due to both intermolecular relaxation processes and the reduction in the fluorescence quantum yields of Rhodamine 6G and Rhodamine 110 (Figs. 4.2.3 and 4.2.4), begin to dominate, with the result that the lasing threshold, would begins, as a rule, to increase, leading finally to the collapse of lasing ($\tau_R >> \tau_f$ and $\Delta E_g^{Fc} \approx 0$) [16-19].

It would be emphasized that, in the case of Rhodamin B, if the increase in the fluorescence quantum yield alone is not sufficient to explain the considerable reduction, at the initial stage of cooling, in the lasing threshold, then, It is possible that positive effects due to the gradual reduction in the triplet states losses, provide the additional amount necessary to explain the considerable reduction in the lasing threshold.

As might be expected, for the case of Rhodamine B, as shown in Fig. 4.2.6, at the initial stage of cooling, there is a considerable increase in the lasing ouput power with decreasing temperature. However, for the case of Rhodamine

6G and Rhodamine 110 (Fig. 4.2.6), there is a slight or almost no increase in the lasing ouput power with decreasing temperature.

Finally, it should be pointed out that these results are in contrast to the results obtained for most other dye solutions (e.g. solutions of Rhodamine 6G in methanol, Rhodamine C in methanol and 3-amino-N-methylphthalimide in methanol) [20-23], where quantum yields are already high at room temperature, and where cooling has initially little or no impact, and further cooling results in reduction in laser output and increase in threshold requirements, in conformity with the theory of universal intermolecular interactions.

In conclusion, one might be able to classify organic dye solutions, when used as a lasing media under laser excitation, and according to the temperature effects, at the initial stage of cooling, on their lasing characteristics, into three different classes:

1) Dye solutions, in high viscosity solvents where quantum yields are low at room temperature, and where cooling results in an increase in their fluorescence quantum yields, and consequently reduction in threshold requirements and a corresponding increase in their laser output. This could be explained by the fact that, at the initial stage of cooling, where negative effects due to intermolecular relaxation processes are

almost absent, there is a linear correlation between the lasing threshold and the fluorescence quantum yield. Thus, this reduction in the lasing threshold is explained by the fact that as the temperature is reduced the value of the quantum yield of spontaneous luminescence sharply increases, overriding any possible negative effects due to intermolecular relaxation processes. On the other hand, if the reduction in the lasing treshold is significant, as the case, examined here, for Rhodamine B-ethylene glycol laser solution, so that the increase in the fluorescence quantum yield alone is not sufficient to explain the considerable reduction. Then, positive effects due to the gradual reduction in the triplet states losses, provide the additional amount necessary to explain the considerable reduction in the lasing threshold. For those dyes, where cooling results in sharp increase in their fluorescence quantum yields, however, with a slight reduction in threshold requirements. It is entirly possible that the position of the T-T absorption spectra of these dyes, is such that it does not affect lasing characteristics, and hence, the second positive factor does not contribute to the lasing efficiency.

2) Dye solutions, in high viscosity solvents where quantum yields are low at room temperature, and where initial cooling results in a further reduction in their fluorescence quantum yields (e. g. Rhodamine 6G and Rhodamine 110-ethylene glycol laser solutions), however, with a slight or almost no reduction in threshold requirements. This could be explained by the fact

that, at the initial stage of cooling, positive effects due to the reduction in the triplet states losses override any possible negative effects due to both intermolecular relaxation processes and the reduction in the fluorescence quantum yield.

3) Dye solutions, in low viscosity solvents, (e.g. solutions of Rhodamine 6G in methanol, Rhodamine C in methanol and 3-amino-N-methylphthalimide in methanol) [20-23], where quantum yields are already high at room temperature, and where cooling has initially little or no impact on their fluorescence quantum yields nor on their lasing characteristics. This could be explained by the fact that, at the initial stage of cooling, positive effects, if there is any, due to the reduction in the triplet states losses would be almost canceled by any possible negative effects due to both intermolecular relaxation processes (which is almost absent at the initial stage of cooling).

Finally, for almost all dye solutions, with further cooling negative effects due to intermolecular relaxation processes begin to dominate, with the result that the lasing threshold, would begins, as a rule, to increase (the temperature at which the increase start to take place might vary from dye to another), leading finally to the collapse of lasing ($\tau_R >> \tau_f$ and $\Delta E_g^{Fc} \approx 0$) [16-19], in conformity with the theory of universal intermolecular interactions.

An understanding of the temperature effects on the spectrum and lasing efficiency of dye solutions, particularly at the initial stage of cooling, is therefore require an explanation beyond the framework of the theory of universal intermolecular interactions.

As a final remark, it should be noted that attempts at a more comperhensive explanation of temperature effects would be complicated because of the complex structure of dye molecules. Dyes always possesses one or more specific polar groups (auxochromes) [23], which, in most of the cases, enter into specific interactions with the dye molecules. These interactions are responsible for the existence of dyes in several different forms, consequently, dyes in solutions are often represented simultaneously in several forms with similar spectral-luminescence characteristics.

4.3 REFERENCES:

[1] Joseph R. Lakowicz, Principles of flourescence spectroscopy, third edition, Plenum press, New York, (1986).

[2] M. U. Belyi, and A. B. Leontev. Opt. Spektrosc. Vol. 34, PP. 715-721, April (1972).

[3] F. P. Schafer, Dye lasers, second revised edition, Springer-Verlag Berlin Heidelberg New York, (1977).

[4] N. G. Bakhshiev and Yu. T. Mazurenko, Optical Spectrosc. PP. 25, (1970).

[5] N. G. Bakshiev and I. V. Piterskaya, Opt. Spectrosc. PP21, (1966).

[6] V. P. Klochkov and S. M. Korotkov, Opt. Spectrosc. PP. 16, (1970).

[7] A. V. Aristov and Yu. s. Maslyukov, Opt. Specrosc. PP. 835, (1968).

[8] N. G. Bakshiev, Opt. Spectrosk. Vol. 32, PP. 1151, (1972).

[9] N. G. Bakshiev, O. P. Grin, and V. I. Studenov, Opt. Spectrosk. Vol. 39, PP. 54-59, July (1975).

[10] N. G. Bakshiev, Opt. Spectrosk. Vol. 32, PP. 979, (1972).

[11] V. A. Alekseev, L. K. Denisov, V. I. Kozintsev, and N. A. Kozlov. J. Appl. Spectrosc. Vol. 31, PP. 848, (1979).

[12] L. V. Levshin, T. D. Slavnova, and V. I. Yuzhakov. J. Appl. Spectrosc. Vol. 24, PP. 698, (1976).

[13] V. I. Studenov, N. G. Bakhshiev, and V. S. Smirnov. Reports of the 7th-All-Union conference, Tashkent, pp. 406, (1974).

[14] A. N. Rubinov and V. I. Tomin Opt. Spektrosk. Vol. 29, PP. 1802, (1970).

[15] A. V. Aristov, N. G. Bakhshiev, and I. V. Piterskaya. Opt. Spektrosk. Vol. 30, PP. 143, (1971).

[16] V. I. Studenov, and N. G. Bakhshiev. Opt. Spektrosk. Vol. 36, PP. 392, (1974).

[17] V. I. Studenov, I. V. Piterskaya, and N. G. Bakhshiev. Opt. Spektrosk. Vol. 39, PP. 308,(1975).

[18] N. G. Bakhshiev, The Spectroscopy of intermolecular interactions Nauka, Leningrad, (1972).

[19] N. G. Bakshiev, Opt. Spectrosk. Vol. 32, PP. 1151, (1972).

[20] N. G. Bakhshiev, and V. I. Studenov. Opt. Spektrosc. Vol. 33, PP. 62-65 (1972).

[21] V. I. Studenov, and N. G. Bakhshiev. Opt. Spektrosk. Vol. 39, PP. 661-665, October (1975).

[22] N. V. Korol' Kova, and B. M. Uzhinov. Zhurnal prikladnoi Spektroskopii, Vol 39, No. 3, pp. 406-412, September (1983).

[23] V. M. Krasnoshchekov, A. B. Nikolaev, and V. V. Rylkov. Opt. Spektrosk. Vol. 54, PP. 118-122, January (1983).

[24] A. M. Samson (editor) , Quantum Electronics and Laser Spectroscopy, Nauka i Teknika, Minsk (1974).

[25] S. A. Davydov and V. V. Gruzinskii, Zh. Prikl. Specktrosk. Vol. 26, PP. 30, (1977).

CHAPTER 5
TEMPERATURE EFFECTS ON OPTICAL PROPERTIES OF RHODAMINE DYES

5.1 BACKGROUND:

The optical constants of an isotropic material are the index of refraction n and extinction coefficient k. They are the real and imaginary components of the complex index of refraction N = n - jk. They can be measured at a given wavelength by direct methods or inferred form photometric or polarimetric measurements. A number of methods exist for extracting n and k from specular-reflectance measurements at both normal and oblique incidence and for semi-infinite media as well as layers on substurates. Here we will discuss the most useful methods for obtaining n and k and the problem encountered in applying these methods.

Humphreys-Owen [4] lists nine methods by which n and k can be deduced from reflectance measurements at oblique incidence. These methods are divided into two classes:

(1) two reflectance measurements at one angle of incidence or one reflectance measurements at each of two angles of incidence and

(2) one reflectance measurement at any angle of incidence and measurement of a special angle of incidence capable of

supplying the necessary second measurement. There are two special angles:

1- the principal angle of incidence, which must be determined by polarimetric methods and so it will not be discussed, and

2- the Brewster, or pseudo-Brewster(pB), angle. The Brewster angle is defined only in terms of dielectric media and is given by

$$n = \tan fB \qquad (5.1.1)$$

At this angle Rp = 0. As k increases, Rp always has a minimum value, but it is not zero. The angle at which this minimum occurs is the pB angle and, if

$$k > 0, \; fpB > fB \; .$$

Humphreys-Owen's list has been rearranged as follows:

Class 1

Method 1 Reflectance at two angles of incidence using natural or polarized radiation; sometimes referred to as the reflectance versus-angle of incidence method

Method 2 The ratio Rp / Rs at two angles of incidence

Method 3 Rs and Rp at one angle of incidence

Class 2

Method 4 Pseudo-Brewster angle and Rs or Rp at that angle

Method 5 Pseudo-Brewster angle and Rp / Rs at that angle

Method 6 Pseudo-Brewster angle and Rs , Rp or Rp / Rs at an other angle of incidence

In principle, only two measurements are required, but, because of possible errors in the measurements, a redundancy of measurements is more useful and will give an indication of the errors involved in determining n and k.

Although these methods can be used at any wavelength, their sensitivities to errors in measurements of reflectance, of the angles involved, or of the state of polarization are functions of both n and k, as well as the angle of incidence and the state of polarization. Thus there may be parts of the n, k plane, angles of incidence, and state of polarization, for which the lack of sensitivity reduces their accuracy to unacceptable values.

Since the sensitivities of the methods are dependent on n, and k, hence on the shape of the R-versus-f curves, a collection of these curves is shown in Fig. (5.1.1)[12] for reference during the ensuing discussion. The large numbers give the values of n and k used in calculating a particular set of curves. These values covers the range of n and k most likely to be encountered in the VUV. The small numbers along the abscissa and ordinate show the angle of incidence and percent reflectance, respectively. The upper curve is always Rs, the lower curve Rp, and the curve between Ra. Generally, for a given n, as k increases the reflectance at normel incidence

increases, the change in R with f becomes small, especially for Ra, except at the pB angle, and the pB angle becomes large. For a given k, as n increases the reflectance at normal incidence decreases, the change in R with f becomes more pronounced, especially for Rp, and again the pB angle becomes larger. The value of Rp at the pB angle appears to be zero for $n > 1.3$ and $k = 0.3$. This is not so, but the values are extremely small.

Method 1:

The sensitivity of this method is most easily investigated by means of isoreflectance curves. An isoreflectance curve is the locus of points in the n, k plane corresponding to a given value of R for a specific value of f. If isoreflectance curves are plotted for perfect data, i.e., reflectance values calculated using the Fresnel formula, an insight into the sensitivity of the method can be obtained. Fig. (5.1.2) [12] show such a set of curves for the parallel component covering that part of n, k plane

$$0.3 < n < 2.3 \text{ and } 0.3 < k < 3.3.$$

An indication of the sensitivity is the angle of intersection of the isoreflectance curves. If there is an error in the reflectance, the isoreflectance curve will be shifted parallel to its self by an amount depending on the magnitude of the error

and in a direction depending on its sign. Thus, if two curves intersect at a small angle, a slight displacement of one with respect to the other may shift the intersection point by a large amount. Such a displacement could be due either to an error in measuring R or an error in measuring f. The figure indicates that for n = 0.3, the sensitivity with respect to k decreases as k increases. Thus for small n and k > n, the R-versus-f method can provide reasonable values, e.g., Al, Mg, etc., usually have small n and k > n. For example, at 1216 A, Al has n 0.06 and k 1.0.

For n > 0.3, the isoreflectance curves for small angles of incidence are more nearly parallel than those for the larger angles. Thus, the sensitivity is greatest if measurements are made at the larger angles of incidence. For n = 0.3, however, the maximum sensitivity for small k is obtained using small angles and as n increases, maximum sensitivity is shifted only slowly to larger angles. Generally, the angles with which maximum sensitivity is obtained are those angles at which the curvature in R is maximum, which is not necessarily the angles at which R changes most rapidly with f. Similar sets of isoreflectance curves have been calculated for Rs and Ra[12].

Although the curves in Fig. 5.1.2 furnish an idea of the sensitivity of the method, the accuracy of the method can only be found by using false data.

By adding positive and negative errors to perfect reflectance data, the magnitude of the displacement of the isoreflectance curves can be obtained and the accuracy of the method determined. Hunter [12] has investigated the accuracy of method 1 using angles of incidence of 20o and 70o. His results are shown in Fig. 1.3 for both Rp and Ra. The blackened parallelopipeds represent the error in determining n and k for + 1 o/o erroes in measuring the reflectance. The parallelopipeds correspond to the values of n and k shown in large numbers. Lines connect the extermities of these parallelopipeds to indicate the magnitude of the errors at intermediate points. The magnitude of the errores is in keeping with the sensitivity as discussed in connection with Fig. 5.1.2 For example, for small n (0.3), the error in n as k increases grows comparatively slowly, but the corresponding error in k becomes large quite rapidly because the parallelopipeds are almost parallel to the k axis. As n increases and for large k, the long axis of the parallelopipeds rotates in a clockwise direction so that the error in determining n increases while that for k decreases. It is evident that Rp is more tolerant of errors than Ra.

In using the R-versus-f method it is not necessary to know the actual R values[12]. The fact that reflectance is defined as the ratio of the reflected intensity at angle f to the incident intensity is equvalent to normalizing the reflected intensity at angle f to the reflected intensity at 90o angle of

incidence, which is defined as unity. For use in the R-versus-f method, normalization can be done at any angle of incidence and is referred to as oblique normalization. Field and Murphy [13] have puplished an analysis of the R-versus-f method for oblique normalization. For oblique normalization the angle between the isoreflectance curves may not be a good indicator of sensitivity, and one should plot known errors in the obliquely normalized reflectance values to get a correct indication of sensitivity. Oblique normalization has no advantages over the usual mode of normalization and is only used when the physical arrangement of the reflectometer makes measurement of the incident intensity impractical.

Method 2:

Figure 5.1.4 shows two sets of curves for the ratio Rp / Rs. To the left is a set for small angles of incidence and to the right a set of large angles. According to Humphreys-Owen, an indication of the sensitivity is the spacing between contours- if the spacing is large, the sensitivity is good and vice versa. As suming that his assertion is correct, the large-angle contours are obviously not useful if n and k are large but might be used to obtain good values if n and k are small. The small-angle contours are only useful if n and k are small. Humphreys-Owen showed a limited set of contours of Rp/Rs for 80^{o} and 60^{o}, and a more extended, calculated set indicates that these two angles

may be more useful than those shown here for larger values of n and k.

Method 3:

Figure 5.1.5 shown two sets of curves for Rs and Rp at both 20^{o} and 70^{o} angles of incidence. Judging from sets of curves obtained for other angles of incidence, these two angles are the most useful. For 20^{o} angle of incidence, the curves of conestant k are spaced 0.01 apart from k = 0 to k = 0.1. The next k contour is for k = 0.2 and thereafter Dk = 0.2. The n contours have Dn = 0.1. The dotted line is the contour of n = 0.364 = tan 20^{o}. This set of curves might be useful for n < 0.5 and k < 0.4.

The set of curves of 70^{o} is less useful for small n and k but more useful for larger values. For this set Rp = 0 when n = 2.747 = tan 70o. Both Dn and Dk are 0.2 for this set.

The envelope of the 20^{o} contours consists of the curves k = 0 and, ultimately, the curves for large n values. The 70^{o} contours are enveloped by the two curves for k = 0, which coincide at Rs = Rp = 0. At 45^{o}, where Rp = Rs2 for any n and k, the envelope is compressed to a line that has the form of a parabola.

Method 4 and 5:

Figures 5.1.6 shows sets of curves for Rp/Rs (method 4) and Rs (method 5) versus the pB angle. The Rp/Rs set favors small values of n and k and the Rs set favors somewhat larger n and k. Not that the Rs curves can give double values. For example, if the pB angle is 15^{o} and Rs = 0.56, k would be 0.3 but n could be 0.2 or 0.3. Thus, the region with double values is not useful. Contours for Rp-versus-pB angle are similar to those for Rp/Rs.

According to Humphrey-Owen, method 6 gives no advantages over the other methods.

In order to obtain quantitative data on the accuracy of methods 2-5, it is necessary to plot the contours for R + DR, or pB + DpB, which has not been done. The existance of large spacing between the contours suggests but does not guarantee small displacements of the contours when errors are introduced Humphrey-Owen points out that Rp, at the pB angle, can be quit small; thus, there may be a large error in measuring it. Furthermore, the minimum in Rp at the pB angle is usually broad, so accurate location of the angle may be difficult.

If method 2 or 5 is to be used, normalization to get acual reflectance values is unnecessary.

The equation for Rp can be manipulated to obtain the pB angle intermes of n and k[4]. It is given below,

$$2(p2 + q)v3 + p2(p2-3)v2 - 2p4v + p4 = 0,$$

where

$$p = n2 + k2, \qquad q = n2 - k2, \qquad v = \sin 2\,fB$$

The experimental values for n and k obtained from the curves can be substituted in the formula to help verfiy the correctness of the results.

5.2 OPTICAL REFRACTIVE AND REFLECTIVE PROPERTIES OF RESONANTLY ABSORBING MEDIA

5.2.1 INTRODUCTION

It is well known that organic Rhdomaine dye solutions are used in different solvents as an active media for tunable dye lasers. Therefore, their optical properties are of obvious scientific and practical interest. Numerous studies [1-10] have shown that lasing characteristics are sensetive to variations in temperature. The correct choice of solvent and optimal temperature of the solutions of organic dyes therefore have opened the feasibility of improving laser characteristics. In

fact, Significant improvements in the performance of some dye lasers [8-10] have been reported as the solvent temperature was reduced below room temperature, namely: a significant reduction in the threshold power requirements and a considerable increase in the attainable output power. Recently [11], we have conducted a theoretical and experimental investigations on the optical properties of An ethanolic solution of Rhodamine B at room temperature. Given the importance of cooling the solutions of organic dyes, when used as a lasing media, on their lasing characteristics, it appears timely to examine the optical properties of organic dye solutions as the solvent temperature is reduced below room temperature.

The optical properties, index of refraction n and the extinction coefficient k, of an isotropic material correspond to the real and imaginary components of the complex index of refraction $N = n - ik$. At a given wavelength they may be obtained by direct methods or inferred from photometric or polarimetric measurements. A number of methods [11-15] exist for extracting n and k from specular reflectance measurements at both normal and oblique incidence. Humphreys-Owen [15] lists nine methods by which n and k can be deduced from reflectance measurements at oblique incidence. These methods are divided into two classes: (1) two reflectance measurements at one angle of incidence or one reflectance measurement at each of two angles of incidence, and (2) one reflectance measurement at any angle of incidence

and measurement of a special angle of incidence satisfying certain specific conditions.

In the work reported here, using the tunable polarized output of a cw dye laser to provide the collimated monochromatic beam, surface reflections measurements vs angle of incidence, at different temperature, at the planar interface of Rhodamine B solution in ethanol and air were made at differen temperatures. Then, optical properties of Rhodamine B in ethanol, for differen temperatures, were extracted from the measured reflectance data. From the minimum reflectivity of parallel polarized light Rp,min(l), at the Pseudo-Brewster angle fpB (l), the optical constants n(l) and k(l) are calculated (method 4 of class two of Ref. 16).

To compare the experimental results with theory, the Fresnel reflectivity equations [16] combined with the Kramers-Kronig relations [17] were used to predict the reflectance in terms of the known absorption coefficient, angle of incidience, and the wavelength.

In this section, the Fresnel reflectivity equation for the P-polarized beam (r_p) is expressed in a simple form and used to relate the intensity (or power) reflectance of a monochromatic collimated light beam at the planar interface between a transparent medium of incidence (usually air, $\varepsilon_0 = 1$) and an absorbing medium of refraction (ε_1 complex) in terms of the absorption coefficient (α) of the medium, the real part (n) of

the complex refractive index of the absorbing medium, the angle of incidence (ϕ), and the wavelength of the incident beam.

Then, using the Kramers-Kronig relationships, an analytical expression for the real part of the complex refractive index is obtained in terms of the absorption coefficient (i.e. the imaginary part of the complex refractive index of the absorbing medium). This result is then combined with the general reflectance expression of step 1, to predict the reflectance of an absorbing medium at any given wavelength, solely in terms of the absorption coefficient of the medium at that wavelength and the angle of incidence.

5.2.2 REFLECTANCE IN TERMS OF n and a

The reflection of a collimated light beam is governed by the Fresnel coefficients [20]

$$r_p = \frac{\epsilon \cos\phi - (\epsilon - \sin^2\phi)^{1/2}}{\epsilon \cos\phi + (\epsilon - \sin^2\phi)^{1/2}}$$

$$r_s = \frac{\cos\phi - (\epsilon - \sin^2\phi)^{1/2}}{\cos\phi + (\epsilon - \sin^2\phi)^{1/2}} \qquad (5.2.1)$$

where p and s identify the linear polarizations parallel and perpendicular to the plane of incidence, respectively. ϕ is angle of incidence, and $\varepsilon = \varepsilon_1 / \varepsilon_0$ is the complex ratio of dielectric constants of the two media defined as:

$$\varepsilon = \varepsilon' + j\varepsilon'' \qquad (5.2.2)$$

and rewritten for algeberiac convenience as:

$$\varepsilon = a+jb$$

using the following abbreviations:

$$Q = a - \sin^2 \phi, \qquad |U| = (Q^2 + b^2)^{1/2},$$

$$\theta = \tan^{-1}(b/Q) \qquad Z = \sqrt{|U|} / \cos \phi$$

the reflectance for the P polarized beam, $\Re_p = r_p \dot{r}_p$, can be expressed in the form:

$$\Re_p = \frac{a^2 + b^2 + Z^2 - 2|Z\{a\cos(\theta/2) + b\sin(\theta/2)\}|}{a^2 + b^2 + Z^2 + 2|Z\{a\cos(\theta/2) + b\sin(\theta/2)\}|} \qquad (5.2.3)$$

We next relate the real and imaginary quantities, a and b, to the absorption coefficient of the medium. The complex refractive index , N, is defined by: N = n + jk, where the imaginary part, k, is related to the absorption coefficient, α by:

$$k = \frac{c}{2\omega}\alpha(\omega) \qquad (5.2.4)$$

where c is the speed of light in free space and ω is the angular frequency.

The complex refractive index, N, is also related to the dielectric constant of the medium by the relation:

$$N^2 = \varepsilon = \{n^2 - k^2\} + j2nk = a + jb \qquad (5.2.5)$$

combining Eqs. (5.2.2), (5.2.4) and (5.2.5) gives:

$$a = n^2 - \frac{c^2}{4\omega^2}\alpha^2(\omega) \qquad b = n\frac{c}{\omega}\alpha(\omega) \qquad (5.2.6)$$

This means that all the terms in Eq (5.2.3) are now available in terms of n and α (as well as ω, c, and ϕ).

5.3 REFLECTANCE IN TERMS OF α

We now turn to the second part of the problem to find $n(\omega)$ in terms of the absorption coefficient $\{\alpha(\omega)\}$, so that the solution of Eq.(5.2.3) can be obtained in terms of the absorption coefficient only.

Since the imaginary part $\{k(\omega)\}$ of the complex refractive index is given by Eq. (5.2.4) in terms of α and ω, using the Kramers-Kronig relations, the real part $\{n(\omega)\}$ can also be determined in terms of α and ω within an arbitrary constant (n_1) which can be determined from the specific physical conditions. The Kramers-Kronig relation for the real part $n(\omega)$ is given by [22]:

$$n(\omega') = n_1 + \frac{1}{\pi} P.V. \int_{-\infty}^{\infty} \frac{k(\omega)}{(\omega - \omega')} d\omega \qquad (5.3.1)$$

where P.V. means the Cauchy principal value. It is important to stress the generality of the relation of Eq. (5.3.1). It requires only boundedness and causality [23]. These conditions are necessarily fulfilled by virtue of the fact that the polarization of a wave cannot antecede the arrival of the disturbing electric field that produces it [24].

Rewriting Eq. (5.3.1) in terms of α (Eq. 5.3.4) gives:

$$n(\omega') = n_1 + \frac{c}{2\pi} P.V. \int_{-\infty}^{\infty} \frac{\alpha(\omega)}{\omega(\omega - \omega')} d\omega \qquad (5.3.2)$$

To obtain reflectance in the vicinity of the absorption resonance, using Eq. (5.2.3), it is first necessary to evaluate the integration of Eq. (5.3.2) over the spectral range of interest, and then substitute the results into Eq. (5.2.3). To evaluate the integration in Eq. (5.3.2), two posibble approaches could be used. The first would be to carry out a numerical integration using the actual measured absorption lineshape (Fig. 5.3.1).

The second approach is to assume a Lorentzian approximation for the absorption lineshape in the vicinity of the peak, and to analytically integrate Eq. 5.3.2 to get an analytical expression for $n(\omega)$. For this approach, we assume a

Lorentzian function for the absorption coefficient $\alpha(\omega)$, given by:

$$\alpha(\omega) = \frac{\alpha(\omega_0)\gamma^2}{(\omega - \omega_0)^2 + \gamma^2} \tag{5.3.3}$$

where:

$\gamma = (\Delta\omega / 2)$, and $\alpha(\omega_0)$ is the absorption coefficient at resonance Substituting Eq. (5.3.3) into Eq. (5.3.2) and carring out the integration we get (see appendix):

$$n(\omega) = n_1 + \left\{ \frac{c(\omega_0^2 - \omega\omega_0 - \gamma^2)}{2\gamma(\omega_0^2 + \gamma^2)} \right\} \alpha(\omega) \tag{5.3.4}$$

At this point, it should be noted that as long as $\Delta\omega << \omega_0$, the evaluation of the integral in Eq. (5.3.2), depends primairly on the absorption and hence dispersion in the immediate vicinity of the resonance center. The successful use of the Kramers-Kronig relations, depends, in their contest, in the fact that negligible error results from a lack of knowledge of frequency spectrum remote from the point of interest (in our case, outside the vicinity of resonance frquency) [25]. To integrate Eq. 5.3.2 using the Lorentzian approximation, we use actual measured values for magnitude of peak absorption, $\alpha(\omega_0)$, peak

frequency, ω_0, and the linewidth, 2γ. Since in the vicinity of resonance, the actual absorption line shape is almost Lorentzian, one is led to the conclusion that the use of a Lorentzian lineshape in Eq. (5.3.2) can be expected to give almost the same results as the numerical integration in the vicinity of resonance.

For the Lorentzian approximation, combining Eqs. (5.2.6) and (5.3.4) into Eq. (5.2.3) gives the final expression for reflectance for any absorbing medium in terms of basic information about its absorption coefficient. This expression is Eq. (5.2.3), repeated here for convenience:

$$\Re_p = \frac{a^2 + b^2 + Z^2 - 2|Z\{a\cos(\theta/2) + b\sin(\theta/2)\}|}{a^2 + b^2 + Z^2 + 2|Z\{a\cos(\theta/2) + b\sin(\theta/2)\}|} \qquad (5.2.3)$$

where however, now

$$a = \left\{ n_1 + \left[\frac{c(\omega_0^2 - \omega\omega_0 - \gamma^2)}{2\gamma(\omega_0^2 + \gamma^2)} \right] \alpha(\omega) \right\}^2 - \left\{ \frac{c^2}{4\omega^2} \alpha^2(\omega) \right\}$$

$$b = \left\{ n_1 + \left[\frac{c(\omega_0^2 - \omega\omega_0 - \gamma^2)}{2\gamma(\omega_0^2 + \gamma^2)} \right] \alpha(\omega) \right\} \frac{c}{\omega} \alpha(\omega)$$

and Z and θ are as previously defined in terms of a, b and ϕ.

Predictions for reflectance using the actual absorption lineshape (numerical integration) and the Lorentzian approximation are compared with each other and with experimental measurements, in the following section.

5.3.1 EXPERIMENTAL

The solution of Rhodamine B in ethanol was selected as the lossy refractive medium from which reflections of collimated light beams are measured at the air medium interface. Rhodamine B was selected because it has a well defined absorption resonance in the green-yellow spectral region (Fig.5.3.1) which is readily accessible to the cw organic dye laser used to provide the tunable collimated light beam. Furthermore, the absorption spectrum, in the vicinity of the resonance, is reasonably close to the Lorentzian shape assumed in Section 2 above to facilitate the evaluation and the numerical calculations needed to make theoretical predictions (see comparison in Fig. 5.3.1). Actually measured values for magnitude of peak absorption, peak wavelength, and the linewidth, were those used in the Lorentzian approximation to evaluate theoretical expressions.

The actual experimental set up is relatively staight forward. A polarized collimated light beam is obtained from a tunable cw dye laser. By appropriate geometric arrangements of mirrors, the angle of incidence of the laser beam on the dye solution surface can be varied, and the incident and reflected powers at the dye-air interface measured using pv detectors.

To increase sensitivity and accuracy, a phase lock loop amplifier was used in conjunction with the detectors. Measurements and comparisons with theoretical predictions were made for the "p" polarized ray only, since results for the "s" polarization are expected to differ only in some details, that would not be expected to add to the understanding of the process or the confirmation of the models used.

5.4 COMPARISONS OF THEORETICAL PREDICTIONS AND EXPERIMENTAL RESULTS

The following parameters were measured, at room temperature, experimentally and used in theoretical calculations:

i) an absorption peak (λ_o) at 552 nm,

ii) a line width ($\Delta\lambda$) of approximately 40 nm,

iii) a peak absorption coefficient, α (ω_o) of 5 x 10^4 cm^{-1}.

The arbitrary constant (n_1) in Eq. (5.5.4) is assigned a value of 1.364, which is the refractive index of the solvent (ethanol) used in our experiment. This is understood by assuming a zero value to the absorption coefficient (α) in Eq. (5.3.4), thus the medium is now lossless and its refractive index is reduced to the refractive index of the transparent solvent. Experimental results and their theoretical comparisons at room temperature are divided into three different sets.

SET I

Experimental measurements were carried out to determine and measure the reflectance as a function of wavelength at three different angles, 29°, 54°, and 75° respectively. As will be seen later, the significance of choosing the angle 54° is that this is the angle of minimum reflection, or Pseudo-Brewster angle (PB), at the resonance frequency. It is also close to the theoretically calculated and experimentally measured value of Brewster's angle for the ethanol solvent alone.

Figs. 5.4.1, 5.4.2, and 5.4.3 show the experimental results along with theoretical predictions. The theoretical predictions are made:

(i) using the Lorentzian approximation evaluated with actual measured values for magnitude of peak absorption, peak wavelength, and the linewidth, and

(ii) by carring out numerical integrations using the actual absorption line shape.

The theoretical predictions are carried out and compared with each other and with the experimental results of this set in Figs. 5.4.1, 5.4.2, and 5.43. These comparisons show a good agreement between the Lorentzian approximation and the numerical integration using the actual absorption line shape.

Off resonance, where the difference between the Lorentzian line shape and the actual line shape is clear, α has a small value, and R_p values are in general less sensitive to variations in α. In order to more readily appreciate the relationship between the absorption and the reflectance curves, the theoretically assumed (Lorentzian) absorption spectrum is also shown, with, however, the same peak and linewidth as are measured experimentally.

When the angle of incidence is 29^o, the maxima for the reflectance is shifted towards longer wavelengths, when it is 75^o the maxima for the reflectance is shifted towards shorter wavelengths, while there is no shift at all when the angle of incidence is 54^o (PB angle at resonance). It is also interesting that the closest fit between theoretical predictions and experimental results is obtained when the angle of incidence is the PB angle at resonance.

With the reasonableness of the Lorentzian approximation thus established, the remaining figures show only theoretical predictions based on the Lorentzian approximation, along with results of experimental measurements.

SET II

Theoretical predictions using the Lorentzian approximation and experimental measurements were carried out to predict and measure the reflectance as a function of the

angle of incidence for three different wavelengths, 514 nm, 552 nm, and 580 nm respectively. Figs. 5.4.4 and 5.4.5 show the theoretical predictions and the corresponding experimental measurements for the reflectance (R_p) vs. the angle of incidence (ϕ) at these wavelengths respectively. It is seen that there is no angle which corresponds to exactly zero reflection. The angle at which R_p has a minimum value is called the Pseudo-Brewster (PB) angle.

From Fig. 5.4.4 (theoretical result), we have: at λ= 514 nm, ϕ_{pB}(incident angle of minimum reflectance) = 50^o , and the corresponding reflectance Rp = 0.0005. At λ= 552 nm, $\phi_{pB} = 53.7^o$, and Rp = 0.01. At λ = 580 nm, ϕ_{pB} = 57.5^o, and Rp = 0.001.

Again, there is reasonably good agreement between theoretical predictions and experimental results (Fig. 5.4.7) particularly at the resonance wavelength (552 nm). Fig. 5.4.4 is redrawn in Fig. 5.4.6, with a different scale, to more readily distinguish between the data.

SET III

Theoretical predictions again using the Lorentzian approximation and experimental measurements were carried out to predict and measure the Pseudo- Brewster angles and the reflectance corresponding to these angles vs. λ. It would

be emphasized that, for any given λ, the PB angles were not determined by setting R_p in Eq. (5.4.2) equal to zero and then finding the corresponding angle, since such a solution does not exist. Instead, for a given λ, R_p was calculated for all ϕ's from $\phi = 0 - 90^{o}$, with increments of 0.01^{o}, and the angle with corresponding to the minimum reflectance is considered as the PB angle for that λ.

Fig. 5.4.7 shows the theoretical predictions and the experimental measurements for ϕ_{pB} vs. λ. Fig. 5.4.8 shows the theoretical predictions and the experimental measurements for reflectance at the PB angles vs. λ, showing a good fit between experimental and theoretical results and with the reflectance at the PB angles tracking the absorption.

5.5 Temperature effects on reflectivity

The experimental setup for measuring reflection intensity both at room temperatue and as the temperature of the dye solution reduced are shown in Fig. 5.5.1 and 5.5.2, respectivelly. As the temperature of the absorbing medium(Rhodamine B dye solution) reduced, the reflection intensity increased.

5.6 Optical Constants of Rhodamine B in Alcoholic Solutions at different Temperatures.

5.6.1 INTRODUCTION

The optical properties, index of refraction n and the absorption coefficient k, of an isotropic material correspond to the real and imaginary components of the complex index of refraction N = n - ik. At a given wavelength they may be obtained by direct methods or inferred from photometric or polarimetric measurements. A number of methods [13-17] exist for extracting n and k from specular reflectance measurements at both normal and oblique incidence. Humphreys-Owen [17] lists nine methods by which n and k can be deduced from reflectance measurements at oblique incidence. These methods are divided into two classes: (1) two reflectance measurements at one angle of incidence or one reflectance measurement at each of two angles of incidence, and (2) one reflectance measurement at any angle of incidence and measurement of a special angle of incidence satisfying certain specific conditions.

It is well known that organic Rhdomaine dye solutions are used in different solvents as active media for tunable dye lasers. Therefore, their optical properties are of obvious scientific and practical interest. Numerous studies [18-24] have shown that lasing characteristics are sensetive to variations in temperature. The correct choice of solvent and

optimal temperature of the solutions of organic dyes therefore have opened the feasibility of improving laser characteristics. In fact, Significant improvements in the performance of some dye lasers [20-22] have been reported as the solvent temperature was reduced below room temperature, namely: a significant reduction in the threshold power requirements and a considerable increase in the attainable output power. Recently [25], we have conducted a theoretical and experimental investigations of the optical properties for a highly concentrated ethanolic solution of Rhodamine B at room temperature. Given the importance of cooling, the solutions of organic dyes, when used as a lasing media, on their lasing characteristics, it appears timely to examine the optical properties of organic dye solutions as the solvent temperature is reduced below room temperature.

In the work reported here, the optical constants for a highly concentrated solution of Rhodamine B in ethanol, at various temperatures (23, -5, -20, and -60oc), were determined by measuring the reflectivity of parallel polarized light at the Pseudo-Brewster angle (method 4 ,class two of Ref. 5). From these reflectivity measurements both optical constants, n and k, are determined.

The absorption spectra at low concentration (2 x 10-5 m/l) were also measured (transmission measurements in cells of known thickness with a spectromete) and compared with those at high concentration. It was found out that, at high

concentration, the absorption spectra are concentration dependent. These deviations, which are more pronounced as the solvent temperature is reduced, are thought to be caused mainly due to the formation of dimers or high aggregates [26-29]. In general dyes dissolve in monomers, dimers, trimers, etc. Dimers are formed by the reaction: $M + M \rightarrow D$, and timers are formed by the reaction: $M + D \rightarrow T$. At low concentrations monomers dominates. With increasing concentrations dimers and higher aggregates may gain importace. Each component (monomer, dimer, etc.) may have a different absorption behavior. At high concentrations the constituting components (monomers, dimers, etc.) of the solution come near together and if two neighbouring components are within an interaction volume [29], the mutual solute-solute interaction changes the absorption behavior.

There is an increase in the fluorescence quantum yield with reduction in temperature [30]. This shows that when dilute Rhodamine B solutions in ethanol are cooled their non-luminescent associates are not formed [30-31]. As already have been reported by the authors [32], this turns out to be of considerable practical implications, when Rhodamine B solutions are used as a lasing media under laser excitation.

5.6.2. EXPERIMENTAL: RESULTS AND ANALYSIS

A polarized collimated light beam is obtained from a tunable cw dye laser. By appropriate geometric arrangements of mirrors, the angle of incidence of the laser beam on the dye solution surface can be varied, and the incident and reflected powers at the dye-air interface measured using pv detectors. To increase sensitivity and accuracy, a phase lock loop amplifier was used in conjunction with the detectors. Rhodamine B was selected because it has a well defined absorption resonance in the green-yellow spectral region which is readily accessible to the cw organic dye laser used to provide the tunable collimated light beam.

The measured absorption spectra at low concentrations (2 x 10-5 m/l) of Rhodamine B solution in ethanol are shown in Fig. 5.6.1 for 23, -5, -20, and -60oc solvent temperature. There is practically no change in the absorption spectra, indicating weak dimer formation (dimer binding energy is small compared to thermal energy). The observed increase in the fluorescence quantum yield for dilute Rhodamine B solutions in ethanol with reduction in temperature [30], is a further indication that non-luminescent associates are not formed [30-31].

The measured minimum parallel reflectivity Rp,min(fpB), and the corresponding Pseudo-Brewster angle fpB are shown in Figs. 5.6.2 and 5.6.3, respectively, for 0.45 moles/liter

conentrations of Rhodamine B in ethanol, at various temperatures, 23oc, -5oc, -20oc, and -60oc. The optical constants n and k are calculated [17] and the results are shown in Figs. 5.6.4 and 5.6.5. for the spectral range of interest. As shown in fig. 5.6.5, the depicted So-S1 absorption bands clearly change with temperatute, and with further cooling, a considerable deformations of their electronic absorption spectra occur. The appearance of a secondary short-wavelength absorption maxima, which are more pronounced at lower temperatures, are indicative of the formation of dimers and perhaps high aggregates [26-29]. It can also be seen that, the lower the temperature, the higher the absorption capacity of the solutions, compared with absorption capacity of dilute solutions (Fig. 5.6.1).

In conclusion, the optical constants n and k of 0.45 moles/liter conentrations of an organic dye, Rhodamine B in ethanol, are determined by measuring the minimum parallel reflectivity Rp,min(fpB), and the corresponding Pseudo-Brewster angle fpB at the dye-air interface, at various temperatures, 23oc, -5oc, -20oc, and -60oc. The absorption spectra at low concentration (2 x 10-5 m/l) were also measured and compared with those at high concentration. It was foud out that, at high concentration, the absorption spectra are concentration dependent. These formations, which are more pronounced as the solvent temperature is reduced, are thought to be caused mainly due to the mutual interaction of neighbouring molecules. In other words, at high concentrations,

the lower the temperature, the stronger the tendency of dimer formation (dimer binding energy UB is larger compared to thermal energy KT [33]).

On the other hand, at low concentration, as the temperature is reduced, the absorption spectra indicate weak tendency of dimer formation. The observed increase in the fluorescence quantum yield for dilute Rhodamine B solutions in ethanol with reduction in temperature [31], is a further indication that non-luminescent associates are not formed.

5.7 CONCLUSION

We have reported experimental work on surface reflections measurements at the planar interface of resonantly absorbing medium and the air for a variety of situations. An ethanolic solution of Rhodamine B, an organic laser dye luminofor with a well defined resonance absorption spectrum, was used as the absorbing medium. It was found that the maxima for reflectance coincide with the maxima for absorption when the angle of incidence is equal to the PB angle at resonance frequency. However, the maxima might be shifted to longer or shorter wavelengths depending on the angle of incidence. It was also found that the PB angle at resonance frequency is equal to the Brewster's angle for the solvent (lossless medium).

The Fresnel reflectivity equations combined with the Kramers-Kronig relations were used to predict the reflectance in terms of the known absorption coefficient. Our experimental results generally confirm the theoretical predictions.

5.8 REFERENCES

[1] S.p.f. Humphreys-Owen, Proc. phys. Soc. (London), Vol. 77, PP. 949, (1961).

[2] R. M. A. Azzam and N. M. Bashara, Ellipsometry and Polarized Light, North-Holand, (1977).

[3] R. M. A. Azzam and A. M. El-Saba, Appl. Opt. Vol. 27, No. 19, (1988).

[4] David L. Greenaway and G. Harbeke, Pergamon Press, (1968).

[5] W. R. Hunter, J. Optical Soc. Am. Vol. 55, PP. 1197, (1965).

[6] G. R. Field and E. Murphy, Appl. Opt. Vol. 10, PP. 1402, (1971).

[7] Barry S. Gourary, J. Appl. Phys. Vol. 28, PP. 3, (1957).

[8] R. Carpenter, J. Opt. Soc. Am. Vol. 40, PP> 225-29, (1950).

[9] W. L. Hyde, J. Opt. Soc. Am. Vol. 38, PP. 663, (1948).

[10] G. N. Ramachandran and S. Ramaseshan, J. Opt. Soc. Am. Vol. 42, PP. 49, (1952).

[11] M. Richartz and H. Y. Hsu, J. Opt. Soc. Am. Vol. 39, PP. 136(1949).

[12] H. Hurwitz, Jr. and R. C. jones, J. Opt. Soc. Am. Vol. 31, PP. 493 (1941).

[13] David L. Greenaway and G. Harbeke, Optical properties and band structure of semiconductors, Pergamon press, (1968).

[14] H. R. Philipp and E. A. Taft, Phys. Rev. Vol. 113, PP. 1002 (1959).

[15] Edward D. Palik, Handbook of Optical Constants of Solids, Academic Press, (1985).

[16] D. E. Aspnes, and A. A. Studna, Phys. Rev. B, Vol. 27, PP. 985, (1983).

[17] S. P. F. Humphreys-Owen, Proc. Phys. Soc. (London), Vol. 77, PP. 949 (1961).

[18] V. I. Studenov, and N. G. Bakhshiev. Opt. Spektrosk. Vol. 36, PP. 392, (1974).

[19] V. I. Studenov, I. V. Piterskaya, and N. G. Bakhshiev. Opt. Spektrosk. Vol. 39, PP. 308, (1975).

[20] N. G. Bakhshiev, The Spectroscopy of intermolecular interactions Nauka, Leningrad, (1972).

[21] N. G. Bakshiev, Opt. Spectrosk. Vol. 32, PP. 1151, (1972).

[22] N. G. Bakhshiev, and V. I. Studenov. Opt. Spektrosc. Vol. 33, PP. 62-65 (1972).

[23] V. I. Studenov, and N. G. Bakhshiev. Opt. Spektrosk. Vol. 39, PP. 661-665, October (1975).

[24] N. V. Korol' Kova, and B. M. Uzhinov. Zhurnal prikladnoi Spektroskopii, Vol. 39, No. 3, pp. 406-412, September (1983).

[25] S. A. Ahmed, and M. A. Ali. J. Chem. Phys. Vol. 91, pp. 3838- 3854, October (1989).

[26] C. A. Parker, Photoluminescence of solutions Elsvier, Amsterdam, (1968).

[27] B. Kopainsky, and W. Kaiser. Chem. Phys. Letter Vol. 8, PP. 357, (1982).

[28] I. L. Arbeloa, and P. R. Ojeda. Chem. Phys. Letter Vol. 8, PP. 556, (1982)

[29] Y. Lu and A. Penzkofer. Chem. Phys. Letter, Vol. 107 PP. 175-184, (1986).

[30] L. V. Levshin, T. D. Slavnova, and V. I. Yuzhakov. zhurnal prikladnoi spektroskopii, Vol. 24, No. 6, pp. 985-990, June (1976).

[31] M. Faraggi, and D. Weinraub. Chem. Phys. Letter Vol. 103, PP. 310, (1984).

[32] J. Moghaddasi, M. A. Ali, and S. A. Ahmed. submitted for publication, IEEE, photonics technology letters, December (1989).

[33] L. V. Levshin, and I. S. Lonskaya. Opt. Spectry. Vol. 11 PP. 2043, (1962).

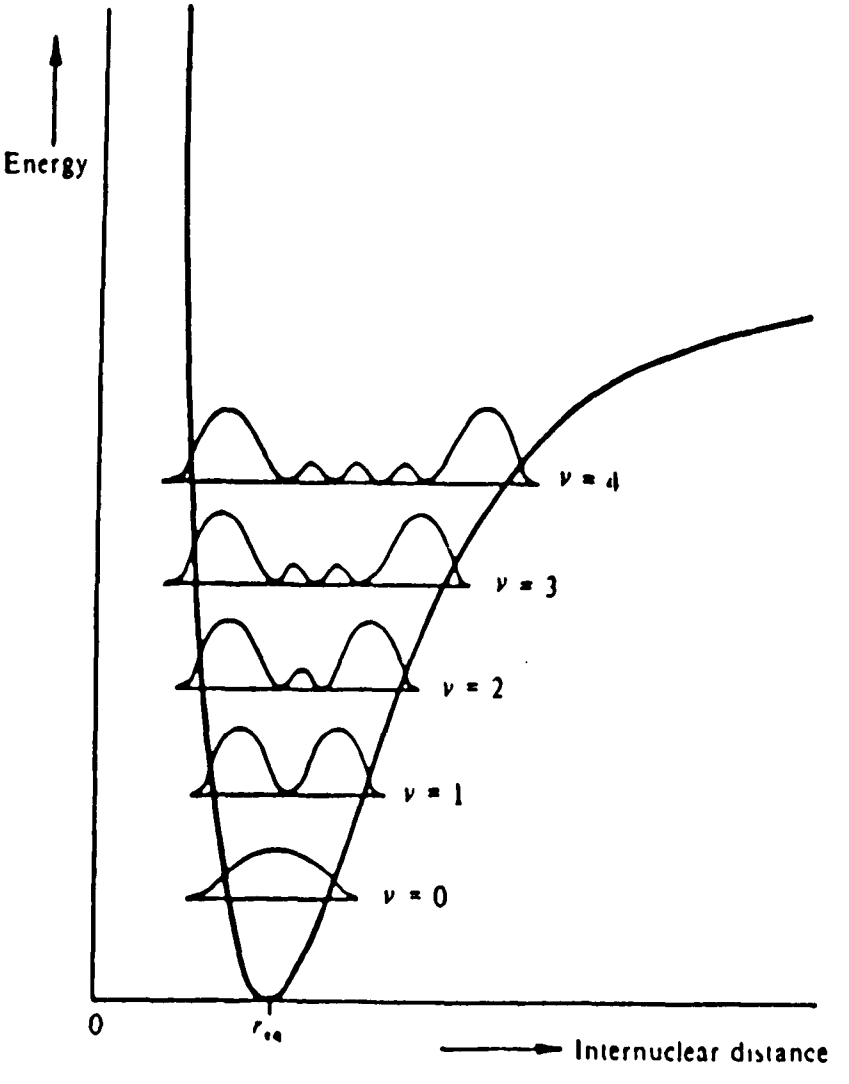

FIGURE 2.1.1 The probability distribution for a diatomic molecule according to the quantum theory. The nuclei are most likely to be found at distances apart given by the maxima of the curve for each vibrational state.

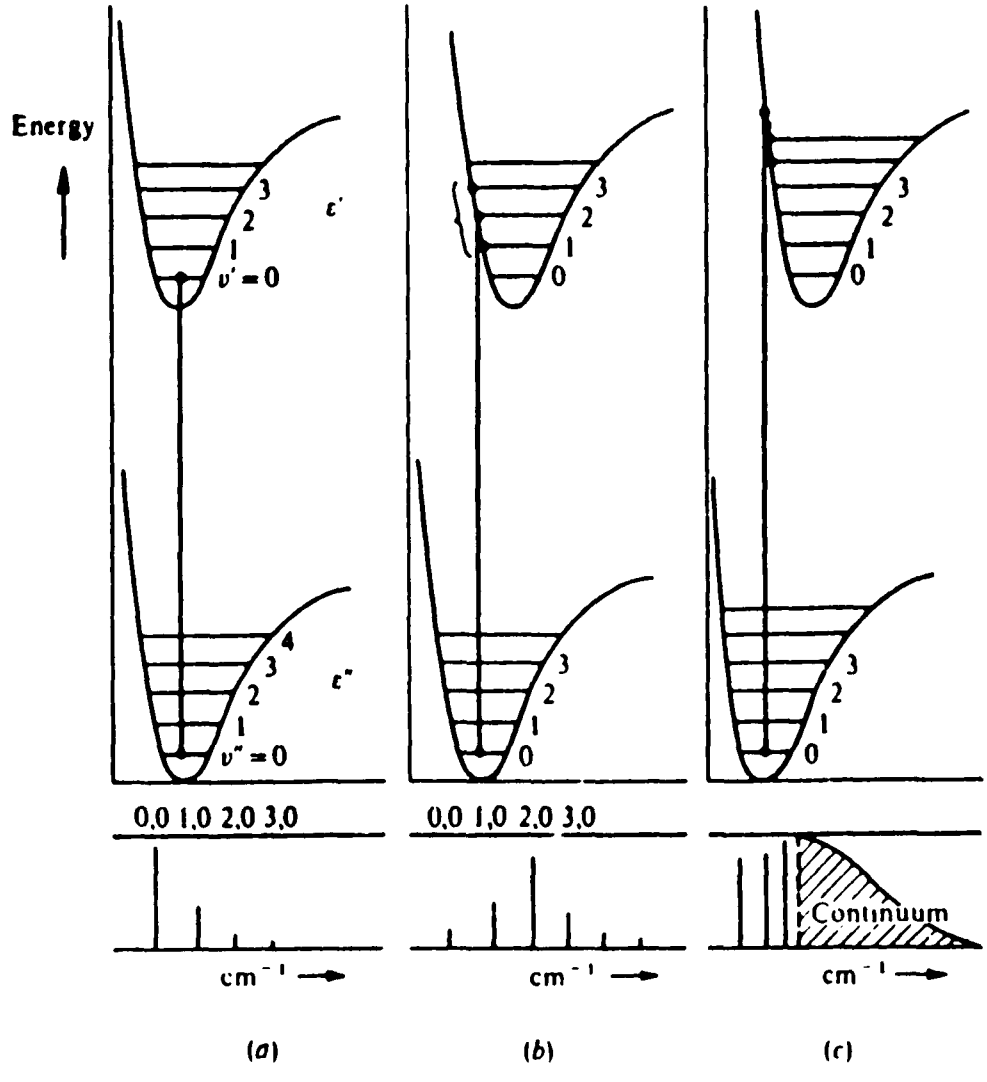

FIGURE 2.1.2 The operation of the Franck-Condon principle for (a) internuclear distances equal in upper and lower states, (b) Upper state internuclear distance a little greater than that in the lower state, and (c) Upper state distance considerably greater.

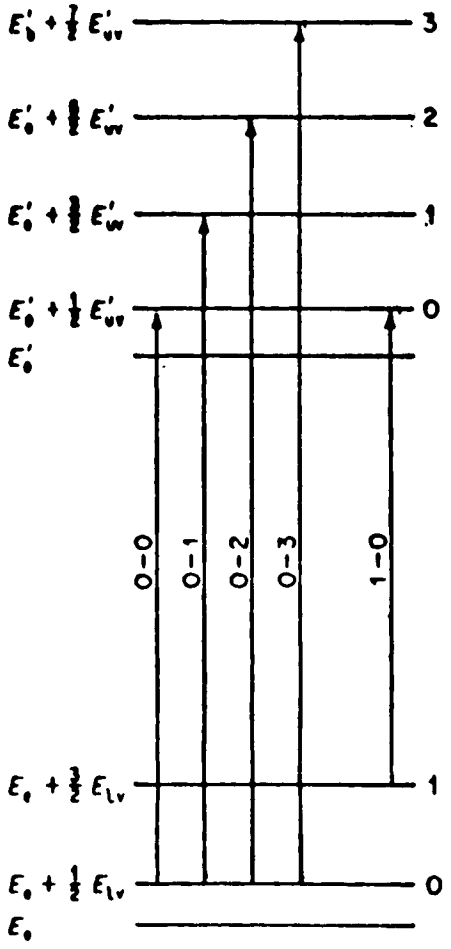

FIGURE 2.2.1 Vibronic absorption transitions.

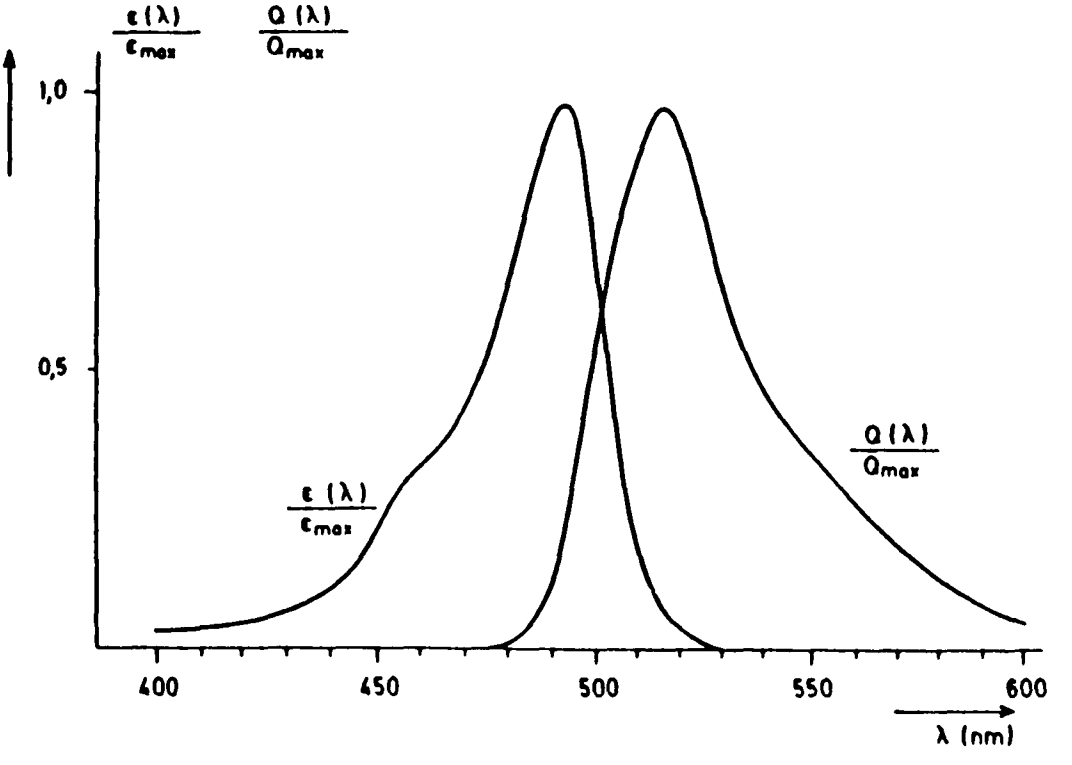

FIGURE 2.2.2 Absorption spectrum, $\varepsilon(\lambda) / \varepsilon_{max}$, and fluorescence spectrum, $Q(\lambda) / Q_{max}$, of a typical dye molecule.

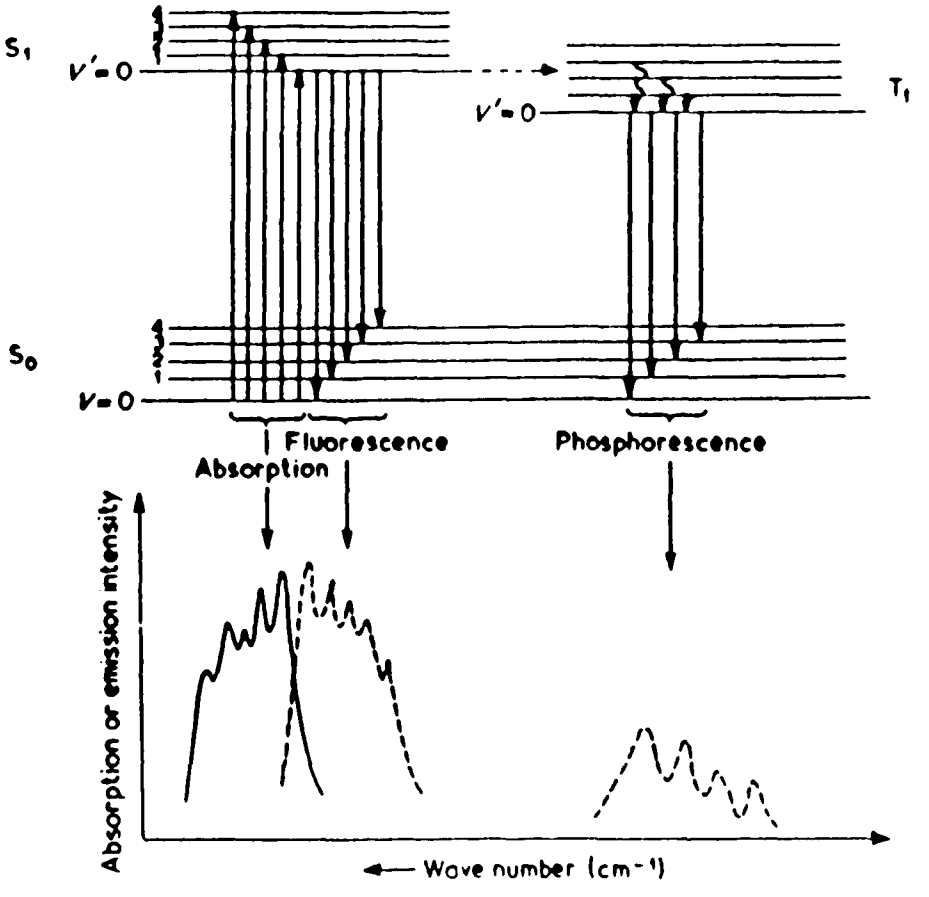

FIGURE 2.2.3 Origin of absorption, fluorescence and phosphorescence spectra.

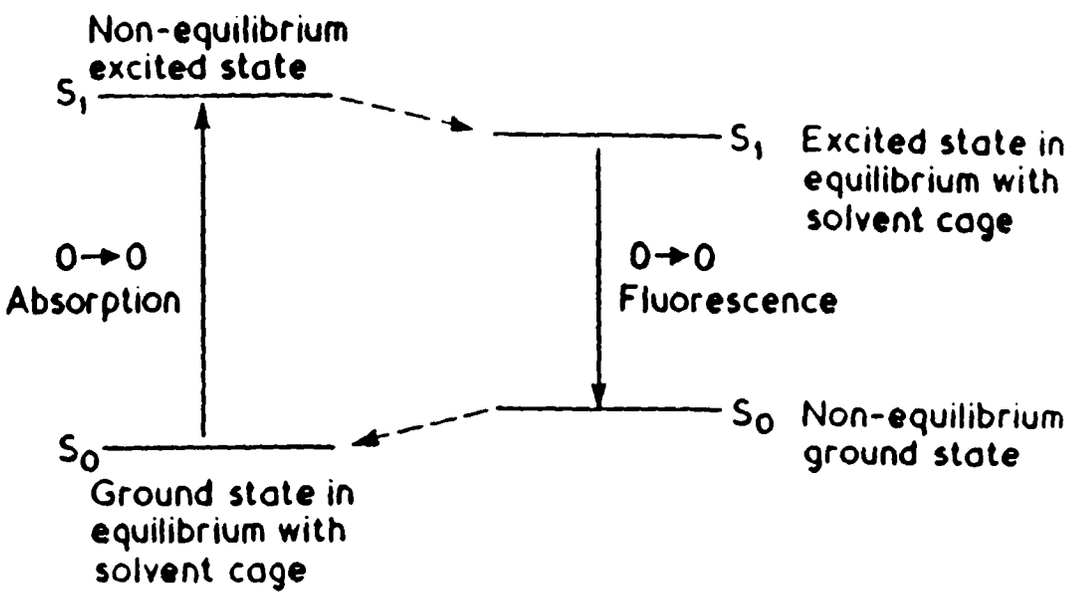

FIGURE 2.2.4 Solvent equilibrium on energy of electronic states.

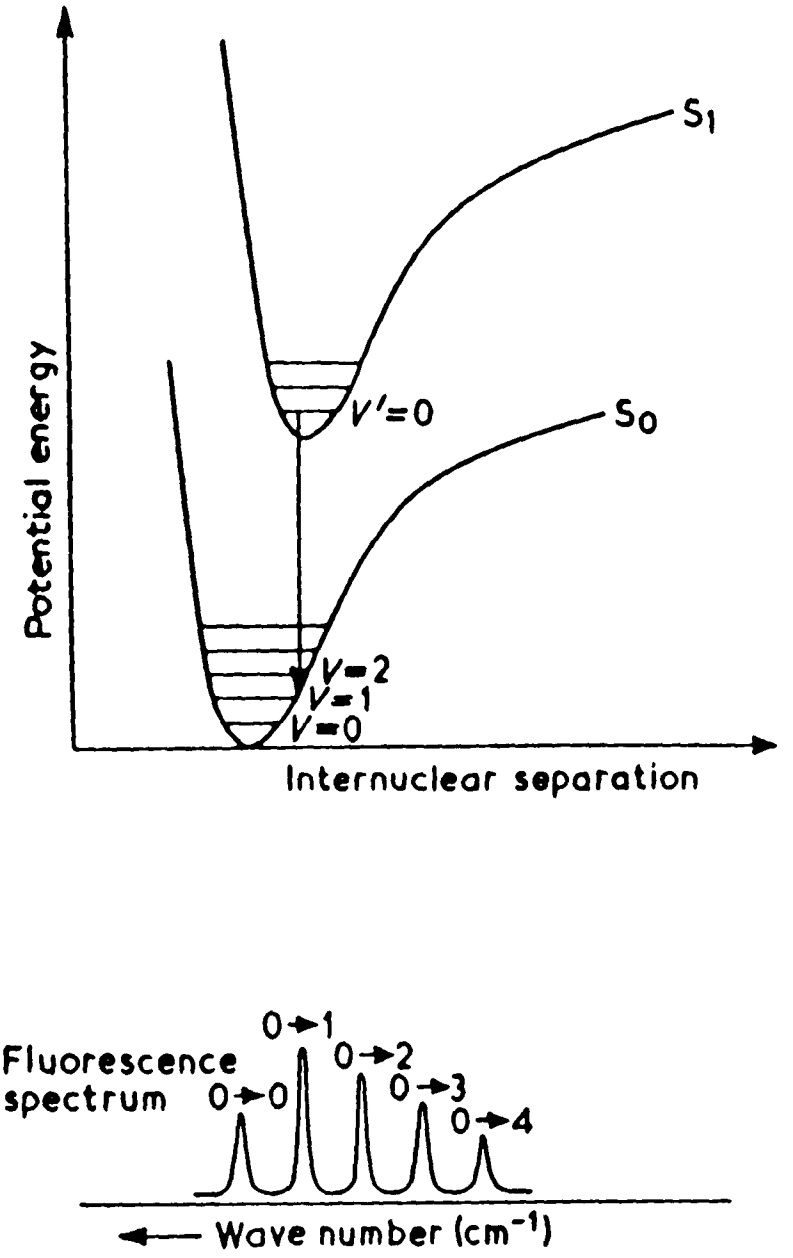

FIGURE 2.2.5 Representation of the fluorescence spectrum of a diatomic molecule showing possible relative intensities of the vibrational bands.

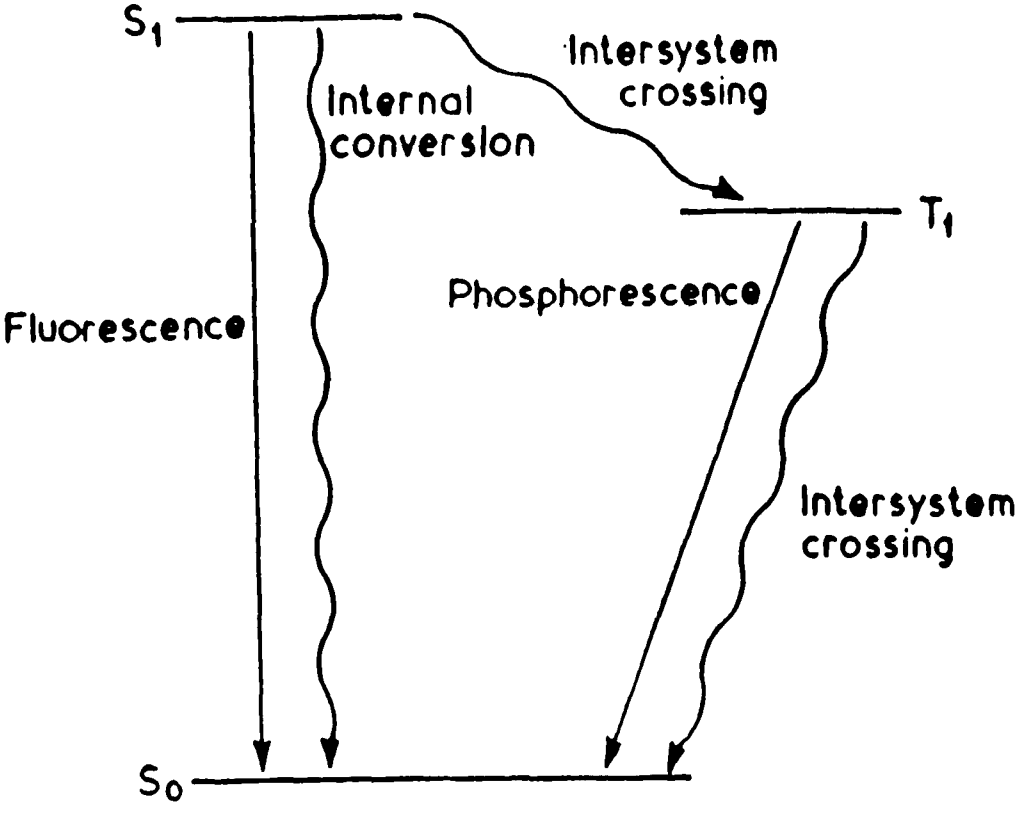

FIGURE 2.2.6 Intramolecular decay processes originating from S_1 and T_1 states.

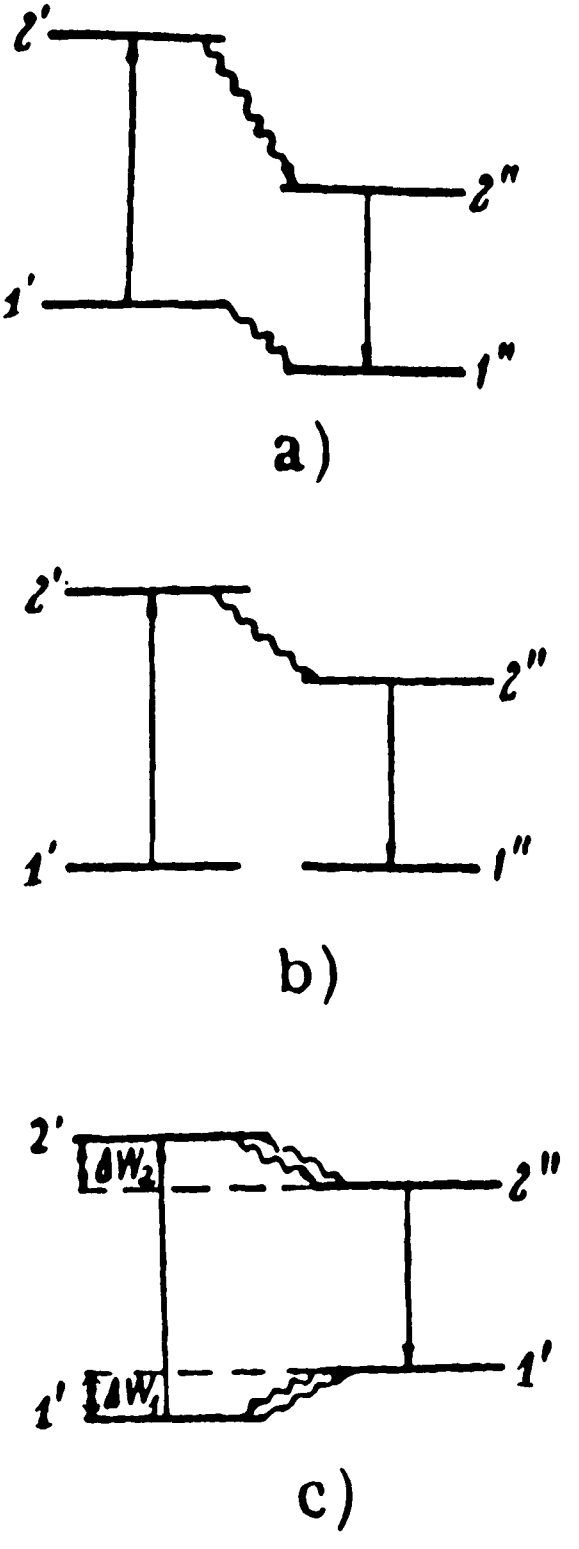

FIGURE 2.3.1 Energy-level scheme for a dipolar molecule in a polar solvent. a) According to Ref. 2,3; b) according to Ref. 6,9; c) energy-level scheme for an elementary cell.

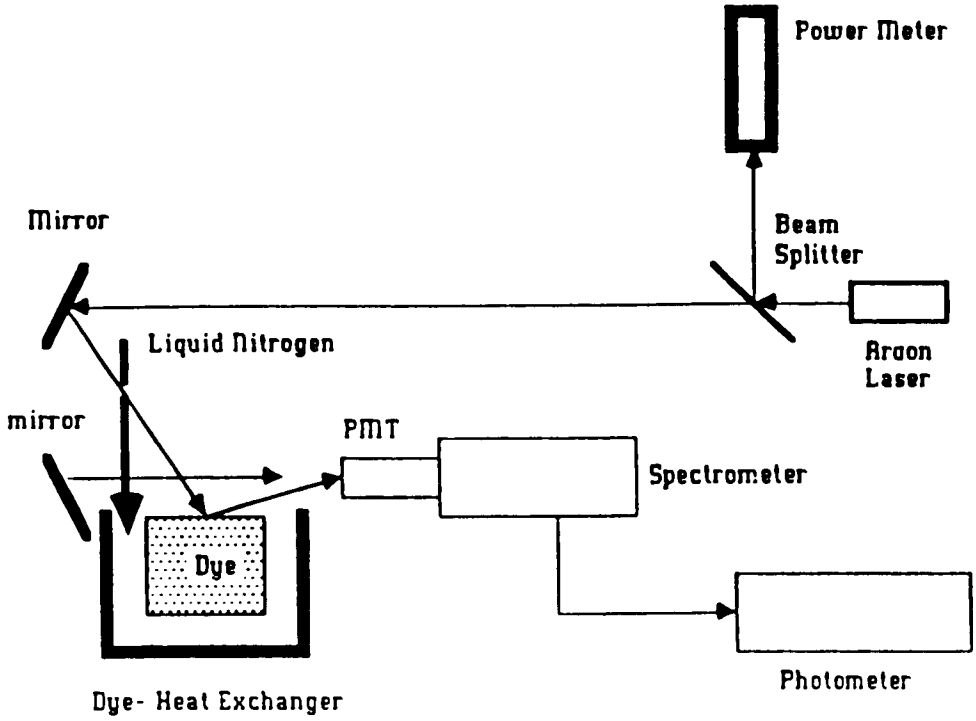

FIGURE 24.1 Experimental setup for fluorescence measurement.

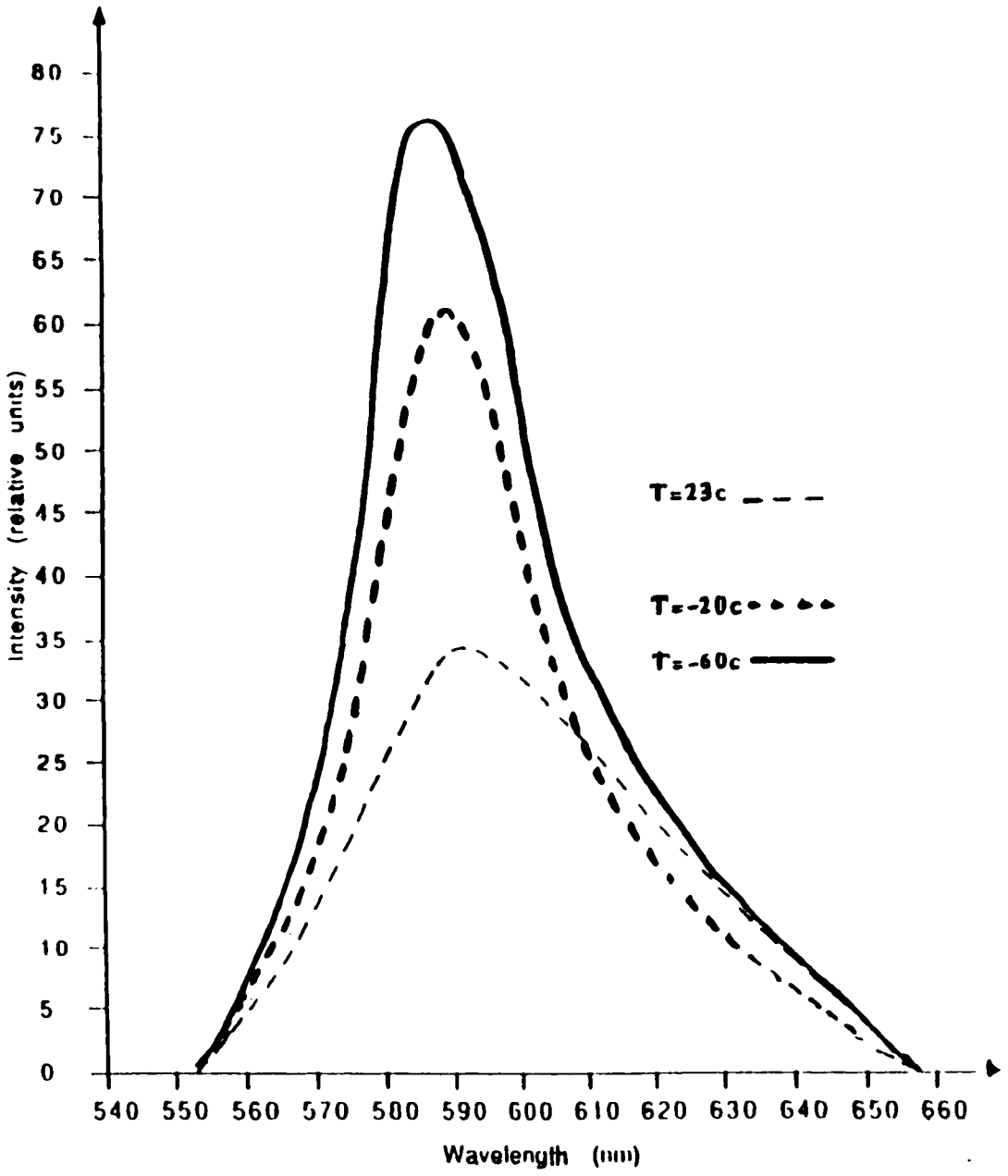

FIG. 2.4.2 Fluorescence spectra of Rhodamine B/ethylalcohol at different temperature

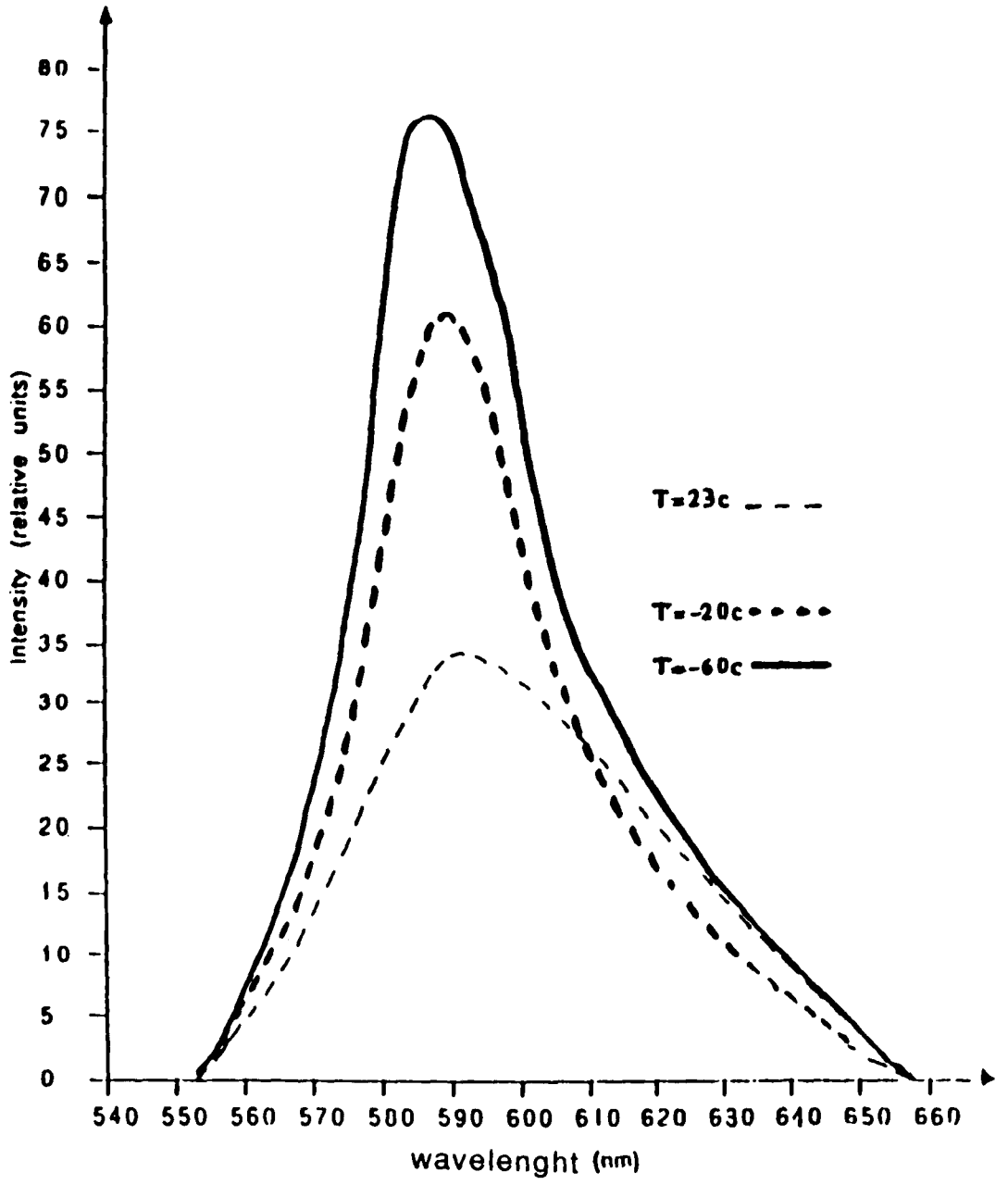

FIG.2.4.3 Fluorescence spectra of Rhodamine B/ethylene glycol at different temperature

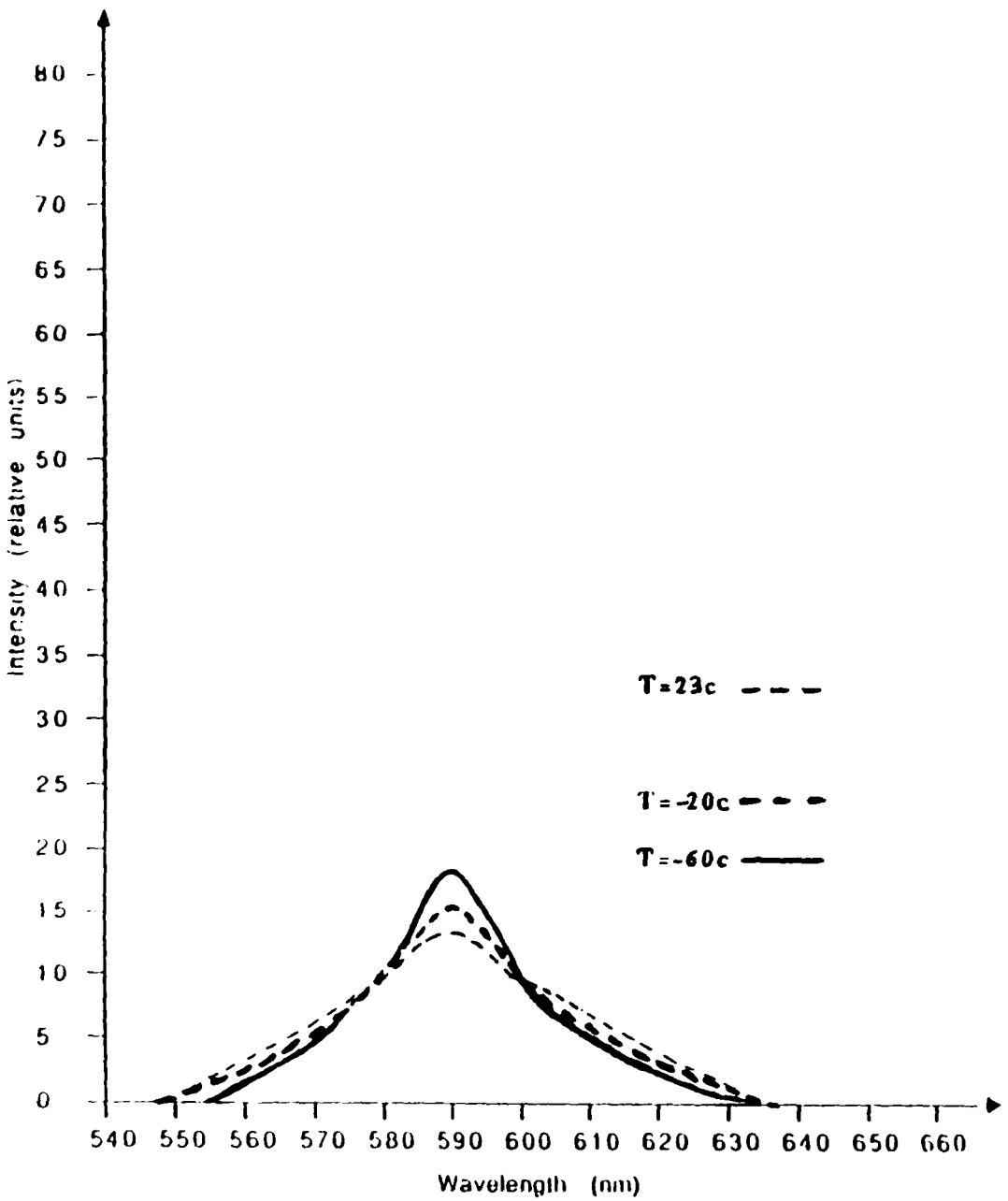

FIG.2.4.4 Fluorescence spectra of RhodamineB/methanol at different temperature

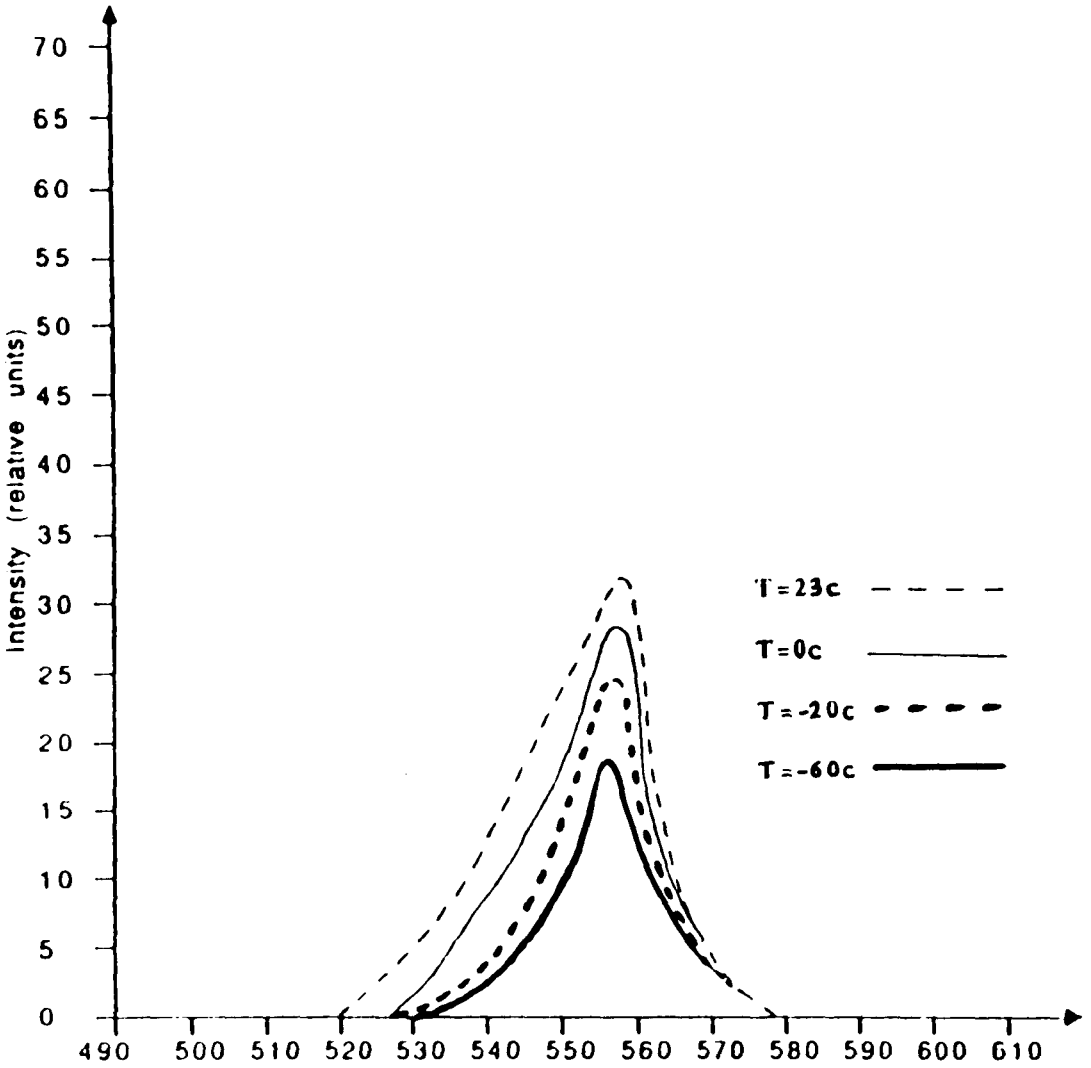

FIG.2.4.5 Fluorescence spectra of Rhodamine 6G/ethylalcohol at different temperature

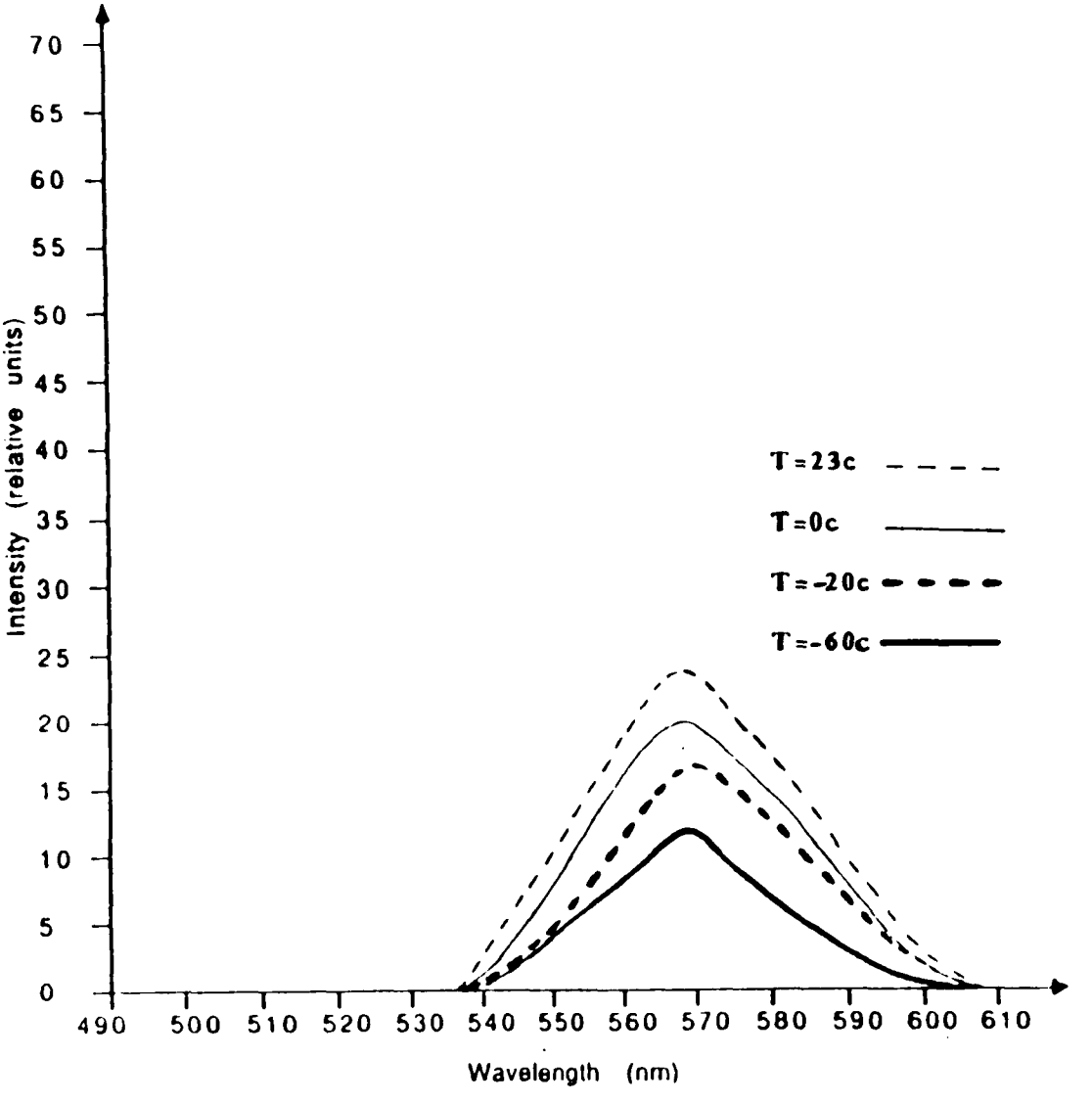

FIG.2.4.6 Fluorescence spectra of Rhodamine 6G/ethylene glycol at different temperature

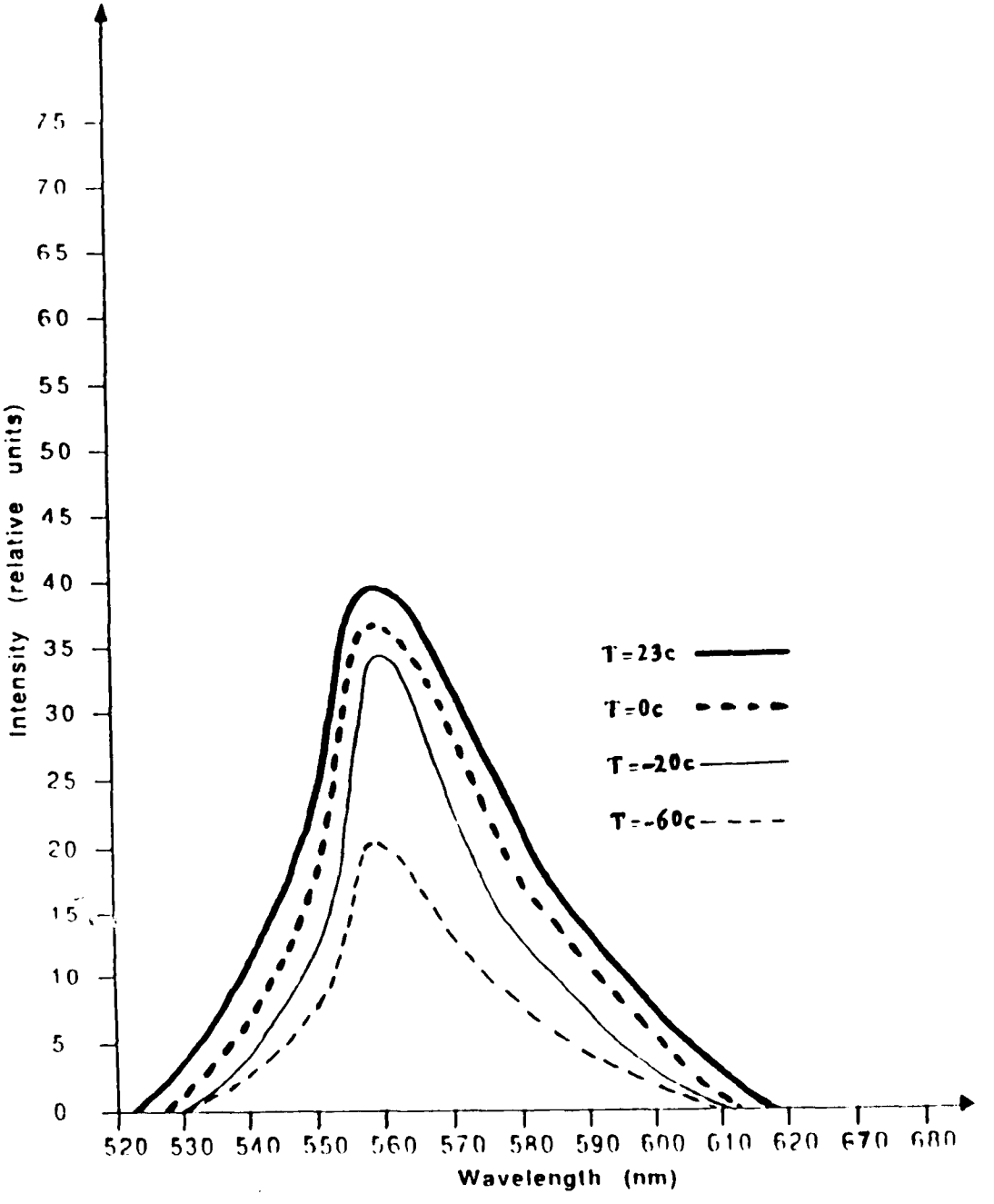

FIG.2.4.7 Fluorescence spectra of Rhodamine 6G/methanol at different temperature

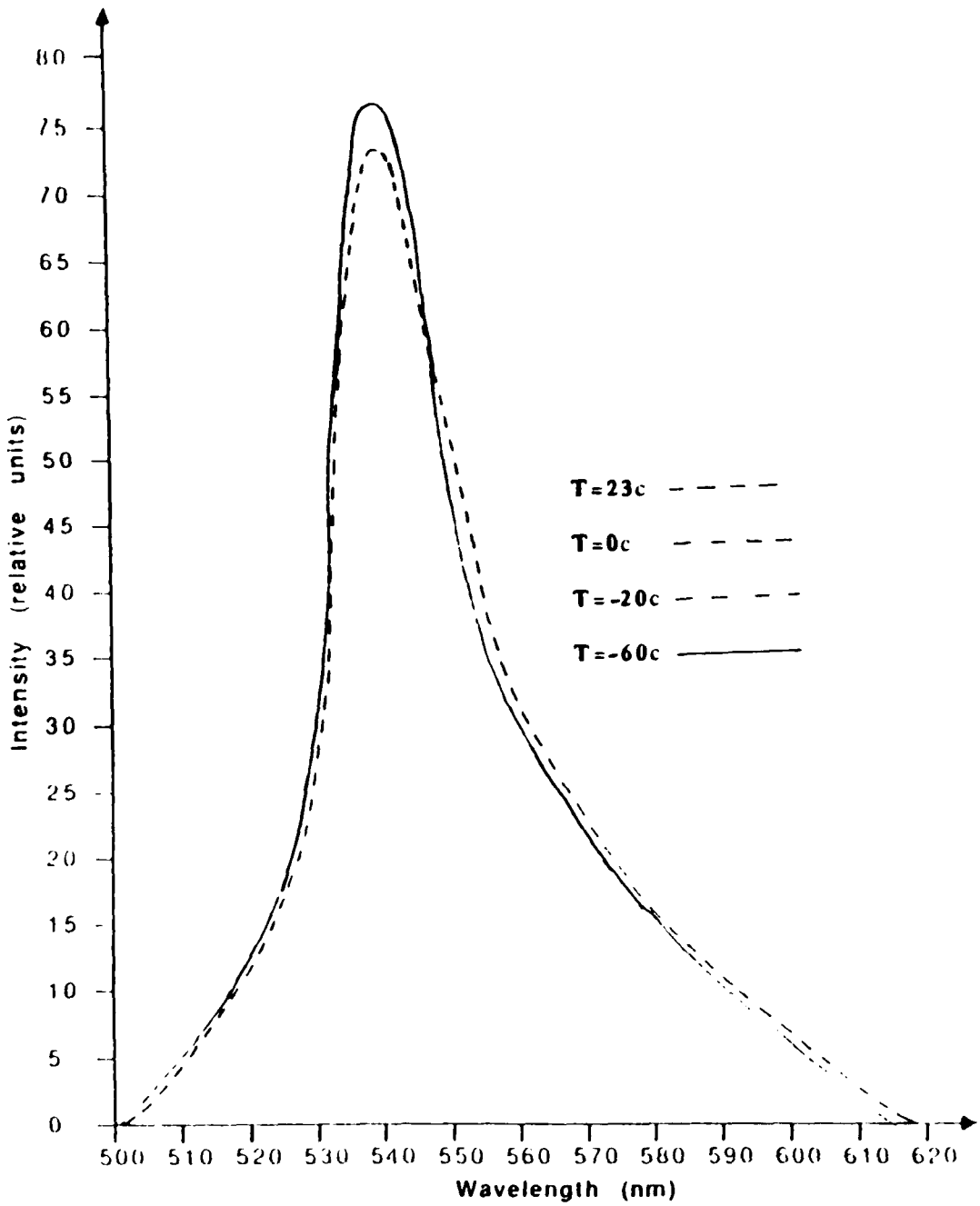

FIG. 2.4.8 Fluorescence spectra of Rhodamine110/ethylalcohol at different temperature

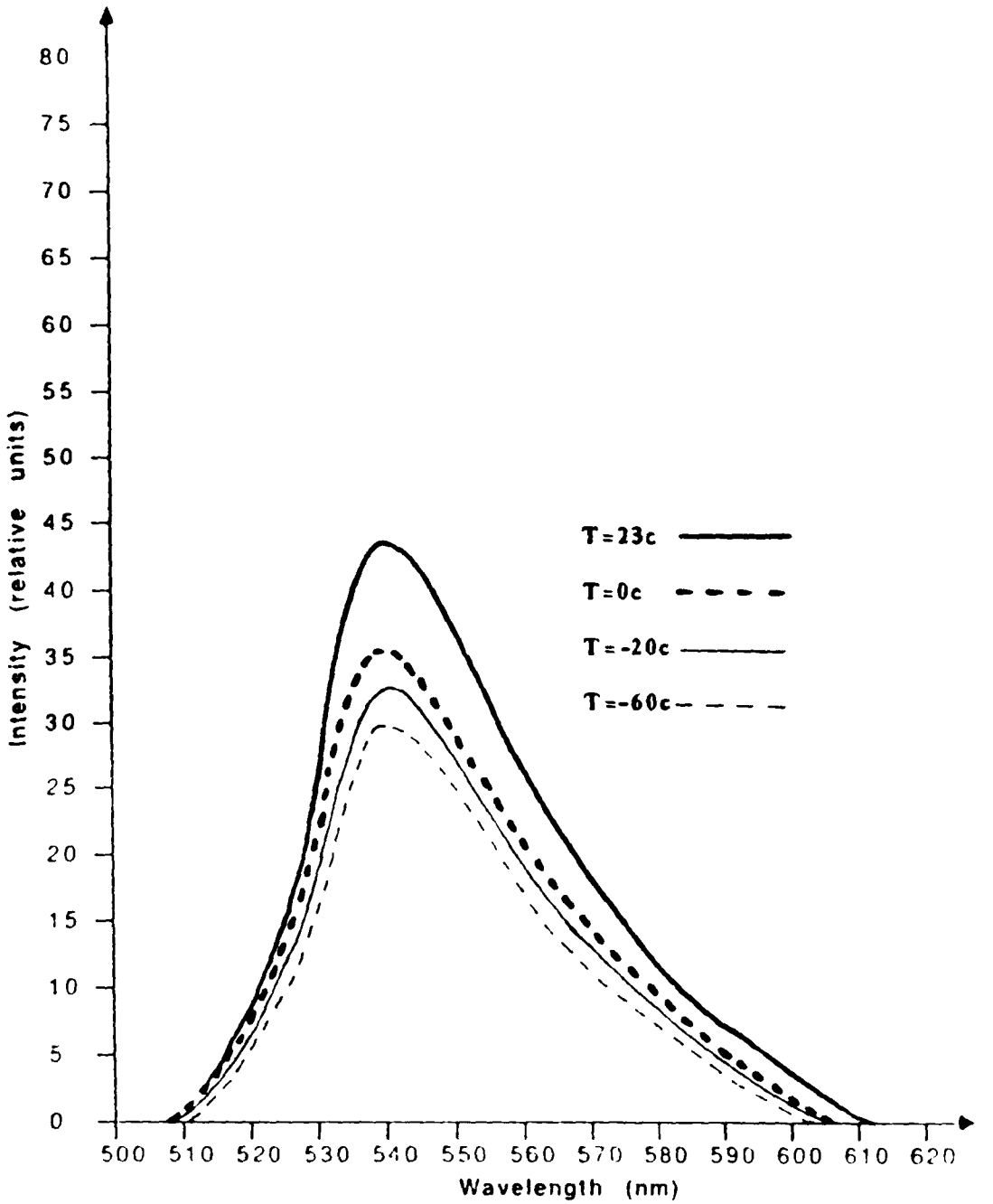

FIG.2.4.9 Fluorescence spectra of Rhodamine 110/ethylene glycol at different temperature

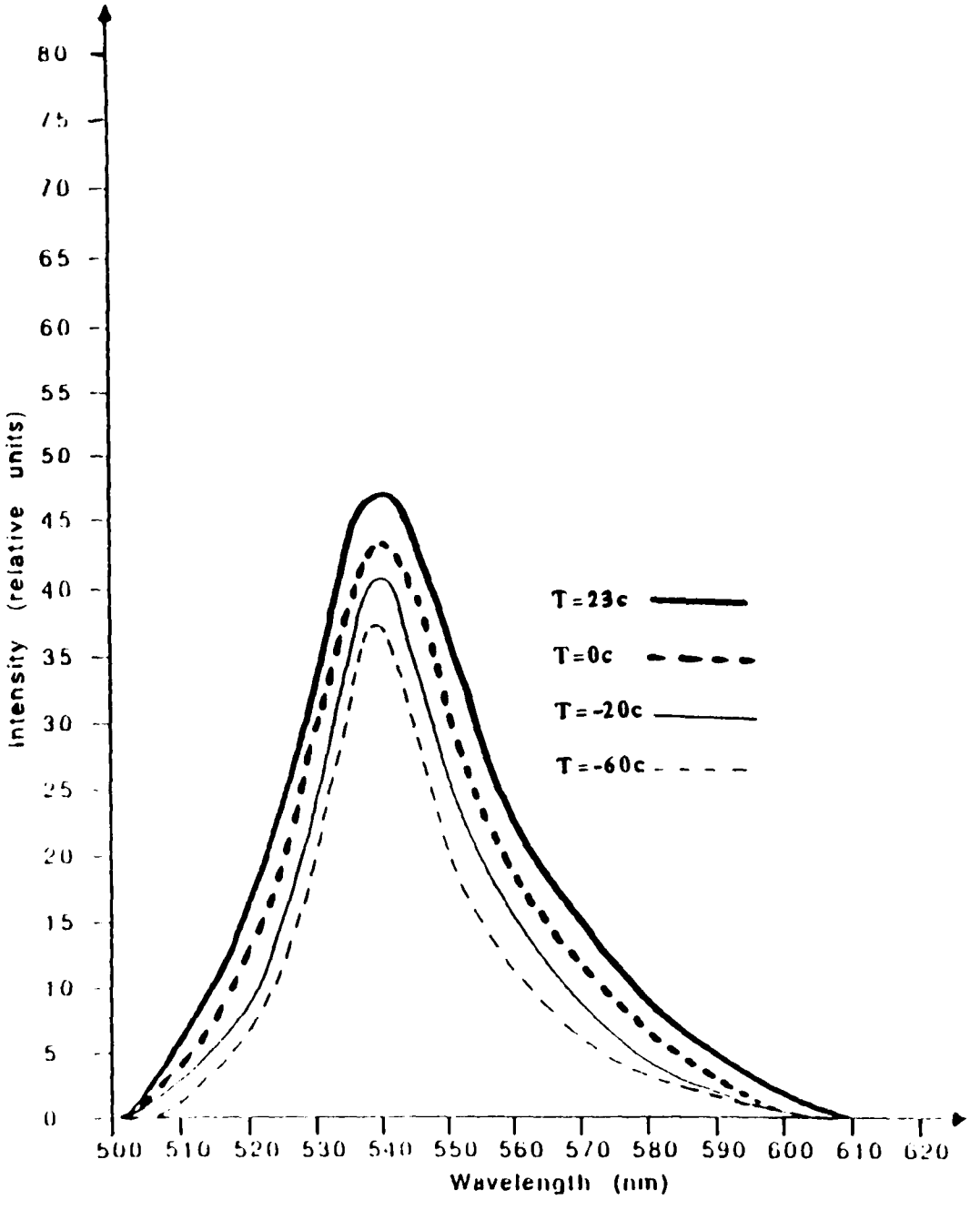

FIG.2.4.10 Fluorescence spectra of Rhodamine 110/methanol at different temperature

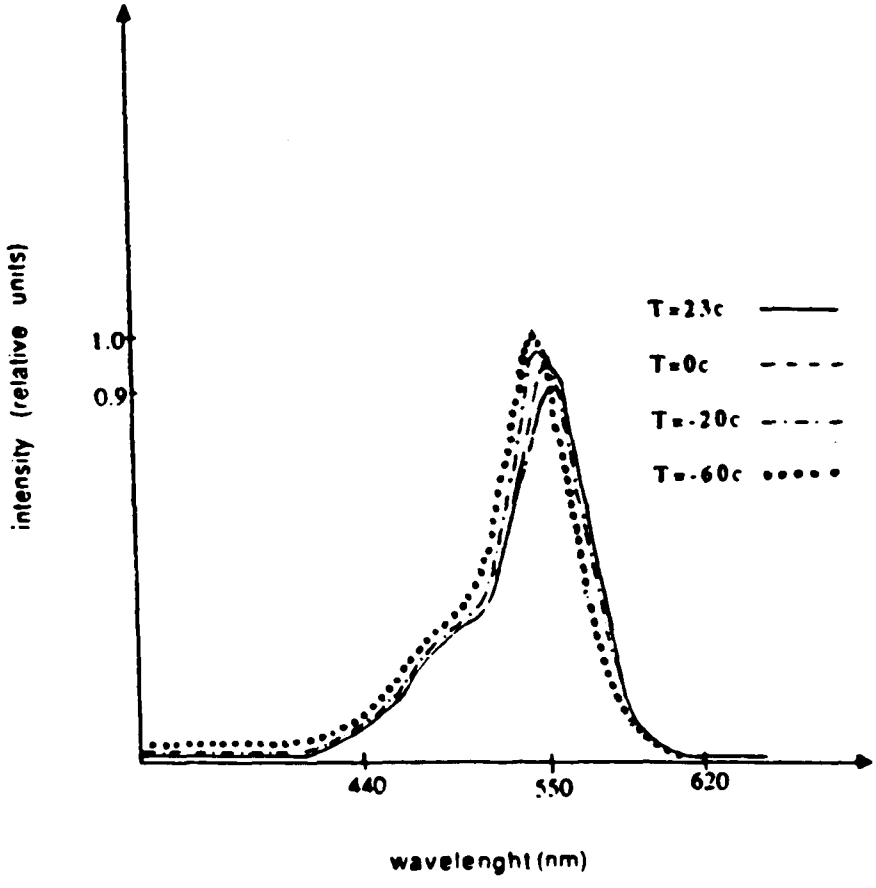

FIG. 2. 4. 11 Absorption spectra of Rhodamine B/ ethylalcohol at different temperature

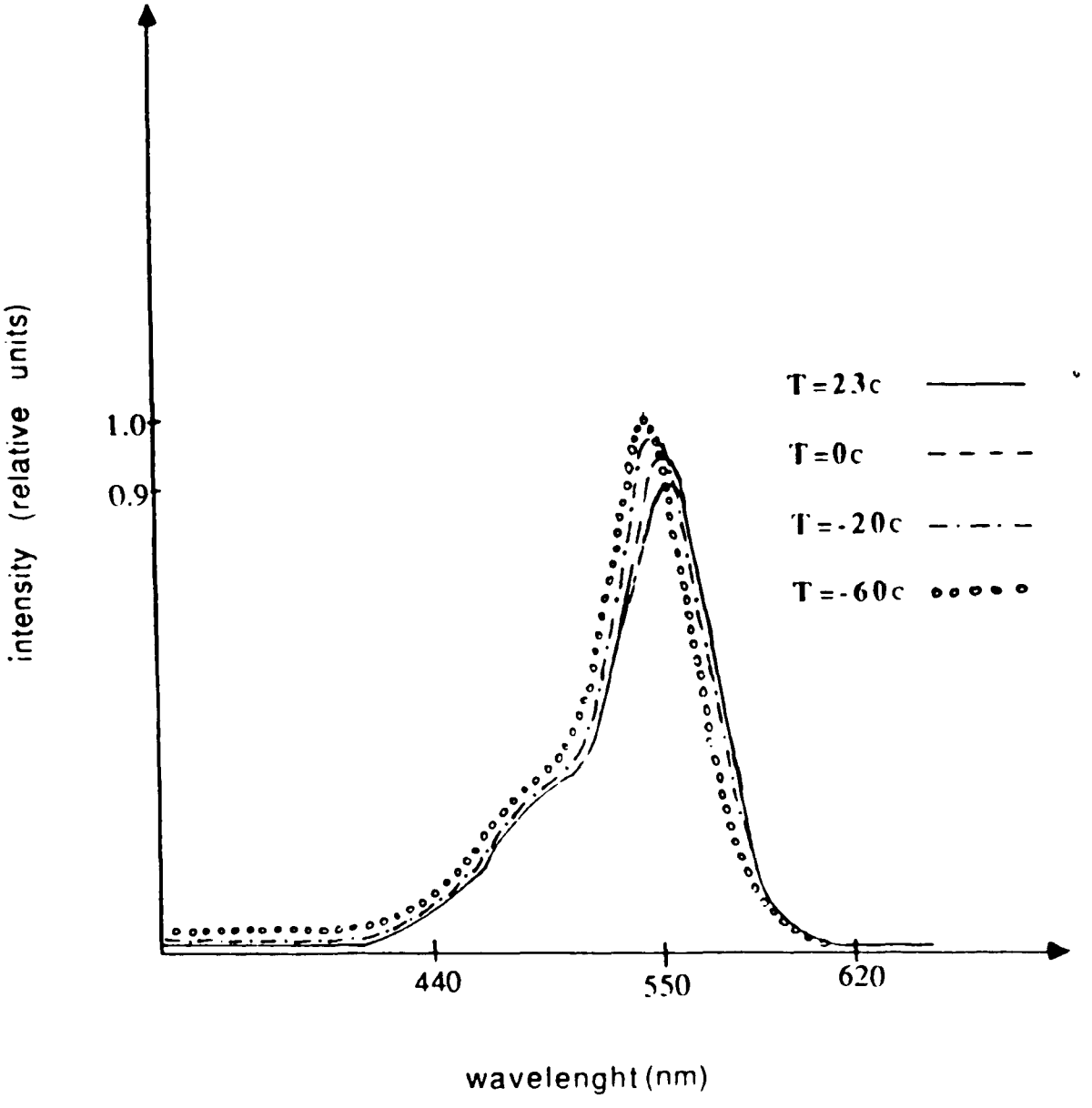

Figure 2.4.12 Absorption spectra of Rhodamine B/ethylene glycol at different temperature.

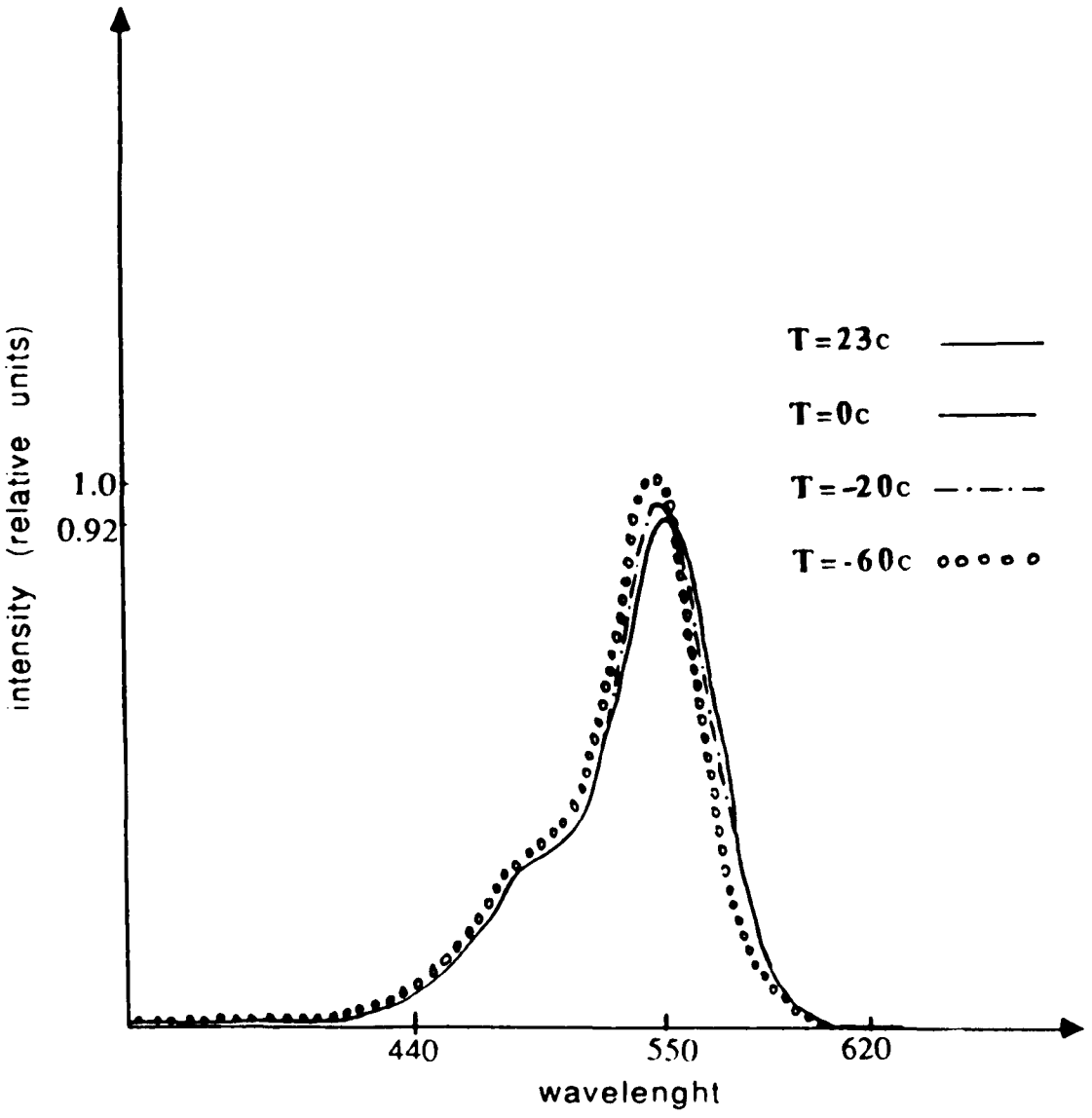

Figure 2.4.13 Absorption spectra of Rhodamine B/methanol at different temperature.

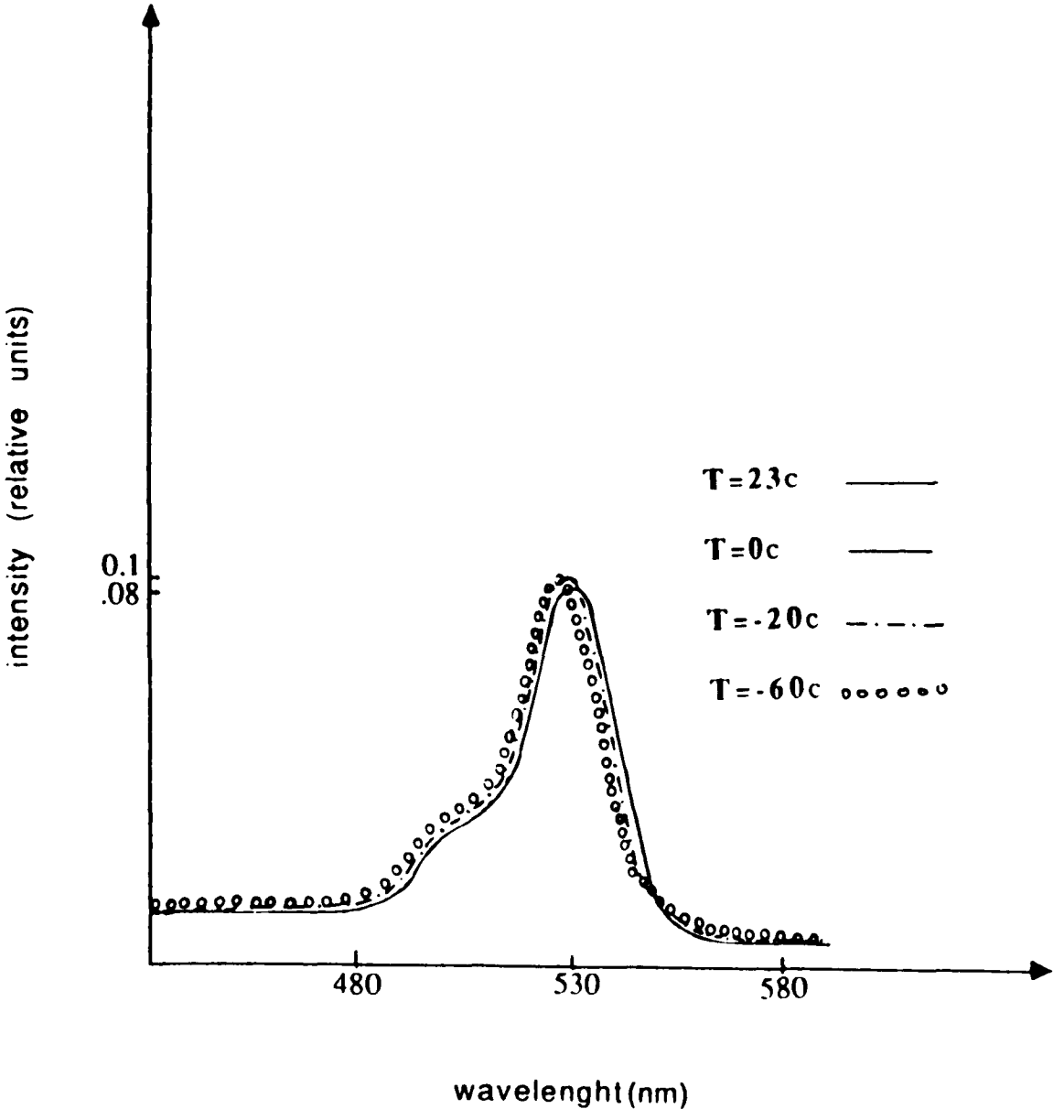

Figure 2.4.14 Absorption spectra of Rhodamine 6G/ethylalcohol at different temperature.

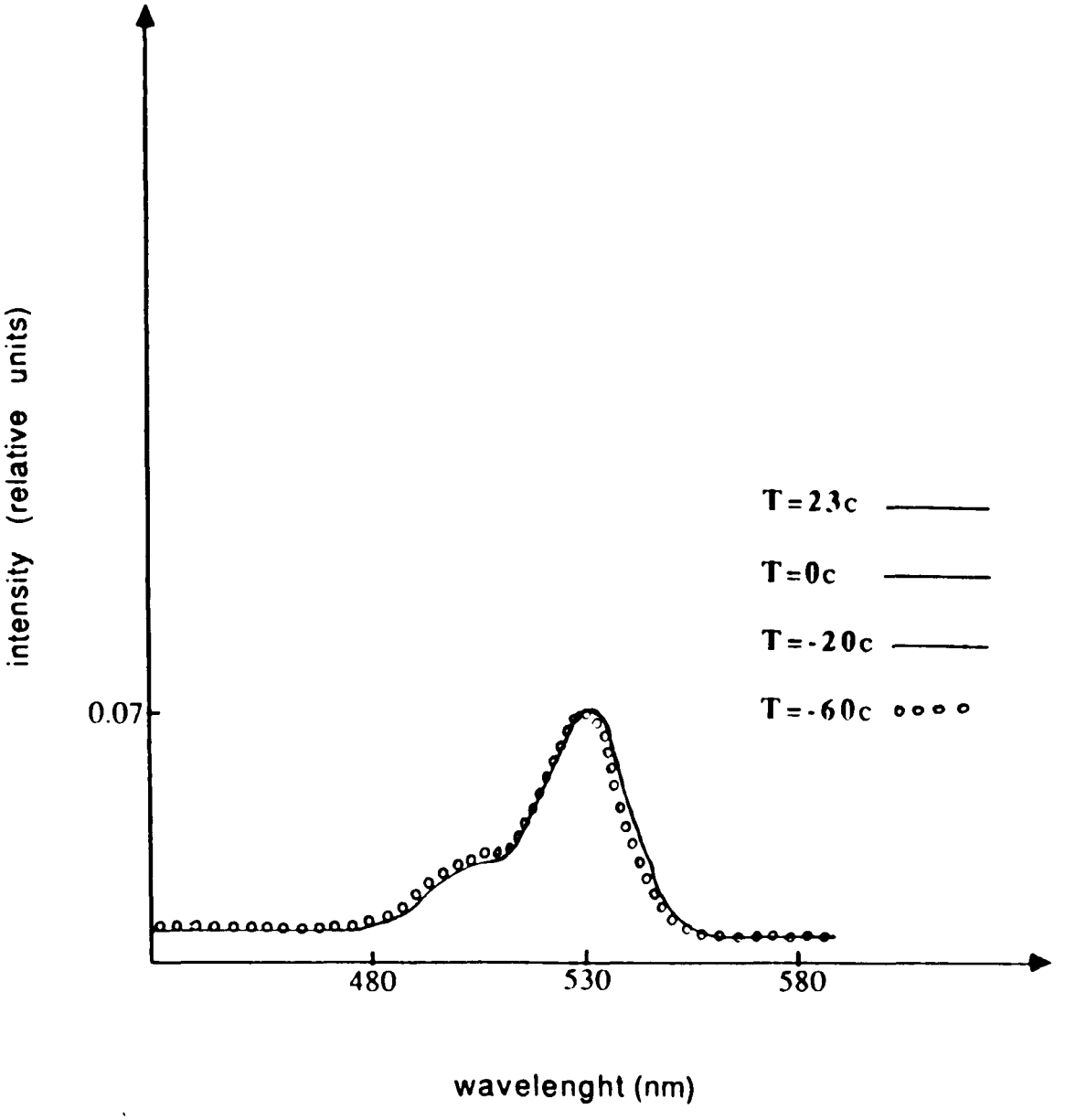

Figure 2.4.15 Absorption spectra of Rhodamine 6G/ethylene glycol at different temperature.

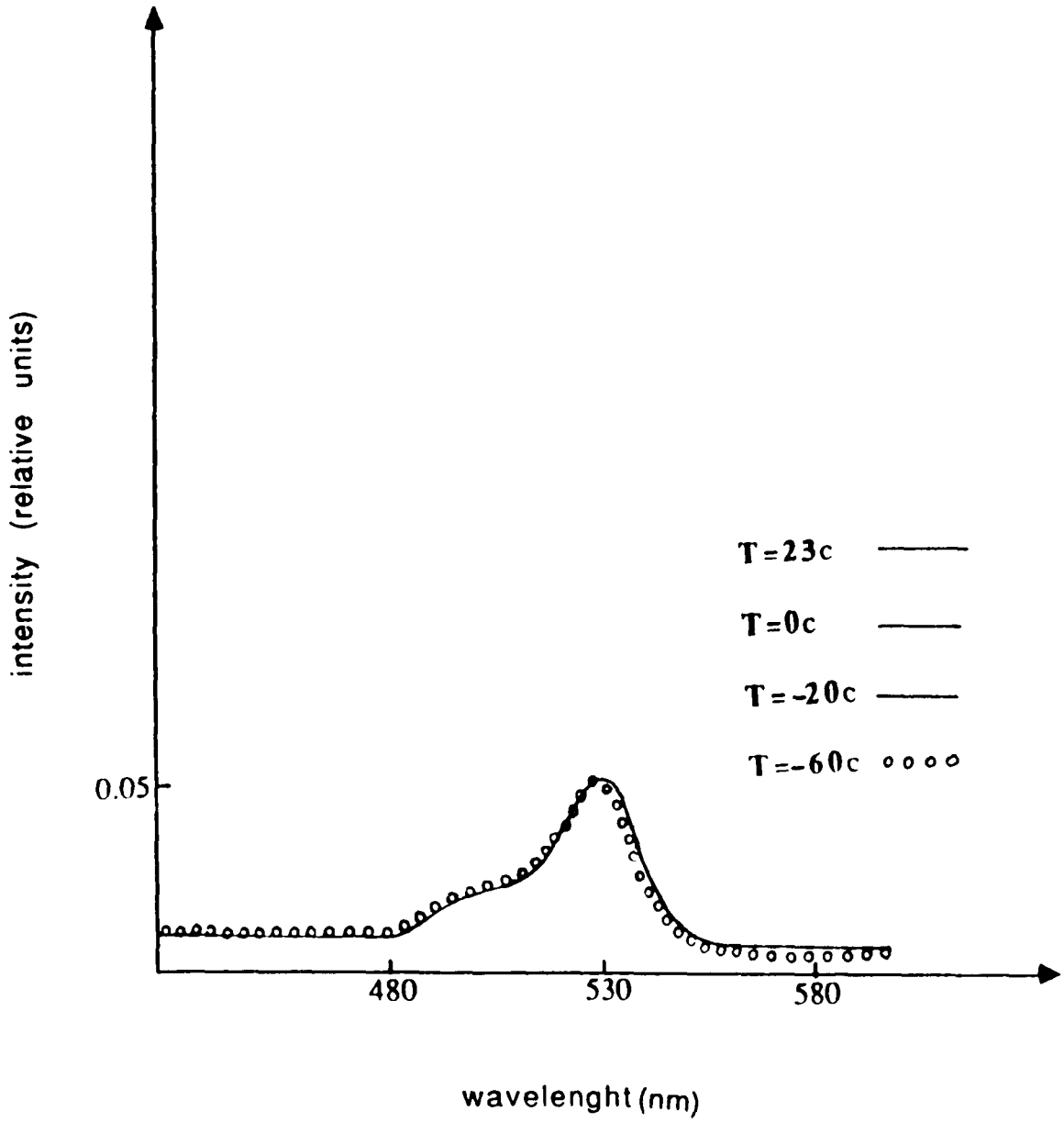

Figure 2.4.16 Absorption spectra of Rhodamine 6G/methanol at different temperature.

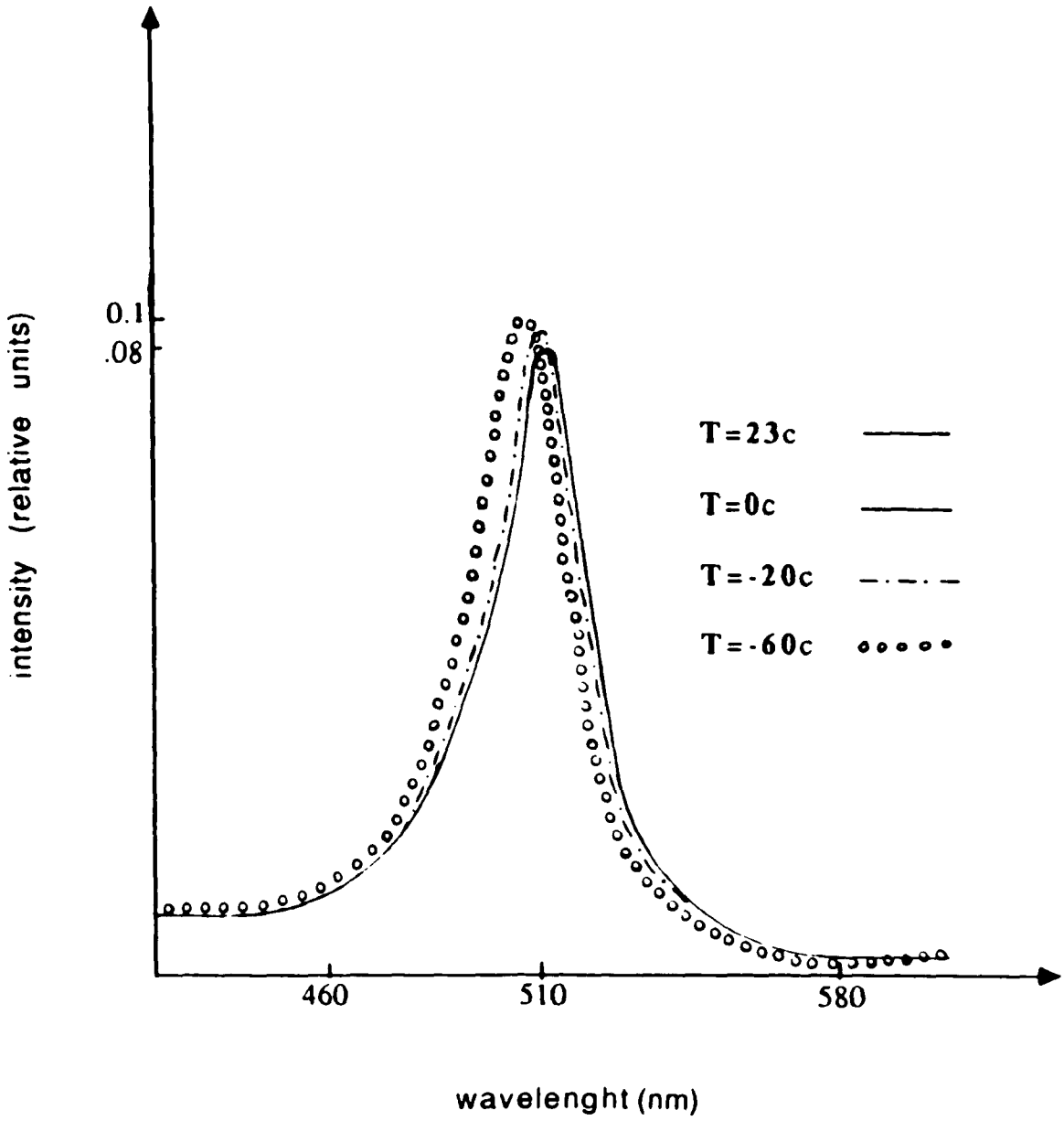

Figure 2.4.17 Absorption spectra of Rhodamine 110/ethylalcohol at different temperature

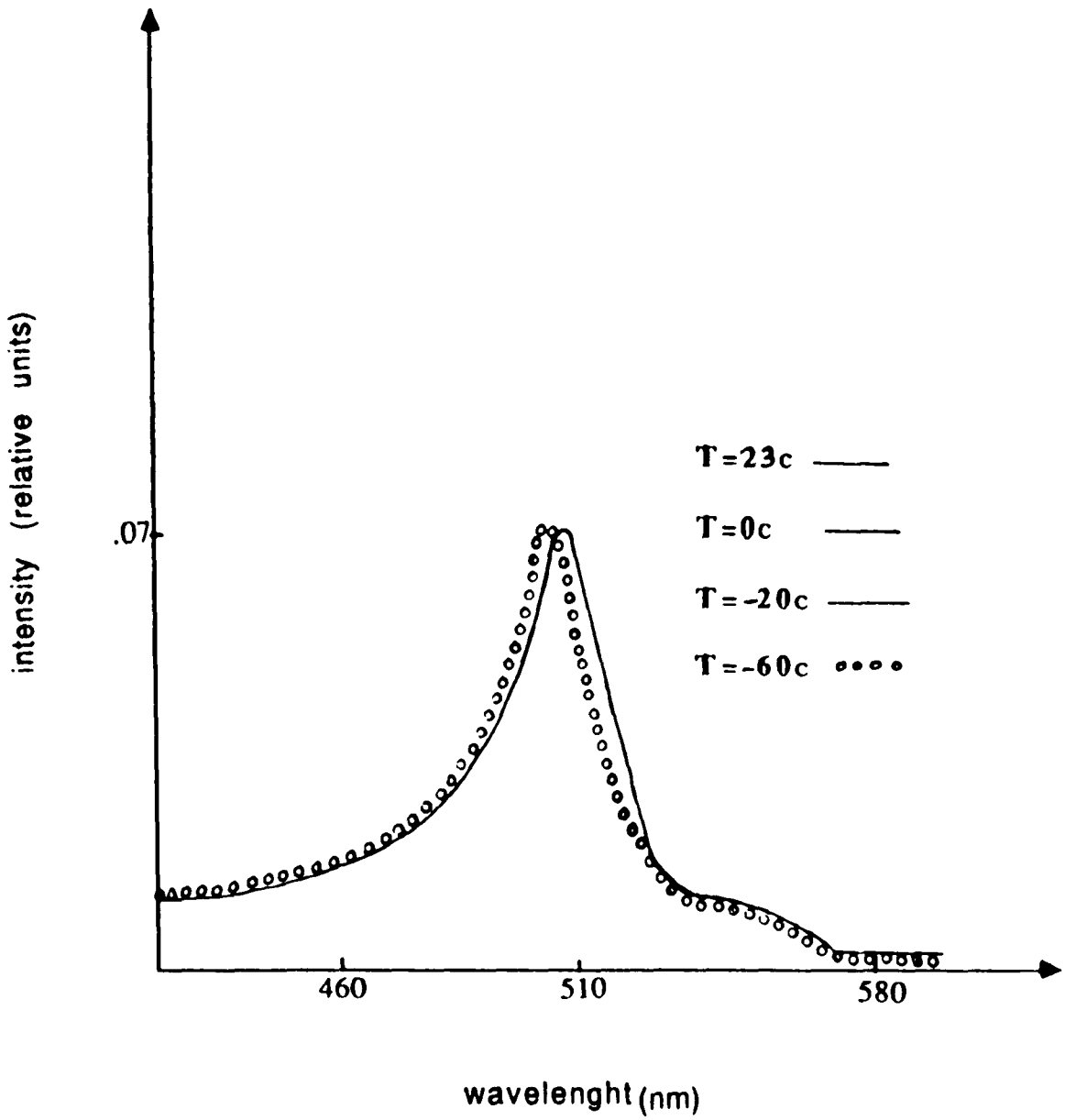

Figure 2.4.18 Absorption spectra of Rhodamine 110/ethylene glycol at different temperature.

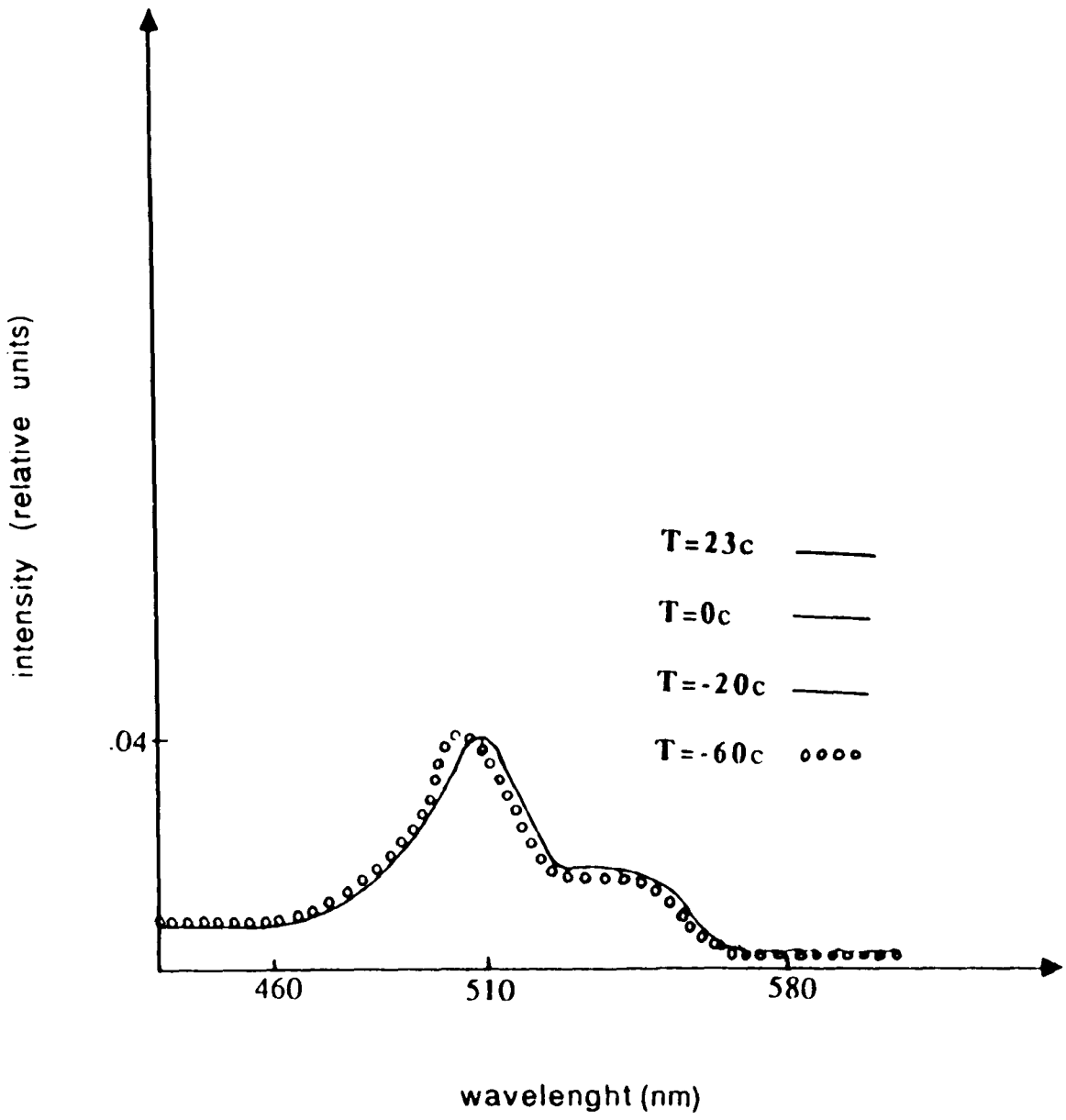

Figure 2.4.19 Absorption spectra of Rhodamine 110/methanol at different temperature.

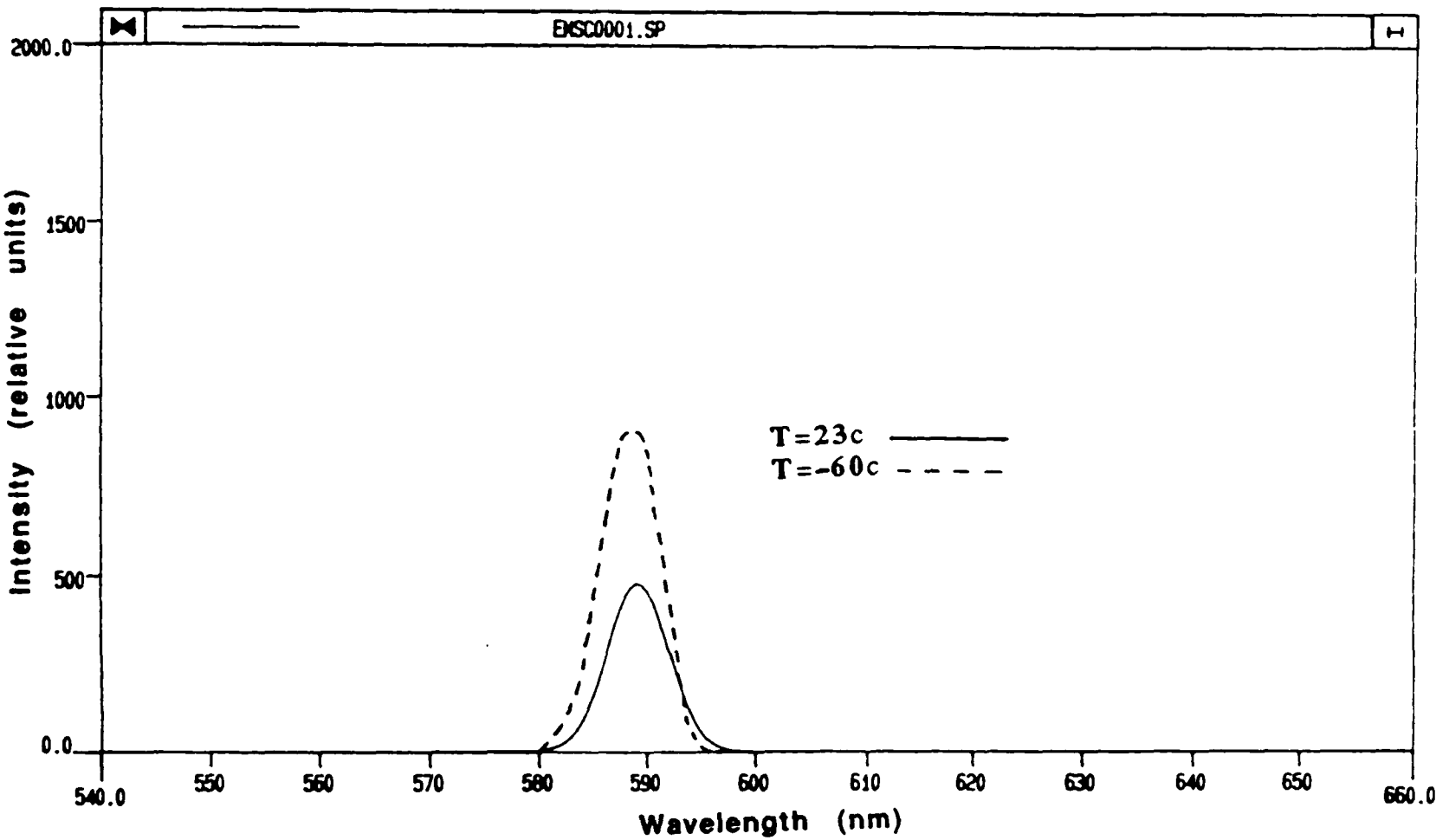

Figure 2.4.20 Fluorescence spectra of Rhodamine B/ethylene glycol under UV lamp excitation.

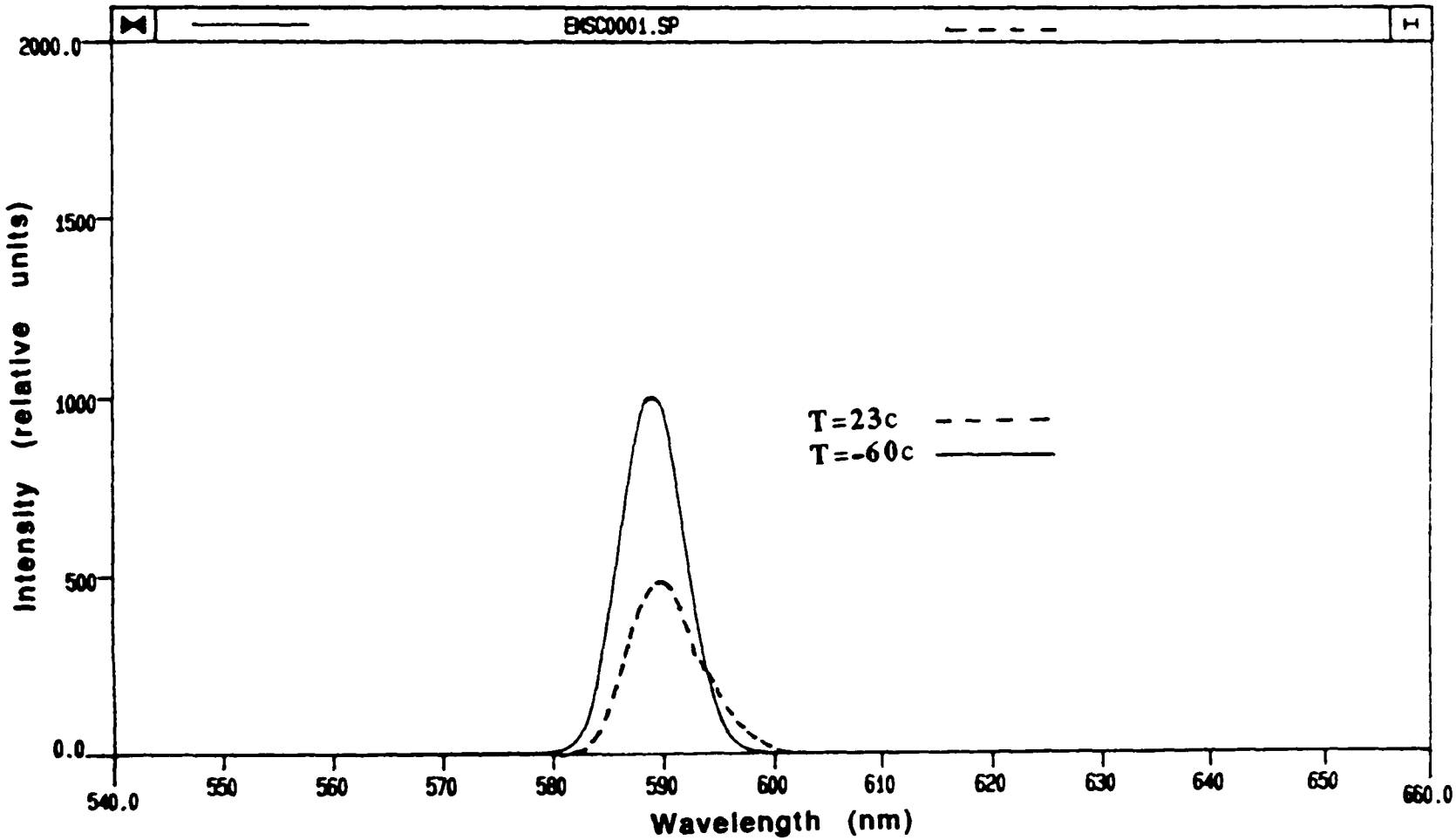

Figure 2.4.21 Fluorescence spectra of Rhodamine B/ethylalcohol under UV lamp excitation.

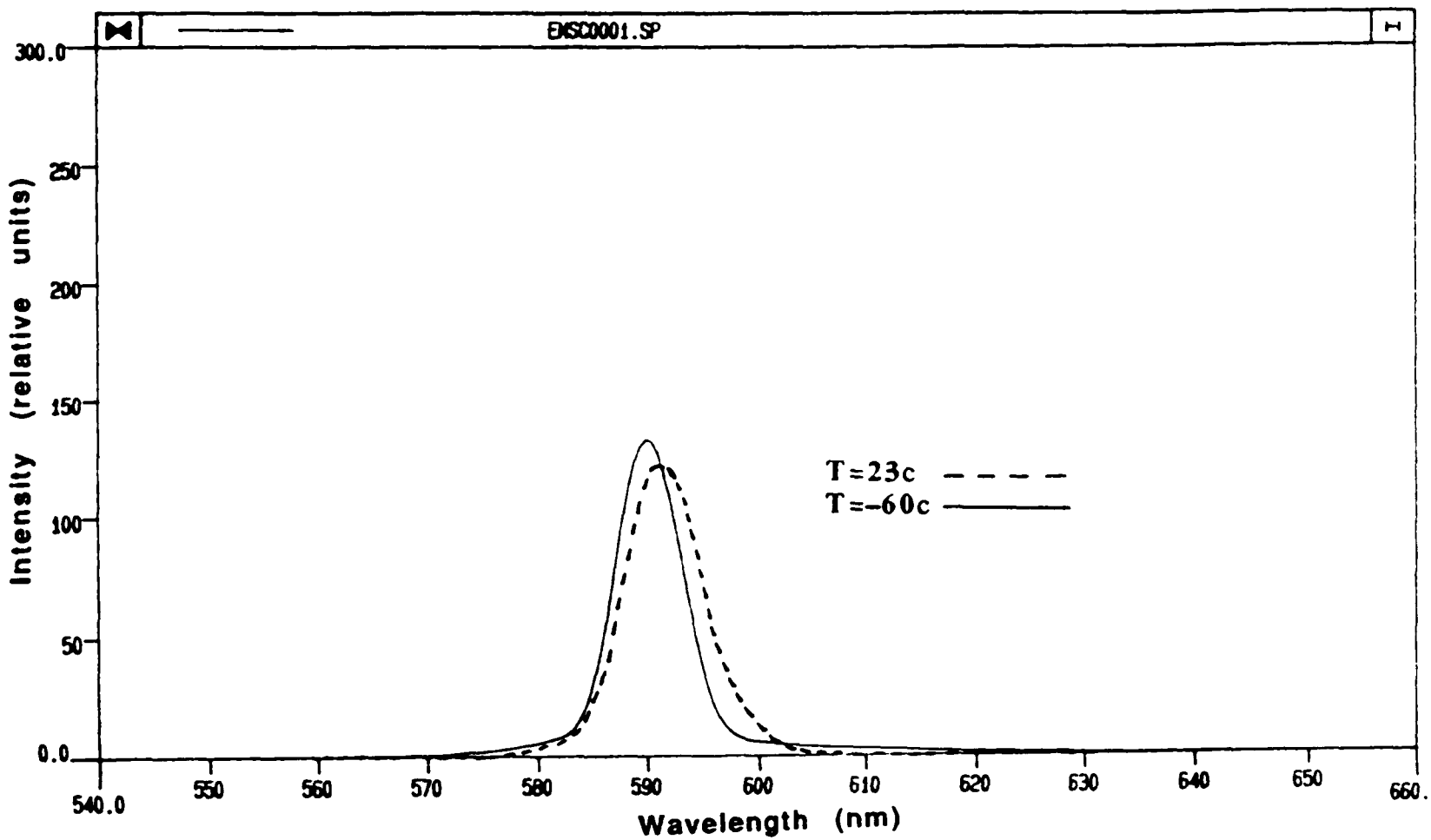

Figure 2.4.22 Fluorescence spectra of Rhodamine B/methanol under UV lamp excitation.

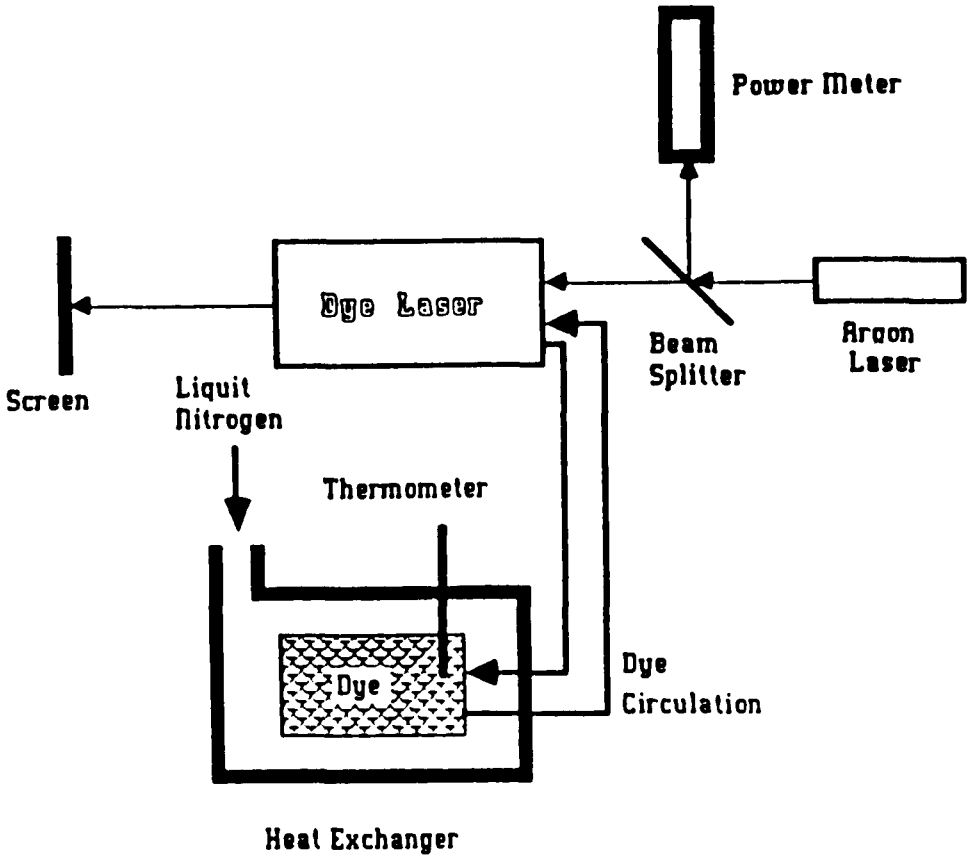

FIFURE 3.4.1 Experimental setup for threshold power measurement

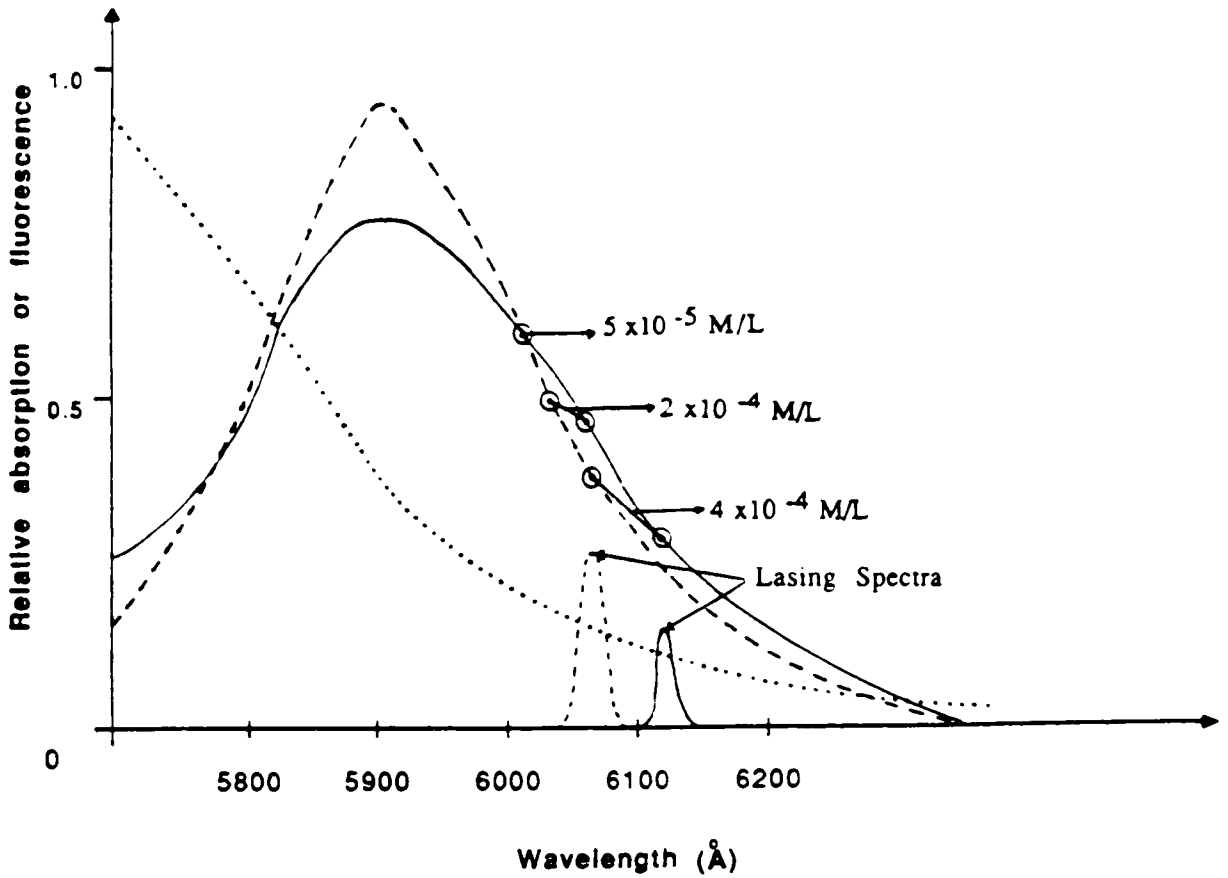

Fig. 3.4.2: Measured absorption and fluorescence spectra. The circles indicate lasing wavelengths at different concentrations.

_ _ _ Fluorescence at -5 °c

____ Fluorescence at 23 °c ..... Absorption

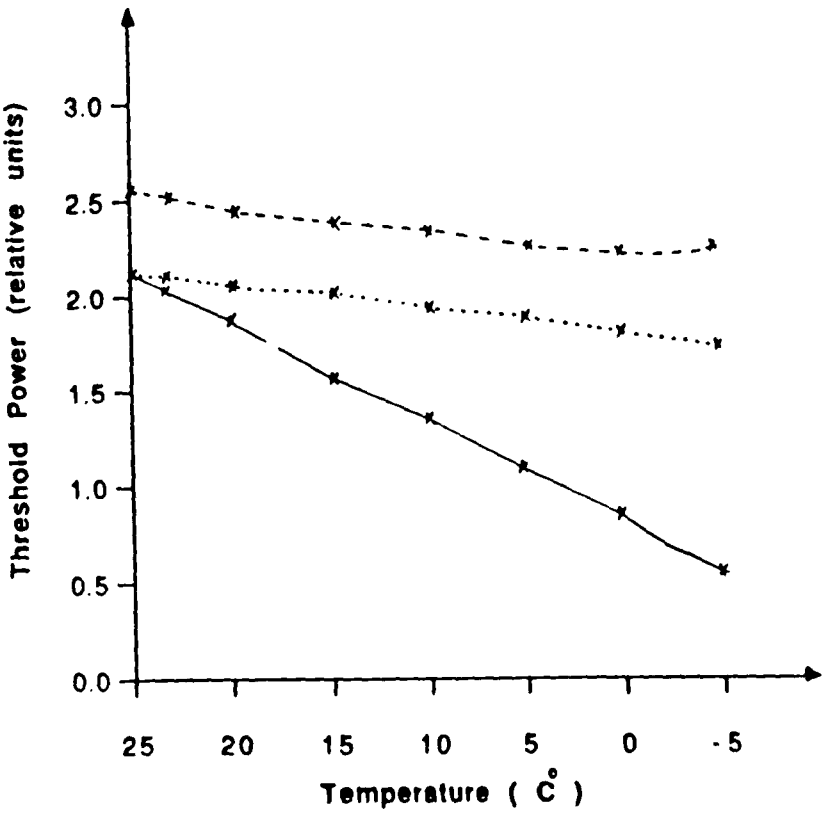

Fig. 4.2.5: Lasing threshold pumping intensity Vs solution temperature for multimode regime. ____ Rhodamine B _ _ _ Rhodamine 110 . . . . Rhodamine 6G

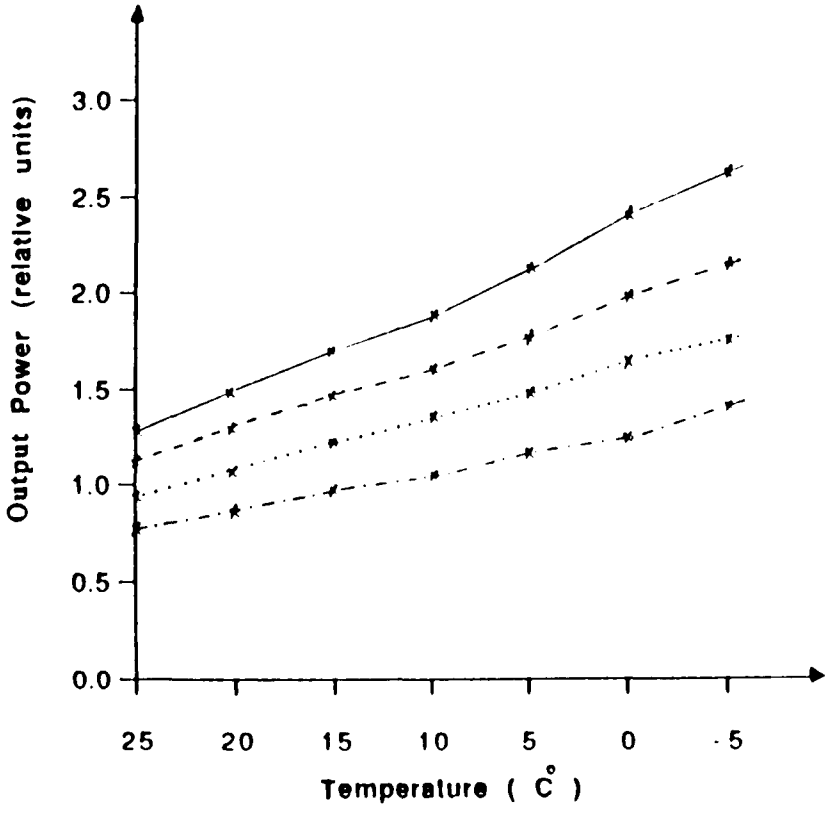

Fig. 3.4.4: Lasing output power Vs solution temperature for multimode regime. ——— 3×10^{-4} M/L – – – 2×10^{-4} M/L . . . . 4×10^{-4} M/L ····· 5×10^{-5} M/L

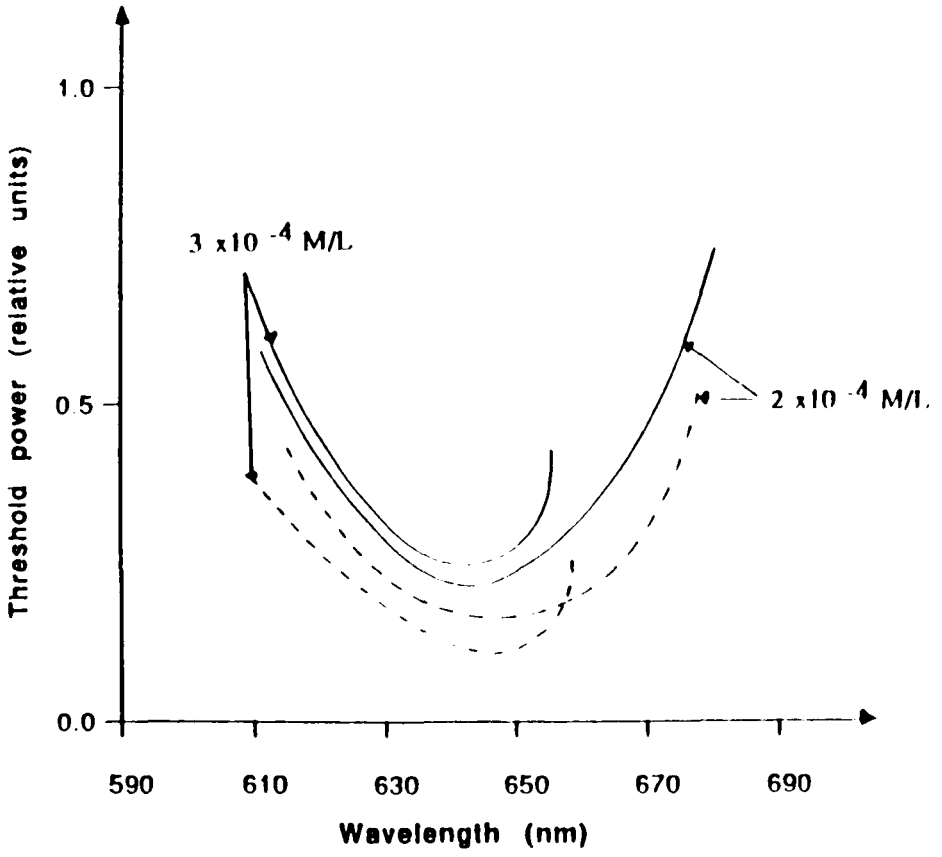

Fig. 3.4.5: Lasing threshold pumping intensity Vs wavelength for single-frequency regime.

_ _ _ T = -5 °c ____ T = 23 °c

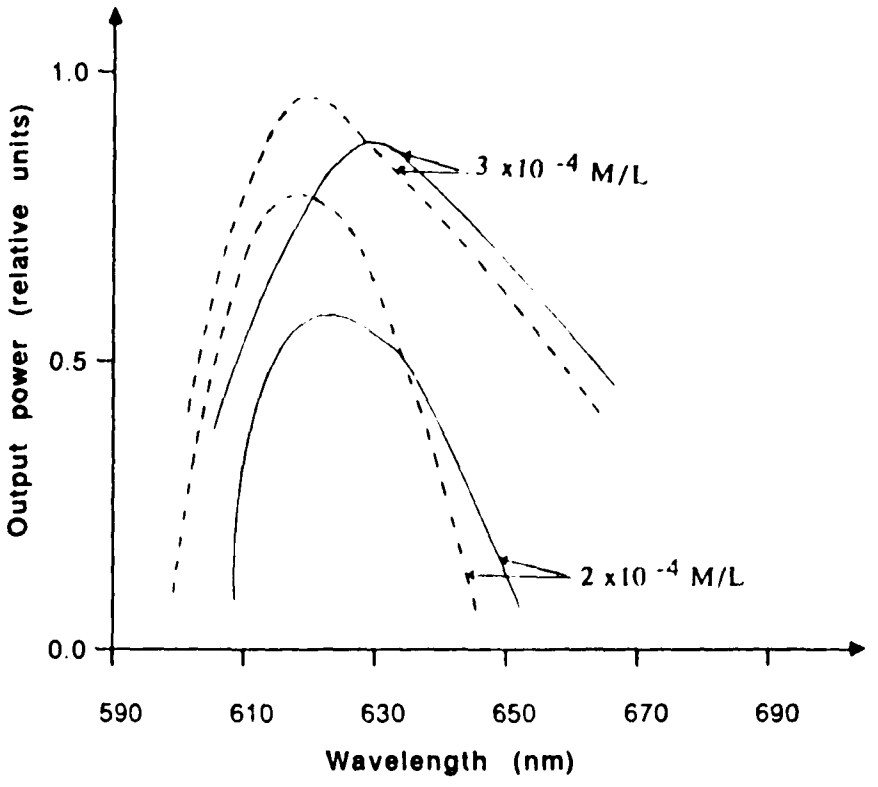

Fig. 3.4.6: Lasing output power Vs wavelength for single-frequency regime. _ _ _ T = -5 °c ___ T = 23 °c

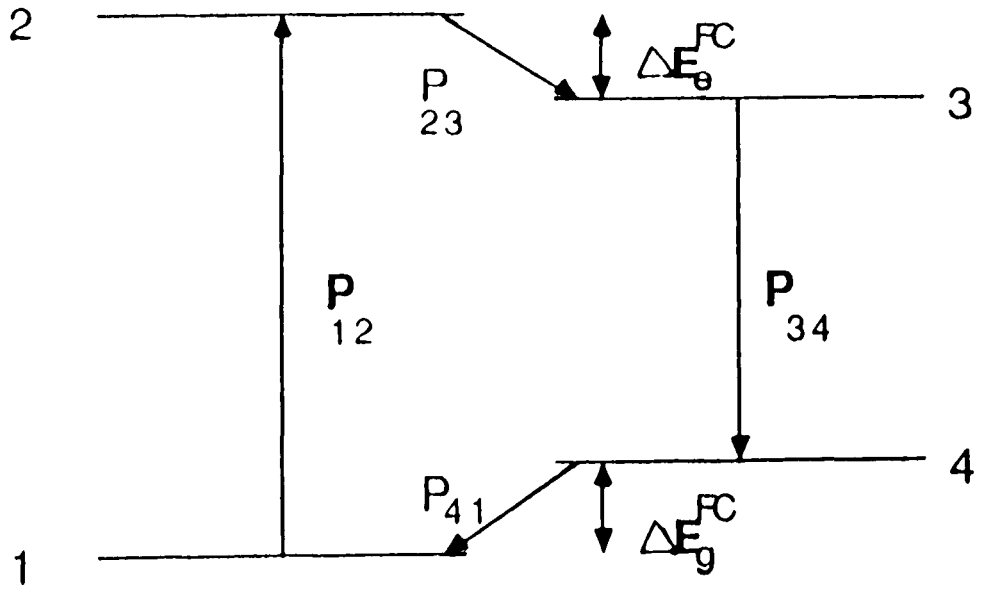

Fig. 4.1.1: Energy level scheme for electronics states of complex dye molecules in a polar solvent. Rhodamine B in Ethanol.

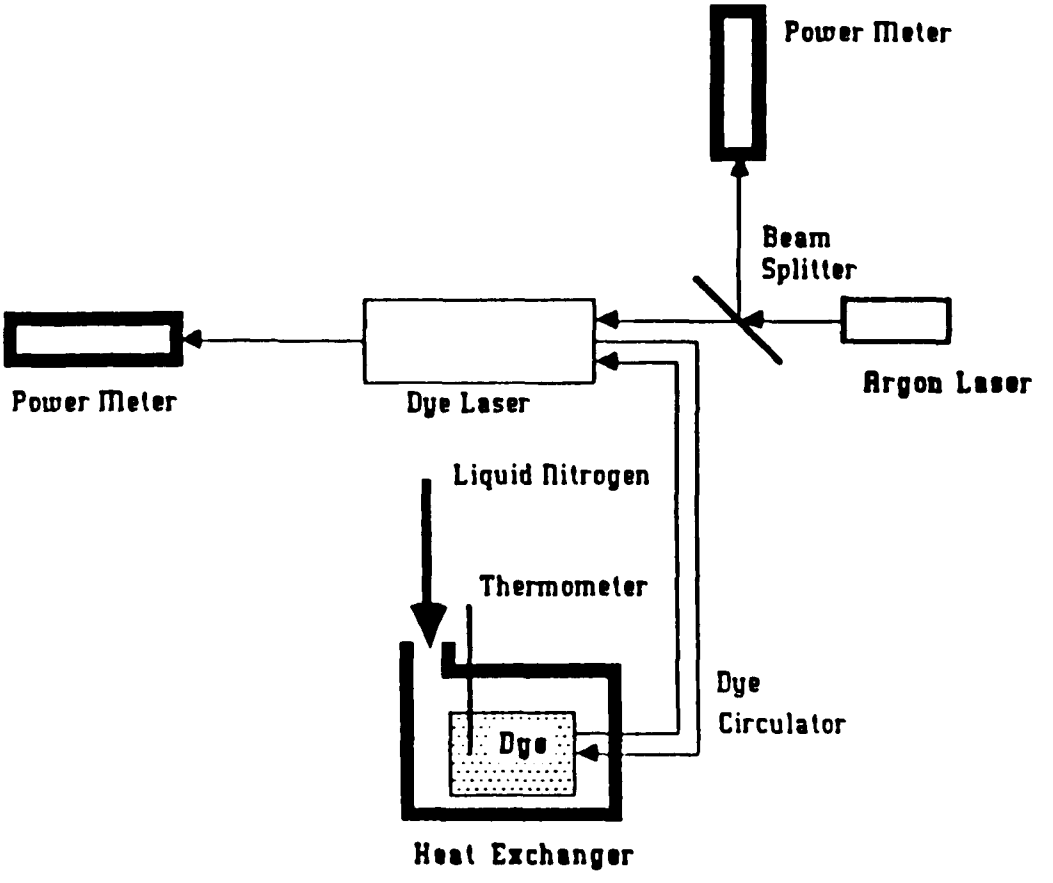

FIFURE 4.2.1 Experimental setup for laser output measurement

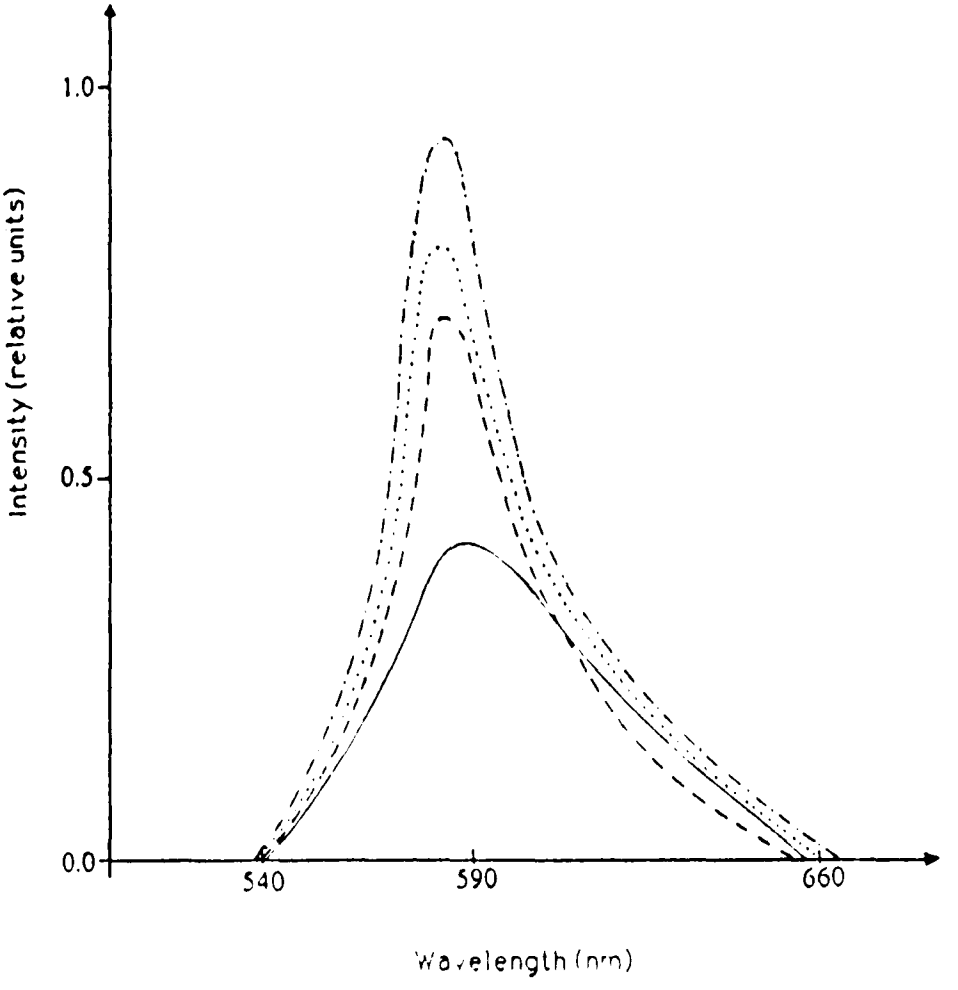

Fig. 4.2.2 Fluorescence spectra of Rhodamine B in ethylene glycol. ——— 23 °c - - - -5 °c ..... -20 °c ····· - 60 °c

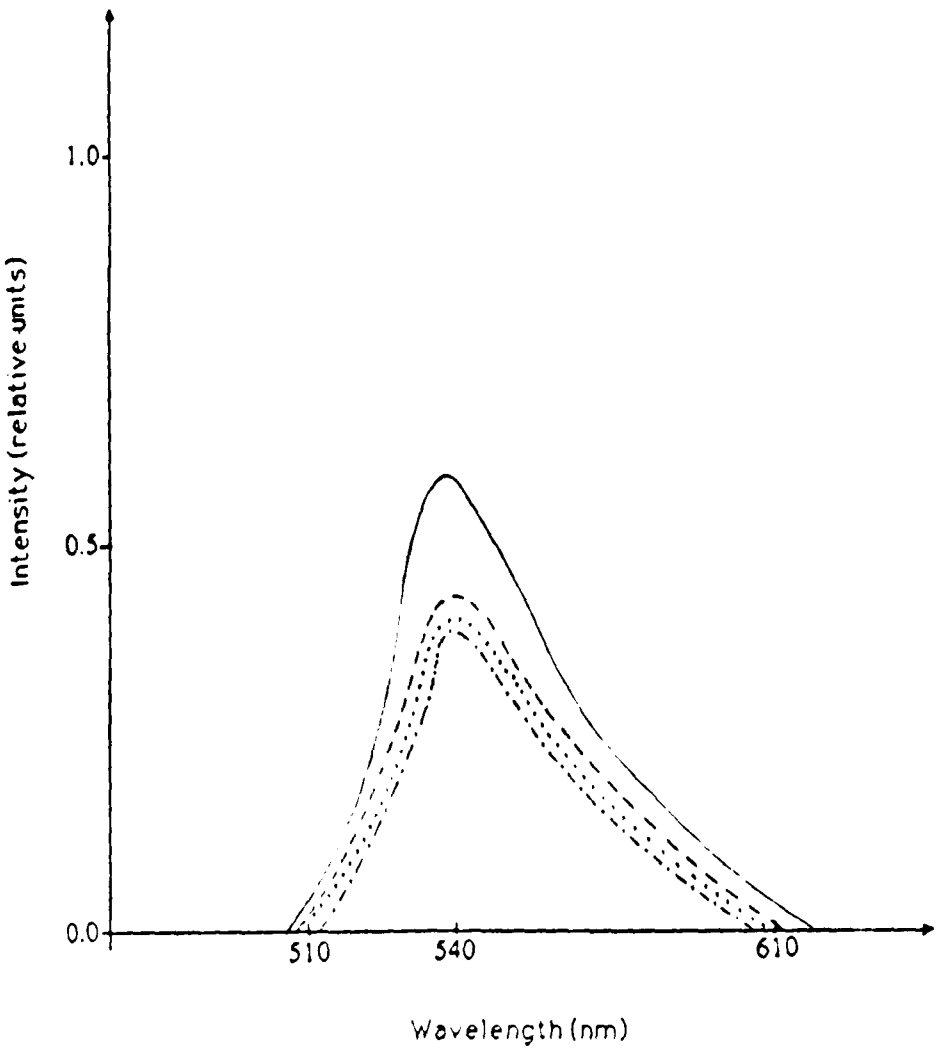

Fig. 4.2.3 Fluorescence spectra of Rhodamine 6G in ethylene glycol. ——— 23 °c - - - -5 °c ..... -20 °c ------ -60 °c

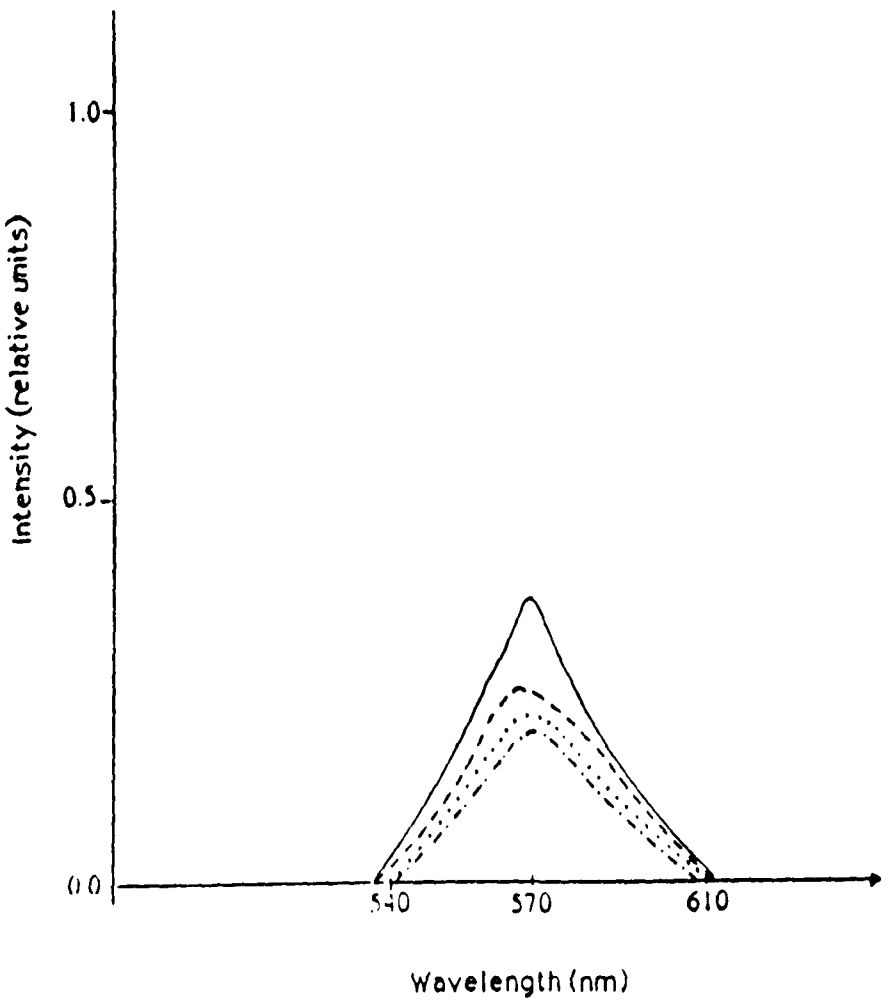

Fig. 4.2.4 Fluorescence spectra of Rhodamine 110 in ethylene glycol ——— 23 °c - - - -5 °c ..... -20 °c ..... - 60 °c

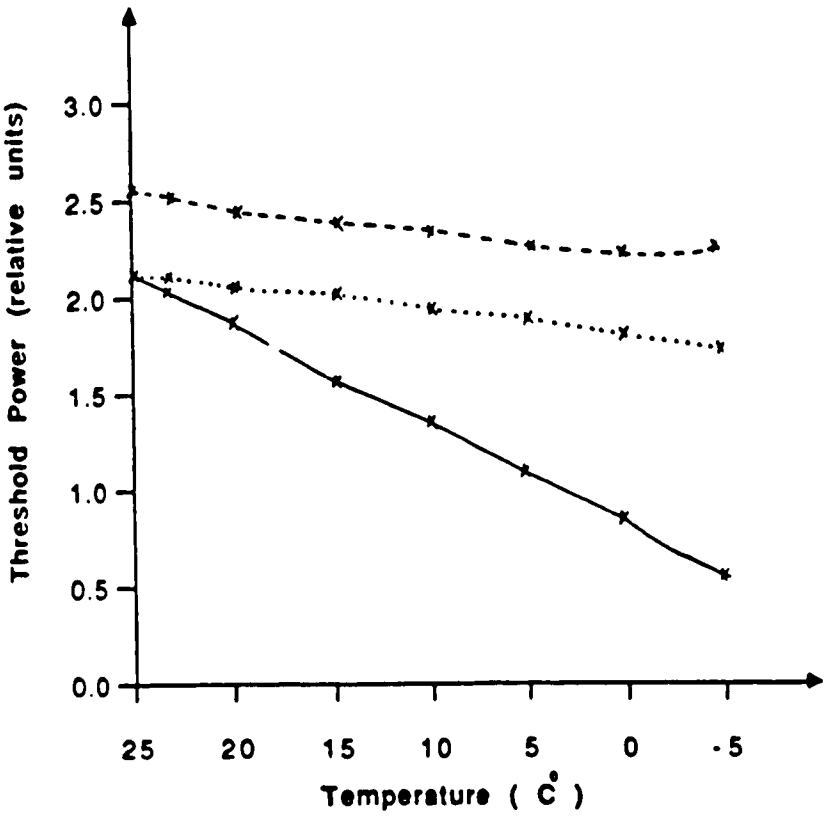

Fig. 4.2.5: Lasing threshold pumping intensity Vs solution temperature for multimode regime. ____ Rhodamine B _ _ _ Rhodamine 110 . . . . Rhodamine 6G

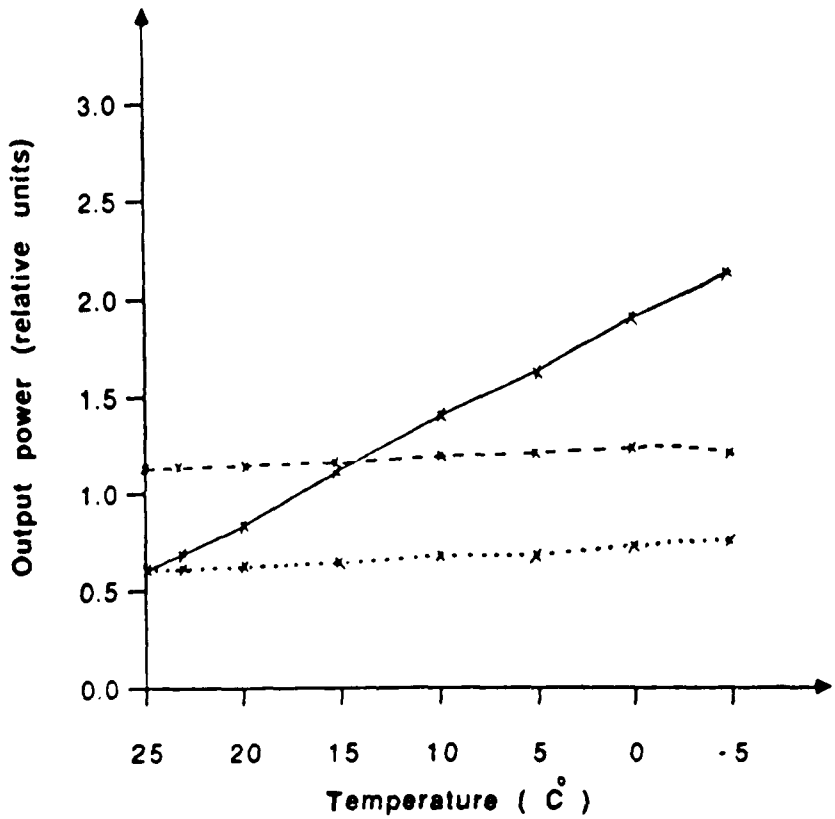

Fig. 4.2.6: Lasing output power Vs solution temperature for multimode regime. ____ Rhodamine B

_ _ _ Rhodamine 110 . . . . Rhodamine 6G

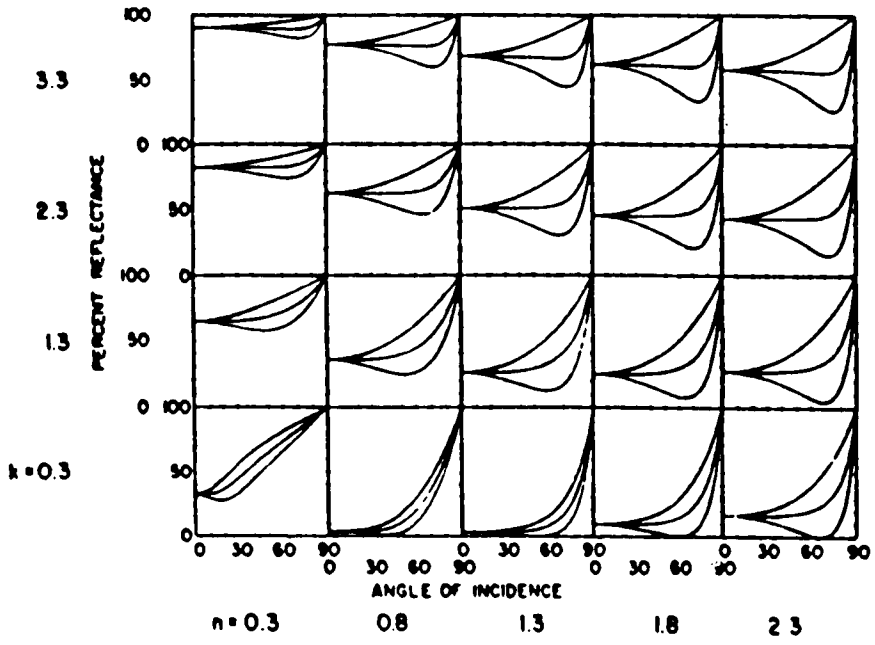

FIG. 5.1.1 R-versus-ϕ curves calculated using the optical constants shown by the large numbers. The small numbers shown on the abscissa and ordinate are the values of ϕ and R, respectively.

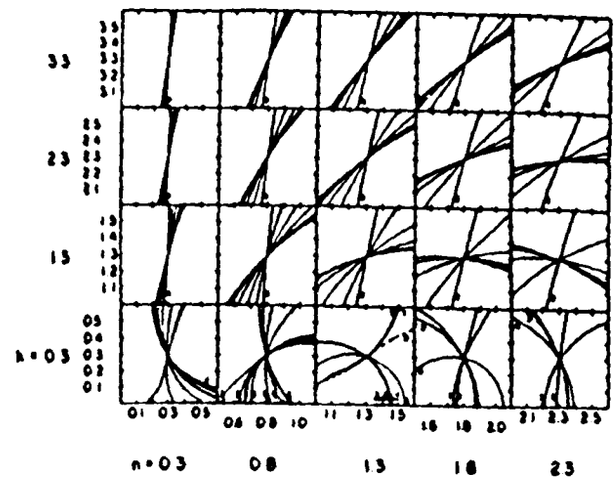

FIG. 5.1.2 Isoreflectance curves for R_p calculated using the optical constants shown by the larger numbers. The small numbers used for the abscissa and ordinate show the scale in the n, k plane. The numeral 8 designates the isoreflectance curve corresponding to 80°. The other curves are for angles of incidence 70, 60, through 10°. The curves usually occur in descending order; when they do not, each curve is labeled with a single digit to avoid confusion (method 1)

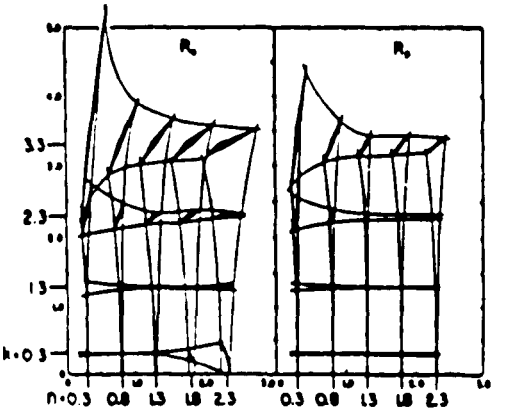

FIG. 5.1.3 The effect of ± 1 o/o error in the measurement of reflectance on the determination of n and k using method 1. The angles of incidence are 20 and 70°

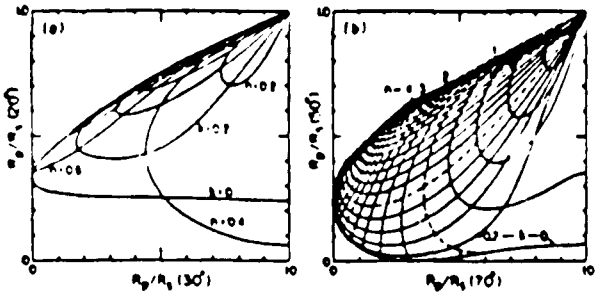

FIG. 5.1.4 Curves of constant n and k as a function of R_p/R_s for (a) small (30-20°) and (b) large (70-50°) angles of incidence. Δn and Δk are each 0.2. Curves for integer n and k values are dashed (method2)

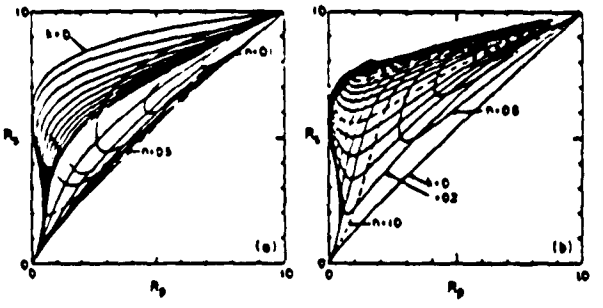

FIG. 5.1.5Curves of constant n and k as a function of R_p and R_s for (a) small (20°) and (b) large (70°) angles of incidence. For (a) Δk is 0.01 for $0 < k < 0.1$; otherwise Δk is 0.2. Δn is 0.1 and the curve for $n = 0.5$ is dashed. The dotted line corresponds to the value of n for the Brewster angle, $n = 0.364$. Fpr (b) $\Delta k = \Delta n = 0.2$. Curves for integer n and k values are dashed (method 3)

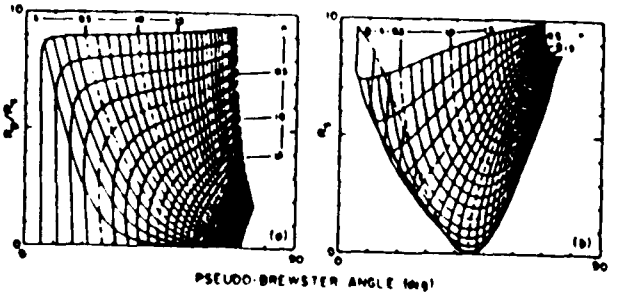

FIG. 5.1.6 Curves of constant n and k as a function (a) of R_p/R_s and the pseudo-Brewster (pB) angle and (b) of R_s and the pB angle (method 4 and 5, respectively). $\Delta n = \Delta k = 0.1$ and curves for integer and half-integer; n and k values are dashed.

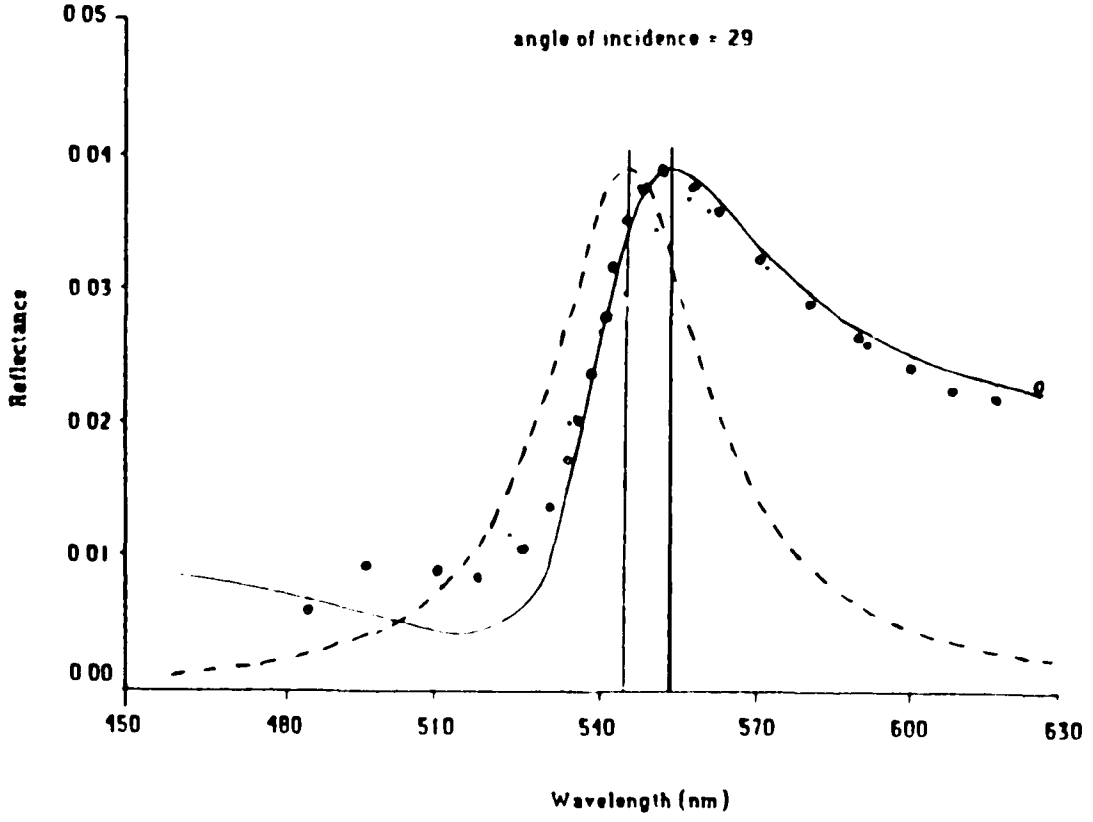

Fig. 5.4.1 Reflectance R_p Vs. λ for Rh B solution at angle of incidence $\phi = 29^{\circ}$

—— theoretical (Lorentzian) • • • theoretical (actual lineshape)

• • • experimental - - - absorption spectrum

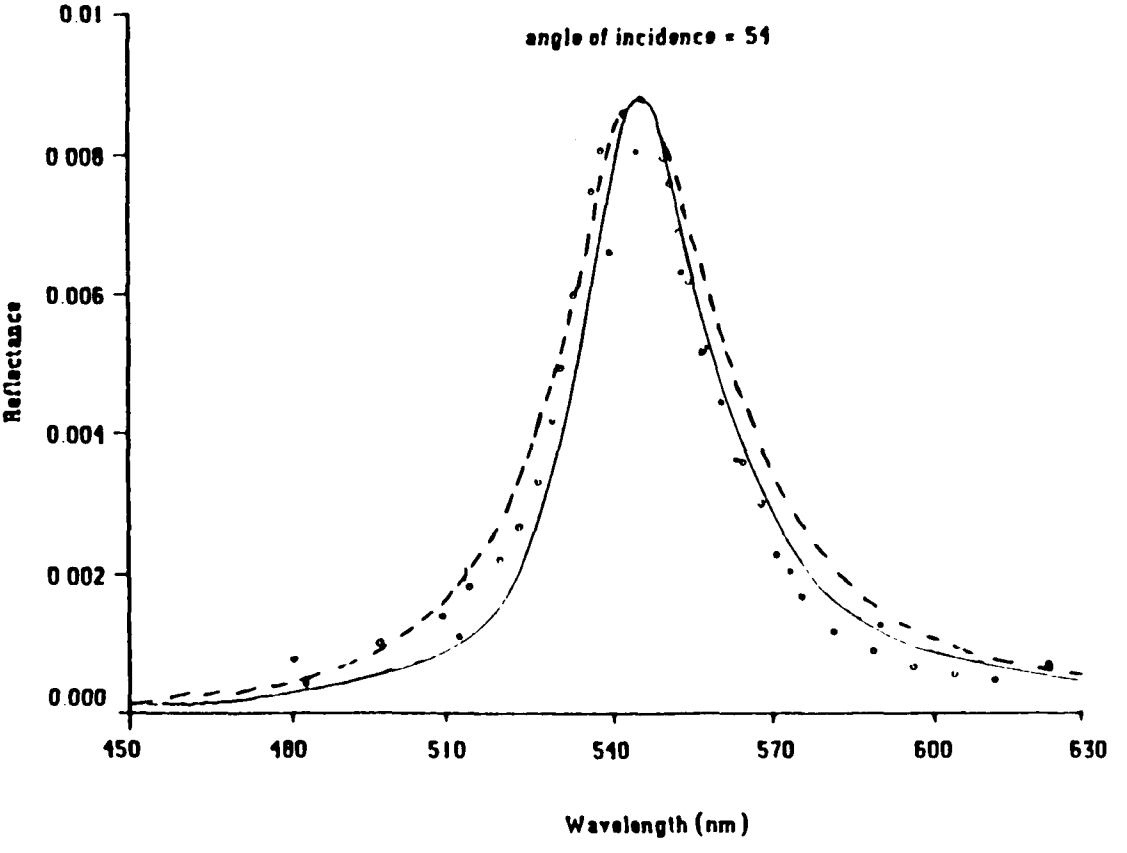

Fig. 5.4.2 Reflectance R_p vs. λ for Rh B solution at angle of incidence $\phi = 54^0$

—— theoretical (Lorentzian) o o o theoretical (actual lineshape)

• • • experimental – – – absorption spectrum

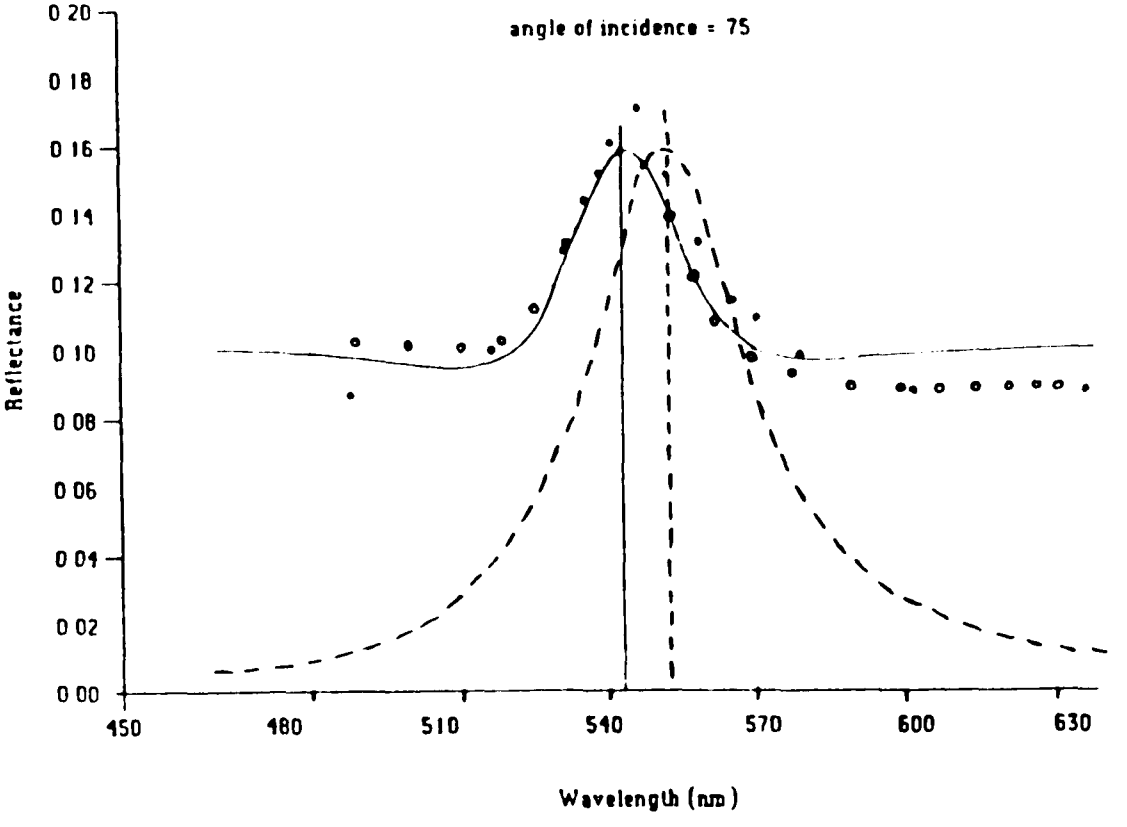

Fig. 5.4.3 Reflectance Rp vs. λ for Rh B solution at angle of incidence $\phi = 75^{\circ}$

—— theoretical (Lorentzian) o o o theoretical (actual lineshape)

• • • experimental – – – absorption spectrum

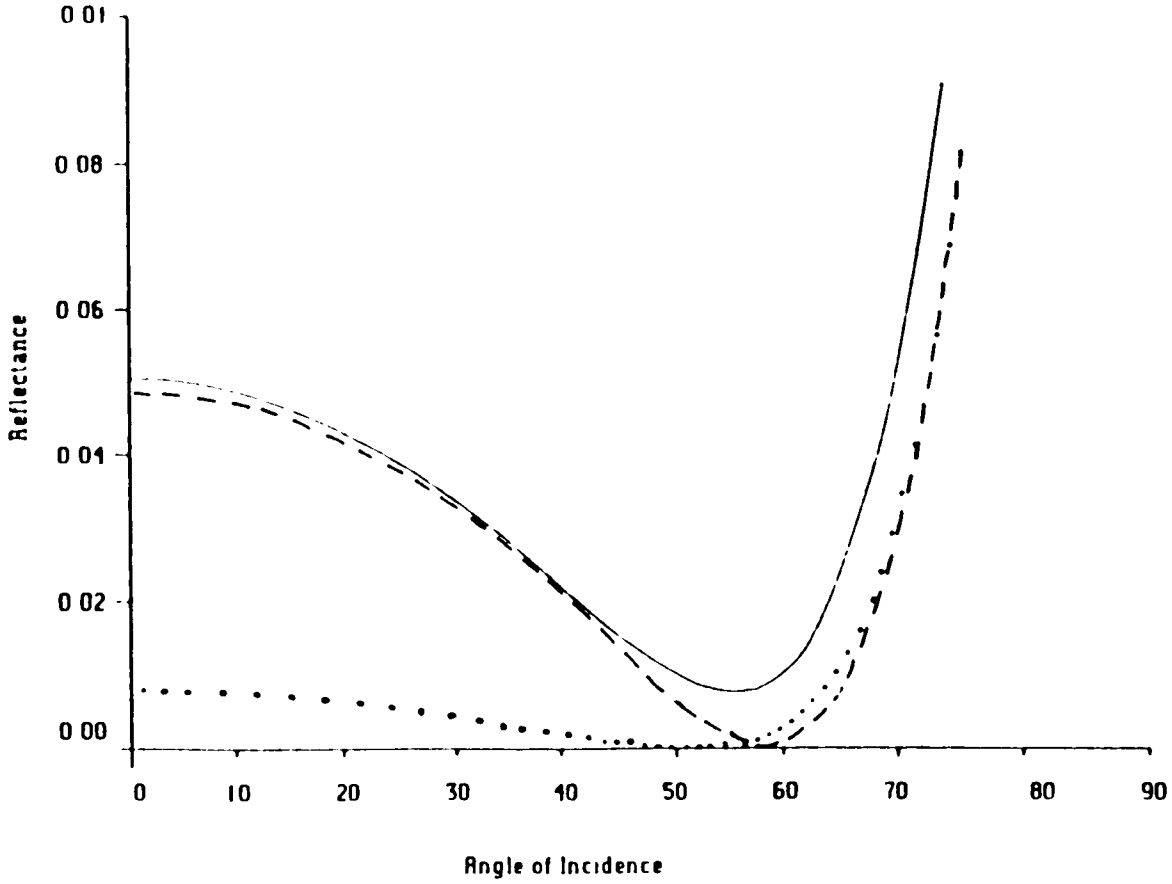

Fig. 5.4.4 Theoretical predictions of reflectance Rp vs. angle of incidence ϕ at wavelengths λ = 514, 552, and 580 nm
___ 552 nm, - - - 580 nm, • • • 514 nm

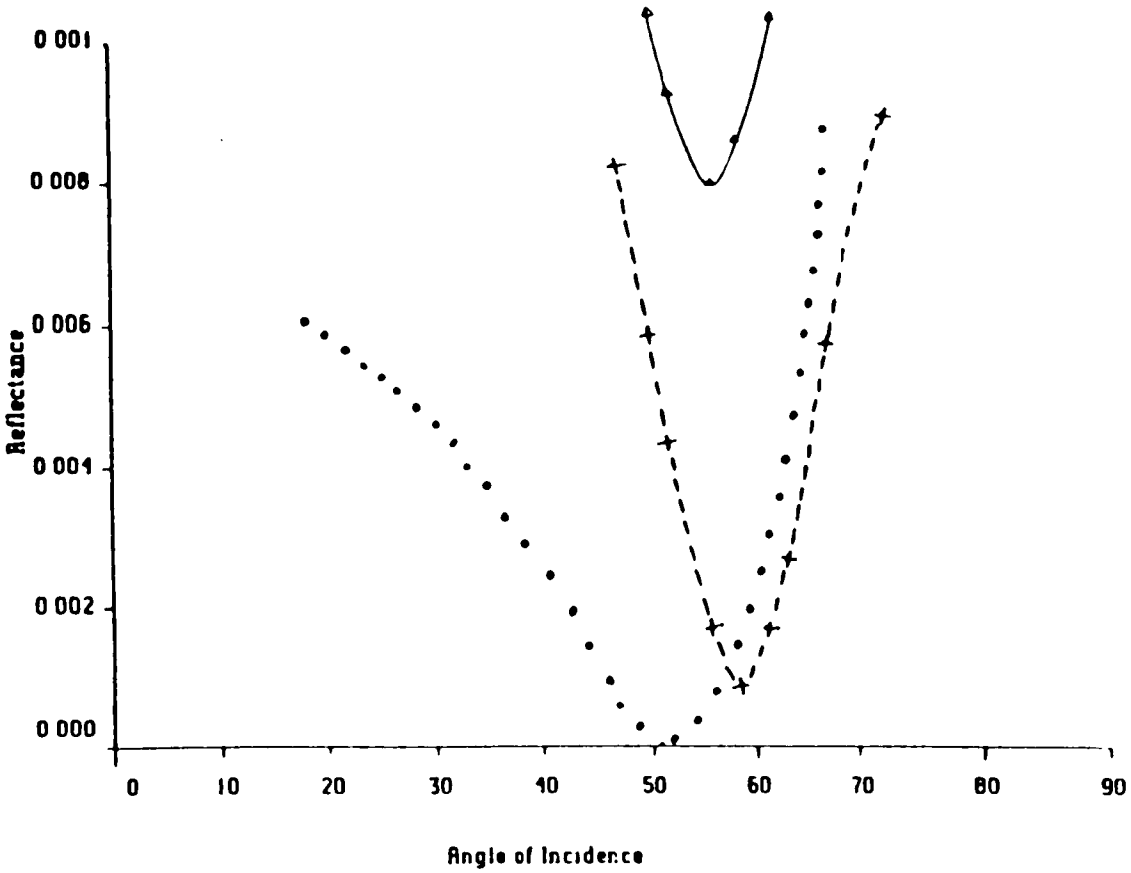

Fig. 5.4.5 Experimental measurements of reflectance Rp vs. angle of incidence ϕ at wavelengths λ= 514, 552,and 580 nm .
Δ Δ Δ 552 nm, + + + 580 nm . . . . 514 nm

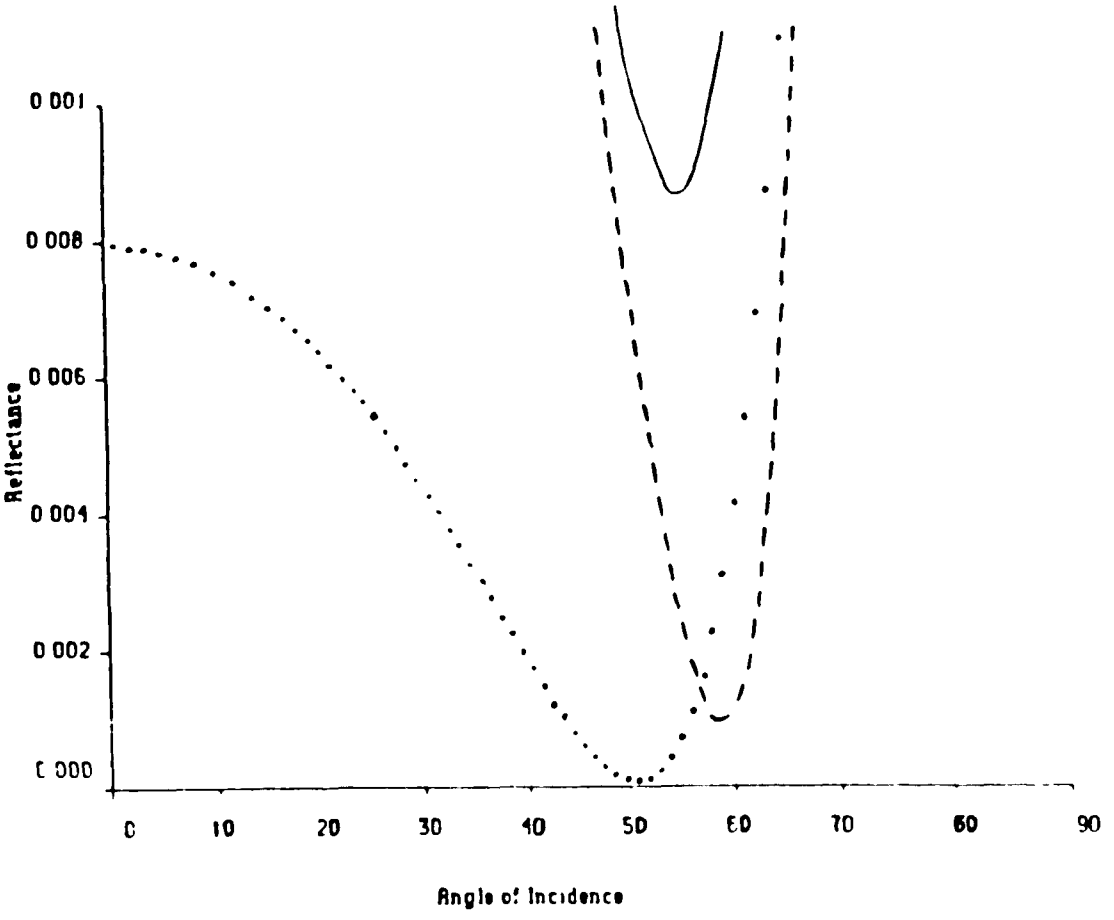

Fig.5.4.6 Expansion of Fig. 5.4.4 with the scale used in 5.4.5 to more readily distinguish between the data.

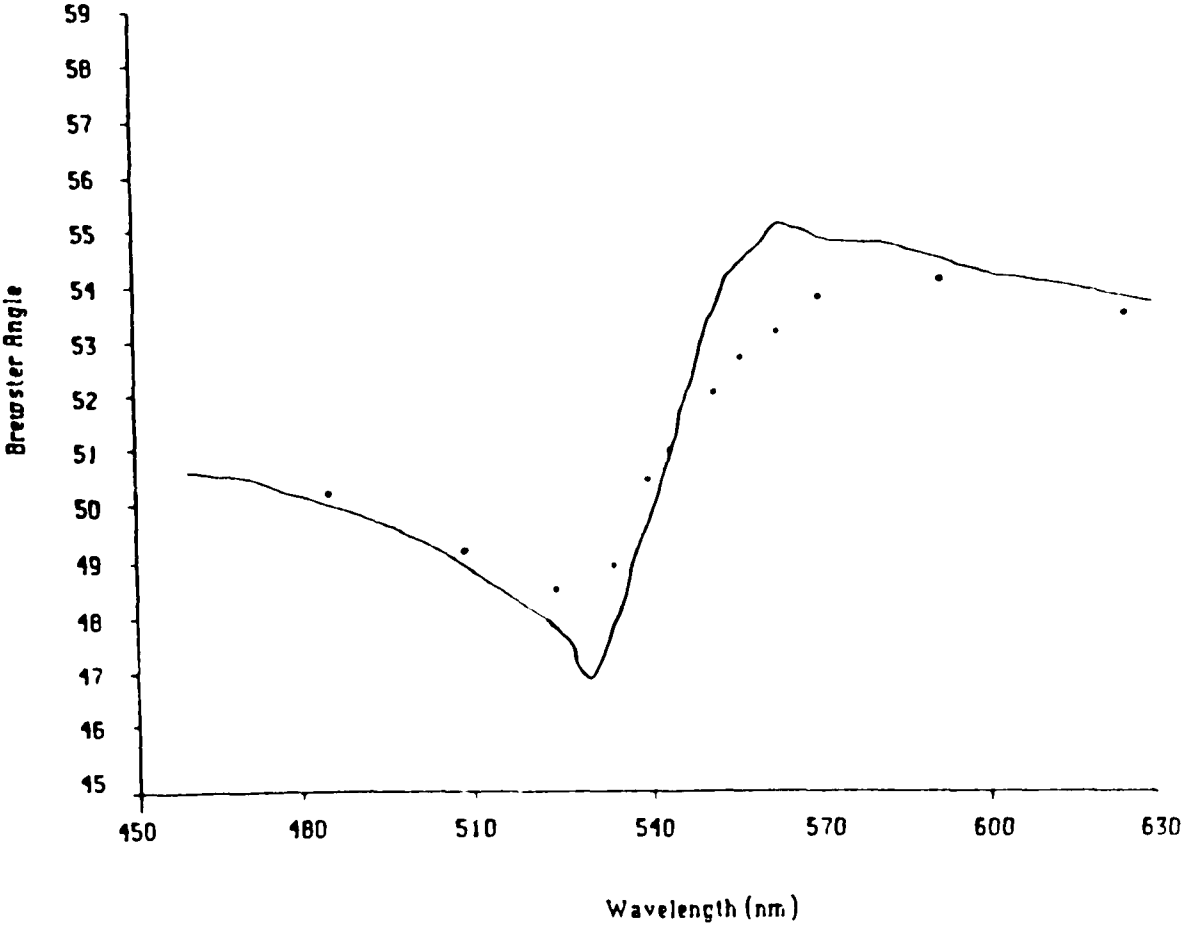

FIG. 5.4.7 Pseudo-Brewster angle ϕ_{pB} vs. λ

——— theoretical

. . . experimental

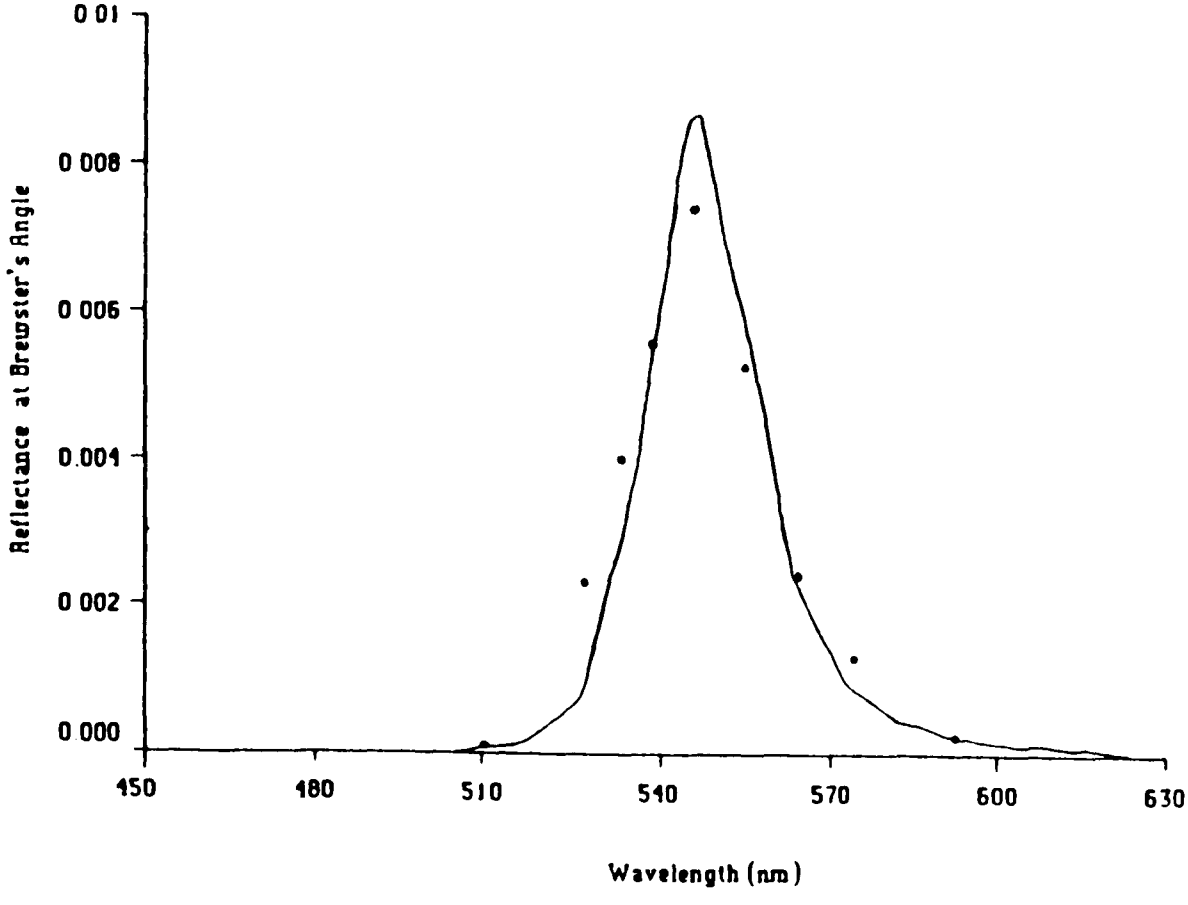

Fig.5.4.8 Reflectance at Pseudo-Brewster angles vs. λ

——— theoretical

. . . . experimental

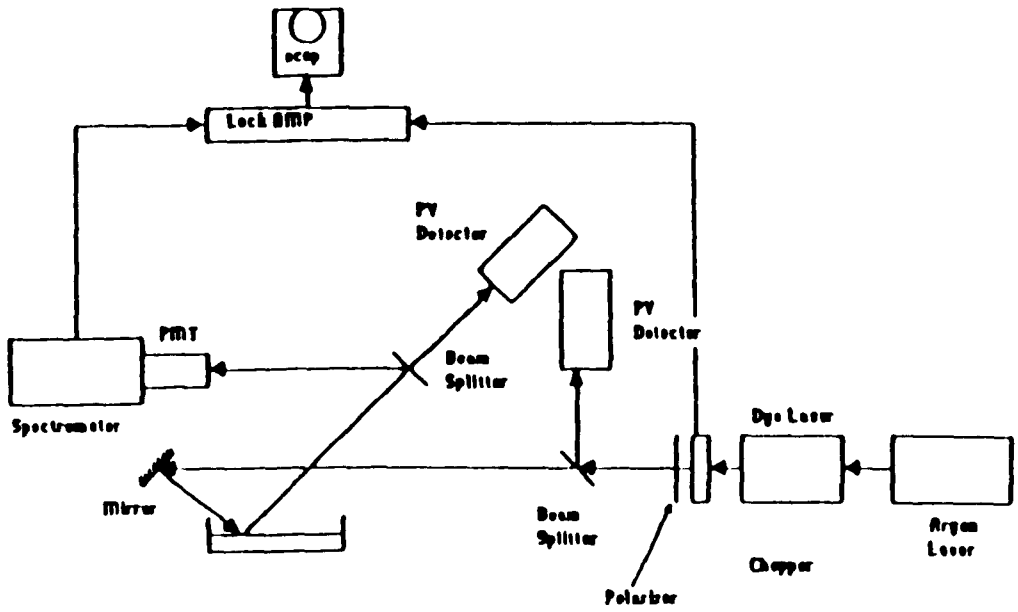

Figure 5.5.1 Experimental setup for reflection measurements.

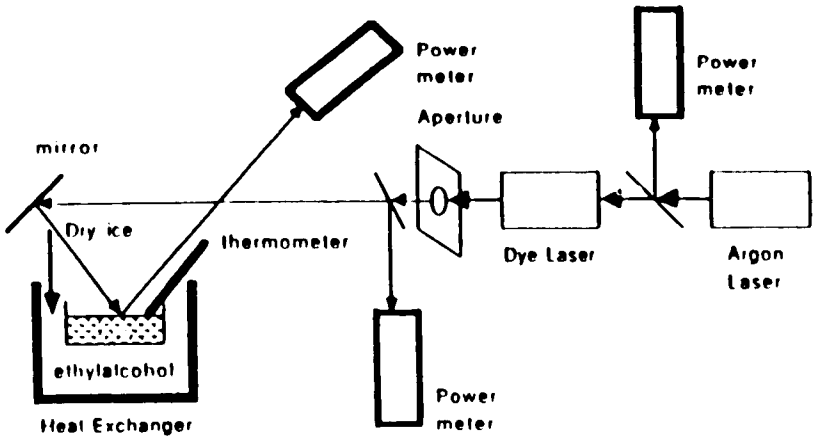

FIGURE 5.5.2 Experimental setup for reflection measurements at different temperature.

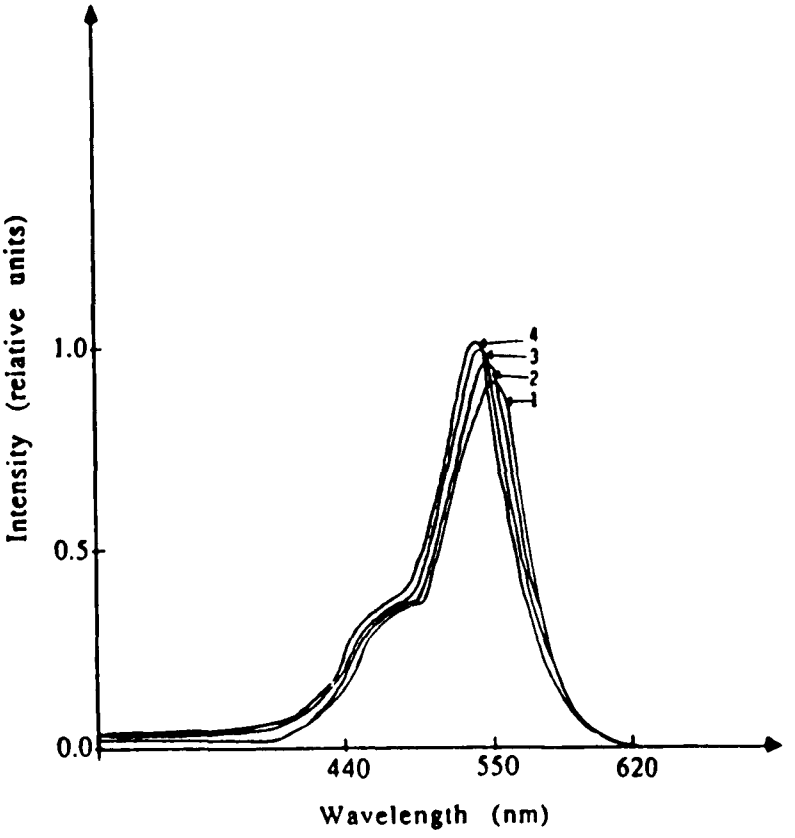

Fig. 5.6.1 Measured absorption spectra at low concentrations (2 x 10^{-5} m/l) of Rhodamine B solution in ethanolthe.
23 °c (1), −5 °c (2), −20°c (3), −60° c (4)..

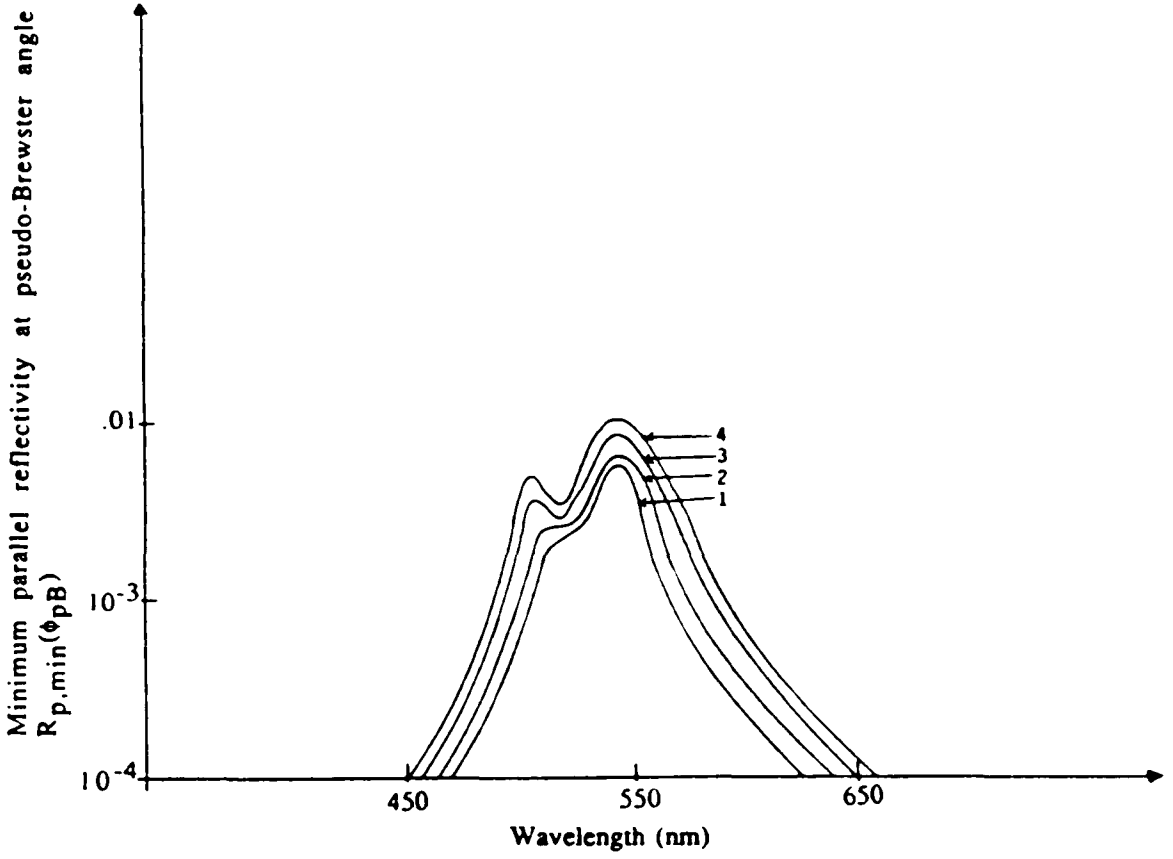

Fig. 5.6.2 measured minimum parallel reflectivity at pseudo-Brewster angle $R_{p,min}(\phi_{pB})$ for 0.45 M/l Rhodamine B in ethanol. 23 °c (1), -5 °c (2), -20°c (3), -60° c (4)..

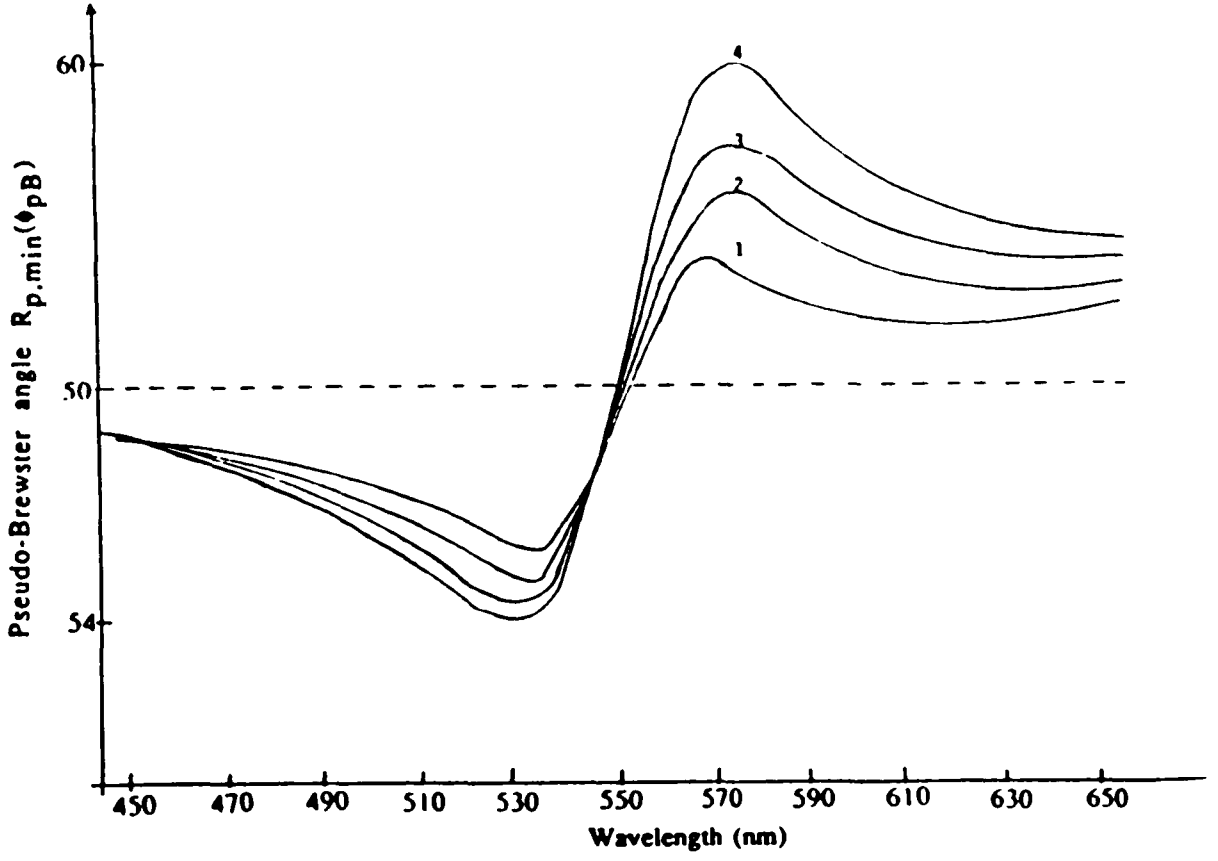

Fig. 5.6.3 Measured pseudo-Brewster angle Vs. wavelength. Dashed curve, ethanol. Solid curves, 0.45 M/l Rhodamine B in ethanol. 23 °c (1), -5 °c (2), -20°c (3), -60° c (4)..

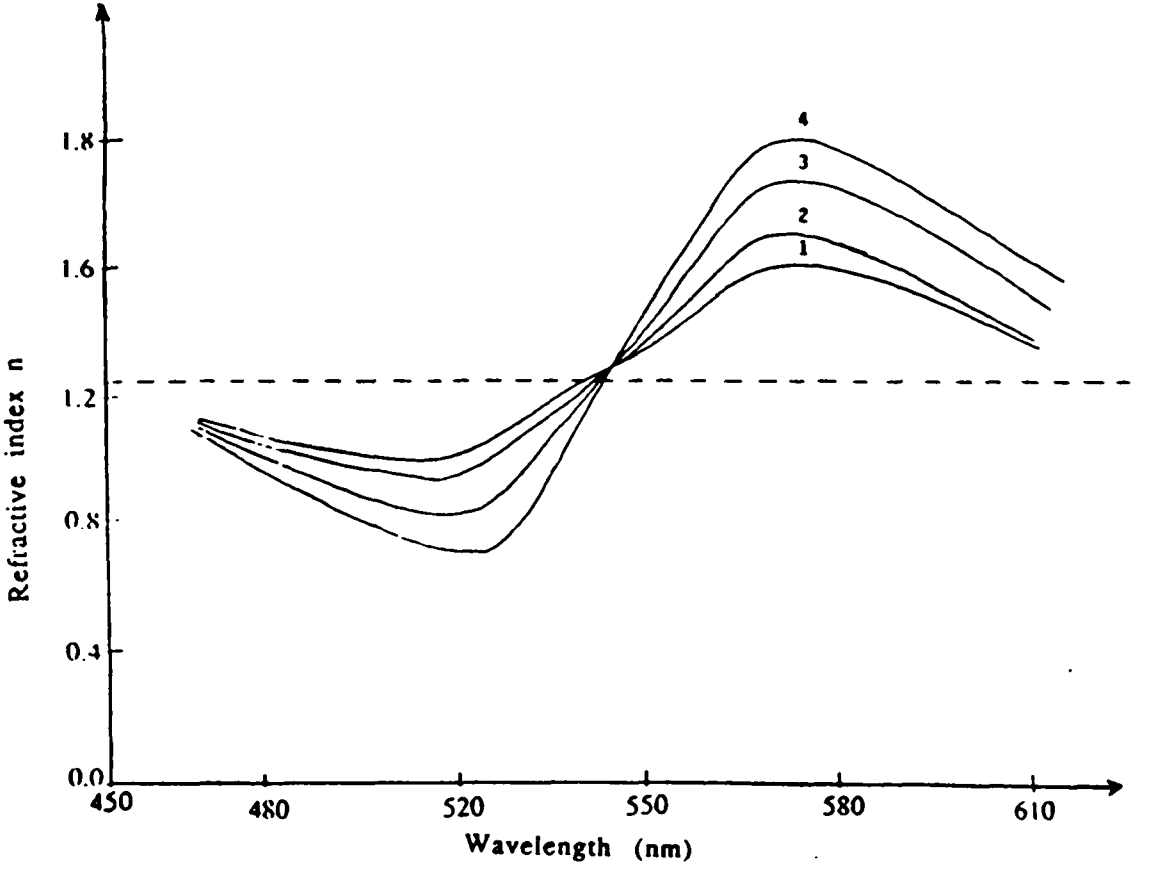

Fig. 5.6.4 Absolute refractive indices Vs. wavelength. Dashed curve, ethanol. Solid curves, 0.45 M/l Rhodamine B in ethanol. 23 °c (1), -5 °c (2), -20°c (3), -60° c (4)..

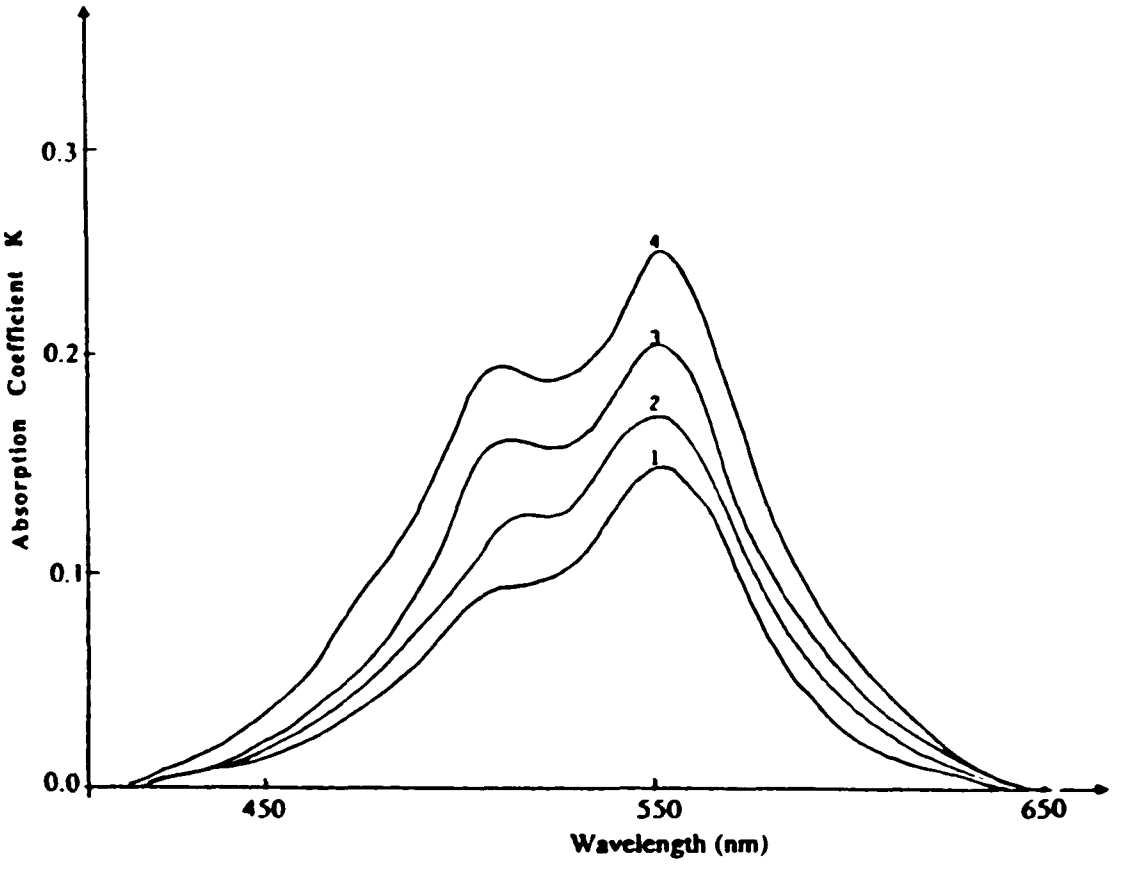

Fig. 5.6.5 Extinction coefficient Vs. wavelength. for 0.45 M/l Rhodamine B in ethanol.
23 °c (1), -5 °c (2), -20°c (3), -60° c (4)..

Appendix

Consider $\oint_c F(\omega)\,d\omega$ where C is the closed contour shown
F(w) is given by:

$$F(\omega) = \frac{d\omega}{\omega(\omega - \omega')\left\{(\omega - \omega_0)^2 + \gamma^2\right\}} \tag{1}$$

integrating the function $F(\omega)$ over the contour shown:

$$\oint_C F(\omega)\,d\omega = \int_{-R}^{-\epsilon} F(\omega)d\omega + \int_{c_1} R\omega)d\omega + \int_{\epsilon}^{\omega'-\epsilon} F(\omega)d\omega + \int_{c_2} R\omega)d\omega + \int_{\epsilon+\omega'}^{R} R(\omega)d\omega + \int_{c_3} F(\omega)d\omega \tag{2}$$

where c_1, c_2, and c_3 are the semicircular arcs of radii, ϵ, ϵ, and R.

we next take the limit of Eq 2 as $R \to \infty$ and $\epsilon = 0$

The integral over C3 vanishes for $R\infty) \to 0$ while the integral over C becomes:

$$\frac{-\pi}{\gamma(\omega_0 + \eta)(\omega' - \omega_0 - \eta)} = P\,V \int_{-\infty}^{\infty} F(\omega)d\omega + \frac{i\pi}{\omega'\left(\omega_0^2 + \gamma^2\right)} - \frac{i\pi}{\omega'\left\{(\omega' - \omega_0)^2 + \gamma^2\right\}} \tag{3}$$

where:

$$\frac{-\pi}{\gamma(\omega_0 + \eta)(\omega' - \omega_0 - \eta)} = 2\pi i \text{ (residue) of } R(\omega) \text{ at } \omega = \omega_0 + i\eta = \text{L.H.S of Eq 2}$$

$$\frac{i\pi}{\omega(\omega_0^2+\gamma^2)} = \int_{C_1} F(\omega)d\omega = -i\pi \text{ (residue) of } F(\omega) \text{ at } \omega = 0$$

$$\frac{-i\pi}{\omega'\left\{(\omega'-\omega_0)^2+\gamma^2\right\}} = \int_{C_2} F(\omega)d\omega = -i\pi \text{ (residue) of } F(\omega) \text{ at } \omega = \omega'$$

from Eq. 3 we get:

$$\text{P.V.} \int_{-\infty}^{\infty} F(\omega)d\omega = \frac{\pi\left\{\omega_0^2-\omega_0\omega'-\gamma^2\right\}}{\gamma(\omega_0^2+\gamma^2)\left\{(\omega'-\omega_0)^2+\gamma^2\right\}} \tag{4}$$

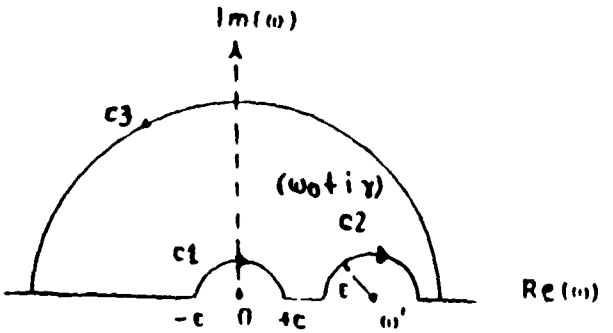

The integration contour used to derive the real (n) of the complex refractive index (N).

BIBLIOGRAPHY

Ahmed S. A. , and Ali M. A. J. Chem. Phys. Vol. 91, pp. 3838-3854, October (1989).

Alekseev V. A. , Denisov L. K. , Kozintsev V. I. and Kozlov N. A. J. Appl. Spectrosc. Vol. 31, PP. 848, (1979).

Arbeloa I. L. and Ojeda. P. R. Chem. Phys. Letter Vol. 8, PP. 556, (1982).

Aristov A. V. and Maslyukov Yu. S. Opt. Specrosc. PP. 835, (1968)

Aristov A. V. , Bakhshiev N. G. and Piterskaya I. V. . Opt. Spektrosk. Vol. 30, PP. 143, (1971).

Aristov A. V., Bakhshiev N. G. and Piterskaya I. V.. Opt. Spektrosk. Vol. 30, PP. 143, (1971).

Aspnes D. E. and Studna A. A. , Phys. Rev. B, Vol. 27, PP. 985, (1983).

Azzam R. M. A. and Bashara N. M., Ellipsometry and Polarized Light, North-Holand, (1977).

Azzam R. M. A. and El-Saba A. M. , Appl. Opt. Vol. 27, No. 19, (1988).

Bakhshiev N. G. and Neporent B.S. , Opt. Spectrosc. Vol16, PP. 191 (1970).

Bakhshiev N. G. and Studenov V. I. . Opt. Spektrosc. Vol. 33, PP. 62-65 (1972).

Bakhshiev N. G. and Studenov V. I. . Opt. Spektrosc. Vol. 33, PP. 62-65 (1972).

Bakshiev N. G. and Piterskaya I. V. , Opt. Spectrosc. PP21, (1966).

Bakhshiev N. G. , and Studenov. V. I. Opt. Spektrosc. Vol. 33, PP. 62-65 (1972).

Bakshiev N. G. , Opt. Spectrosk. Vol. 32, PP. 1151, (1972).

Bakshiev N. G. , Opt. Spectrosk. Vol. 32, PP. 979, (1972).

Bakshiev N. G. , O. P. Grin, and Studenov V. I. , Opt. Spectrosk. Vol. 39, PP. 54-59 (July 1975).

Bakshiev N. G., Opt. Spectrosk. Vol. 32, PP. 1151, (1972).

Bakhshiev N. G., The Spectroscopy of intermolecular interactions, Nauka, Leningrad, (1972).

Bakshiev N. G. and Piterskayal. V. , Opt. Spectrosc. PP21, (1966).

Bakhshiev N. G.and Mazurenko Yu. T. , Optical Spectrosc. PP. 25, (1970).

Bakshiev N. G. , Opt. Spectrosk. Vol. 32, PP. 1151, (1972).

Bakshiev N. G. , Opt. Spectrosk. Vol. 32, PP. 979, (1972).

Bakshiev N. G. , Grin O. P., and Studenov V. I. , Opt. Spectrosk. Vol. 39, PP. 54-59, July (1975).

Bakhshiev N. G. , The Spectroscopy of intermolecular interactions Nauka, Leningrad, (1972).

Bakshiev N. G. , Opt. Spectrosk. Vol. 32, PP. 1151, (1972).

Bakhshiev N. G. , The Spectroscopy of intermolecular interactions Nauka, Leningrad, (1972).

Bakhshiev N. G., Piterskaya I.V. , and A. V. Altaskaya, Opt Spectrosc. Vol. 28, PP. 897 (1970).

Bakhshiev N. G. , Opt. Spectrosc. Vol. 10, PP. 717 (1961).

Bakhshiev N.G. , Opt. Spectrosc. Vol 32, PP. 1151 (1972).

Bakhshiev N. G. , Opt. Spectrosc. Vol. 32, PP. 1152(1972).

Bakhshiev N. G. , Opt. Spectrosc. Vol. 32, PP. 979 (1972).

Bakhshiev N. G. and Mazurenko Yu. T. , Optical Spectrosc. PP. 25, (1970).

Belyi M. U. , and Leontev A. B. . Opt. Spektrosc. Vol. 34, PP. 715-721, April (1972).

Bass M. andSteinfeld J. I. , IEEE J. Quantum Electronics Vol. 4, PP. 53-58, February (1968).

Bass M. and Steinfeld J. I. , IEEE. J. Quantum Electronics. Vol. 4, PP. 53-58, Feb. (1968).

Carpenter R. , J. Opt. Soc. Am. Vol. 40, PP. 225-29, (1950).

Davydov S. A. and Gruzinskii V. V. , Zh. Prikl. Specktrosk. Vol. 26, PP. 30, (1977).

Faraggi M. , and Weinraub D. Chem. Phys. Letter Vol. 103, PP. 310, (1984).

Field G. R. and Murphy E. , Appl. Opt. Vol. 10, PP. 1402, (1971).

Garg S. K. and Smyth C. P. , J. Phys. Chem. Vol. 69, PP. 1294 (1965).

Greenaway David L. and Harbeke G. , Optical properties and band structure of semiconductors, Pergamon press, (1968).

Greenaway David L. and Harbeke G. , Pergamon Press, (1969).

Gourary Barry S. , J. Appl. Phys. Vol. 28, PP. 3, (1957).

Hunter W. R. , J. Optical Soc. Am. Vol. 55, PP. 1197, (1965).

Humphreys-Owen S. P. F. , Proc. Phys. Soc. (London), Vol. 77, PP. 949 (1961).

Hurwitz H. , Jr. and Jones R. C. , J. Opt. Soc. Am. Vol. 31, PP. 493 (1941).

Humphreys-Owen S. P. F. , Proc. phys. Soc. (London), Vol. 77, PP. 949, (1961).

Hyde W. L. , J. Opt. Soc. Am. Vol. 38, PP. 663, (1948).

Klochkov V. P. and Korotkov S. M., Opt. Spectrosc. PP. 16, (1970).

Klochkov V. P. and Korotkov S. M., Opt. Spectrosc. PP. 16, (1971).

Kopainsky B. , and Kaiser W. . Chem. Phys. Letter Vol. 8, PP. 357, (1982).

Korol' Kova N. V. , and Uzhinov B. M. . Zhurnal prikladnoi Spektroskopi, Vol 39, No. 3, pp. 406-412, September (1983).

Korol' Kova N. V. , and UzhinovB. M. Zhurnal prikladnoi Spektroskopii, Vol 39, No. 3, pp. 406-412, September (1983).

Krasnoshchekov V. M., Nikolaev A. B. , and V. V. Rylkov. Opt. Spektrosk. Vol. 54, PP. 118-122, January (1983).

Kuznetsova R. T. Fofova V. I. and Danilva V. I. . Appl. Phys. PP. 1475, (1980).

Levshin L. V. and Akbarova D. M. , Zh. Prikl. Spectrosc., 3, 441 (1965).

Levshin L. V. , Slavnova T. D. and Yuzhakov V. I. . J. Appl. Spectrosc. Vol. 24, PP. 698, (1976).

Levshin L. V. , Slavnova T. D. and Yuzhakov V. I. . J. Appl. Spectrosc. Vol. 24, PP. 698, (1976).

McFarlandb B. B. , Appl. Phys. Letters, Vol. 10, PP. 208-209, April (1967).

Mazurenko Yu. T. and Bakhshiev N.G. , Opt. Spectrosc. Vol. 28, PP. 490 (1970).

Mcrae E. S. and Kasha M. , J. Chem. Phys. 28, 721 (1958).

Moghaddasi J. , Ali M. A. , and Ahmed S. A. submitted for publication, IEEE, photonics technology letters, December (1989).

Parker C. A. , Photoluminescence of solutions Elsvier, Amsterdam, (1968).

Philipp H. R. and Taft E. A. , Phys. Rev. Vol. 113, PP. 1002 (1959).

Palik D. Edward, Handbook of Optical Constants of Solids, Academic Press, (1985).

Ramachandran G. N. and Ramaseshan S. , J. Opt. Soc. Am. Vol. 42, PP. 49, (1952).

Samson A. M. , Methode of Calculation for Organic-Dye Laser with Monochromatic Excitation. Institute of Physics, Academy of science of USSR (1970).

Samson A. M. (editor), Quantum Electronics and Laser Spectroscopy, Nauka i Teknika, Minsk (1974).

Schafer F. P., Dye lasers, second revised edition, Springer-Verlag Berlin Heidelberg New York, (1977).

Schafer F. P. , Dye lasers, second revised edition, Springer-Verlag Berlin Heidelberg New York, (1977).

Permogorov V. I. , Serdyukova L. A. , and Frank M. A. Kamenetskii, Opt. Spectrosc. Vol. 36, PP. 503 (1974).

Sharp T. E. and Rosenstock H. M.. J. Chem. Phys. Vol. 41, PP. 3453 (1964).

Shafer F. P. , W. Schmidt, and Volez Vol J. . 9, PP. 306-309, October (1966).

Snavely B. B. , Peterson O. G., and Reithel R. F., Appl. Phys Letters, Vol. 11, PP. 275-276, November (1967).

Snavely B. B. and Peterson O. G. , IEEE Journal of Quantum Electronics, Vol. QE-4, Vol. 10, October (1968).

Sorner G. C. and Topp M. R. , Chem. Phys. Letter. PP. 36, 265, (1975).

Sorokin P.P. and Lankard J.R. , IBM J Research and develop. Vol. 10, pp. 162-163, March (1966).

Sorokin P. P. and Lankard J. R. , IBM J. Research and Develop. Vol 11, PP. 148, March (1967).

Sorokin P. P. and Lankard J. R., IBM J. Research and Develop. Vol 11, PP. 149, March (1967).

Studenov V. I. , and Bakhshiev N. G. . Opt. Spektrosk. Vol. 36, PP. 392, (1974).

Studenov V. I. , and Bakhshiev N. G. . Opt. Spektrosk. Vol. 39, PP. 661-665, October (1975).

Studenov V. I., Piterskaya I. V. , and N. G. Bakhshiev. Opt. Spektrosk. Vol. 39, PP. 308, (1975).

Studenov V. I., and Bakhshiev N. G. . Opt. Spektrosk. Vol. 36, PP. 392, (1974).

Studenov V. I. , Piterskaya I. V. , and N. G. Bakhshiev. Opt. Spektrosk. Vol. 39, PP. 308,(1975).

Studenov V. I. , Bakhshiev N. G., and Smirnov V. S.. Reports of the 7th-All-Union conference, Tashkent, pp. 406, (1974).

Studenov V. I. , Bakhshiev N. G. , and Smirnov V. S.. Reports of the 7th-All-Union conference, PP. 406, (1974).

Studenov V. I. , and Bakhshiev N. G. . Opt. Spektrosk. Vol. 36, PP. 392 (1974).

Studenov V. I., PiterskayaI. V. , and Bakhshiev N. G.. Opt. Spektrosk. Vol. 39, PP. 308, (1975).

Studenov V. I. , and Bakhshiev N. G. . Opt. Spektrosk. Vol. 39, PP. 661-665, October (1975).

Soffer B. H. and McFarland B. B. , Appl. Phys. Letters, Vol. 10, PP. 266-267, May (1967).

Studenov V. I. , Piterskaya I. V. , and Bakhshiev N. G. . Opt. Spektrosk. Vol. 39, PP. 308, (1975).

Spaeth M. L. and Bortfield D. P. , Appl. Phys. Letters, Vol. 10 PP. 179-181, September (1966).

Tomin V. I. and Rubinov A. N. Opt. Spektrosk. Vol. 29, PP. 1802, (1970).

Tomin V. I. , and Rubinov A. N. Opt. Spektrosk. Vol. 29, PP. 1803, (1970).

Uzhinov B. M. and Korol' Kova N. V. , prikladnoi Spektroskopii, Vol. 39, No. 3, pp. 406-412, September (1983).

Zhurnal prikladnoi, Levshin L. V. , and Yuzhakov. V. I. spektroskopii, Vol. 24, No. 6, pp. 985-990, June (1976).